Quantifying the contributions of atmospheric processes and meteorology to severe PM2.5 pollution episodes during the COVID-19 lockdown in the Beijing-Tianjin-Hebei, China

Ishaq Dimeji Sulaymon[1], Yuanxun Zhang[2], Philip K. Hopke[3], Song Guo[4], Fei Ye[5], Jinjin Sun[1], Yanhong Zhu[1], and Jianlin Hu[1]

[1]Nanjing University of Information Science and Technology
[2]University of Chinese Academy of Sciences
[3]University of Rochester
[4]Peking University
[5]Nanjing University of Information Science & Technology

March 16, 2023

Abstract

A major tool for curtailing the spread of COVID-19 pandemic in China was a nationwide lockdown, which led to significant reductions in anthropogenic emissions and fine particulate matter (PM2.5). However, the lockdown measures did not prevent high PM2.5 pollution episodes (EPs). Three severe EPs were identified in the Beijing-Tianjin-Hebei (BTH) region during the lockdown. The integrated process rate (IPR) analysis tool in the Community Multiscale Air Quality (CMAQ) model was employed to quantify the contributions of individual atmospheric processes to PM2.5 formation during the lockdown in the BTH region. The IPR results showed that emissions and aerosol processes were the dominant sources of net surface PM2.5 in Beijing and Tianjin, constituting a total of 86.2% and 92.9%, respectively, while emissions, horizontal transport, and aerosol processes dominated the net surface PM2.5 in Shijiazhuang and Baoding. In addition, the EPs in Beijing and Tianjin were primarily driven by local emissions, while the EPs in Shijiazhuang and Baoding were attributed to combined local emissions and regional transport. The reductions in PM2.5 in Case 2 relative to Case 1 were attributed to the weaker PM2.5 formation from emissions and aerosol processes. However, the EPs were enhanced by low planetary boundary layer heights, low vertical export of PM2.5 from the boundary layer to the free troposphere, and substantial horizontal import, especially in Shijiazhuang and Baoding. This study improves the understanding of buildup of PM2.5 during the EPs, and the results provide insights for designing more effective emissions control strategies to mitigate future PM2.5 episodes.

Quantifying the contributions of atmospheric processes and meteorology to severe $PM_{2.5}$ pollution episodes during the COVID-19 lockdown in the Beijing-Tianjin-Hebei, China

Ishaq Dimeji Sulaymon[a], Yuanxun Zhang[b,c], Philip K. Hopke[d,e], Song Guo[f], Fei Ye[a], Jinjin Sun[a], Yanhong Zhu[a], Jianlin Hu[a*]

[a] *Jiangsu Key Laboratory of Atmospheric Environment Monitoring and Pollution Control, Collaborative Innovation Center of Atmospheric Environment and Equipment Technology, School of Environmental Science and Engineering, Nanjing University of Information Science and Technology, Nanjing, 210044, China*

[b] *College of Resources and Environment, University of Chinese Academy of Sciences, Beijing 100049, China*

[c] *CAS Center for Excellence in Regional Atmospheric Environment, Chinese Academy of Sciences, Xiamen, 361021, China*

[d] *Center for Air Resources Engineering and Science, Clarkson University, Potsdam, NY 13699, USA*

[e] *Department of Public Health Sciences, University of Rochester School of Medicine and Dentistry, Rochester, NY 14642, USA*

[f] *State Key Joint Laboratory of Environmental Simulation and Pollution Control, College of Environmental Sciences and Engineering, Peking University, Beijing, 100871, China*

---

[*] Corresponding author. *E-mail address:* sulaymondimeji@nuist.edu.cn; jianlinhu@nuist.edu.cn

Key Points:

- Three severe $PM_{2.5}$ pollution episodes were identified in the Beijing-Tianjin-Hebei region during the COVID-19 lockdown.

- The $PM_{2.5}$ episodes were dominated by emissions and aerosol processes, and enhanced by unfavorable meteorological conditions.

- Designing more effective emissions control strategies with both chemistry and meteorology in thought could mitigate future $PM_{2.5}$ episodes.

Abstract

A major tool for curtailing the spread of COVID-19 pandemic in China was a nationwide lockdown, which led to significant reductions in anthropogenic emissions and fine particulate matter ($PM_{2.5}$). However, the lockdown measures did not prevent high $PM_{2.5}$ pollution episodes (EPs). Three severe EPs were identified in the Beijing-Tianjin-Hebei (BTH) region during the lockdown. The integrated process rate (IPR) analysis tool in the Community Multiscale Air Quality (CMAQ) model was employed to quantify the contributions of individual atmospheric processes to $PM_{2.5}$ formation during the lockdown in the BTH region. The IPR results showed that emissions and aerosol processes were the dominant sources of net surface $PM_{2.5}$ in Beijing and Tianjin, constituting a total of 86.2% and 92.9%, respectively, while emissions, horizontal transport, and aerosol processes dominated the net surface $PM_{2.5}$ in Shijiazhuang and Baoding. In addition, the EPs in Beijing and Tianjin were primarily driven by local emissions, while the EPs in Shijiazhuang and Baoding were attributed to combined local emissions and regional transport. The reductions in $PM_{2.5}$ in Case 2 relative to Case 1 were attributed to the weaker $PM_{2.5}$ formation from emissions and aerosol processes. However, the EPs were enhanced by low planetary boundary layer heights, low vertical export of $PM_{2.5}$ from the boundary layer to the free troposphere, and substantial horizontal import, especially in Shijiazhuang and Baoding. This study improves the understanding of buildup of $PM_{2.5}$ during the EPs, and the results provide insights for designing more effective emissions control strategies to mitigate future $PM_{2.5}$ episodes.

Keywords: Fine particulate matter; Pollution episodes; Process analysis; WRF-CMAQ; COVID-19 shutdown.

1. Introduction

For more than two decades, China has been suffering from severe haze pollution, attributed to its population growth, urbanization, fast industrialization, as well as economic advancement (Li et al., 2020; Shi et al., 2017; Zhao et al., 2021). The development of severe haze is caused by a combination of anthropogenic emissions (local and regional) (Sulaymon et al., 2020, 2021a) and adverse meteorological conditions (Chen et al., 2021; Hua et al., 2021; Hu et al., 2016; Shen, et al., 2021; Shi et al., 2020; Sulaymon et al., 2021a, 2021b). Severe air pollution causes reductions in visibility (Jiang et al., 2021; Li et al., 2019; Wang et al., 2018), changes in climate and ecosystem services (Jiang et al., 2021; Zhao et al., 2021), and adverse human health effects (Chen et al., 2017; Croft et al., 2019; Hopke et al., 2019; Shang et al., 2018; Shen et al., 2020; Yan et al., 2018). The global disease burden (GDB) has attributed about 2 million premature deaths per annum to severe air pollution exposure in China (Yin et al., 2020).

The issuance of the new ambient air quality standards (GB3095-2012) in 2012 and the subsequent implementation of the Air Pollution Prevention and Control Action Plan (APPCAP) in September 2013 by the Chinese authorities has led to reduction in the concentrations of fine particulate matter with aerodynamic diameters of ≤2.5 ($PM_{2.5}$) in Chinese cities (Fan et al., 2020; Sulaymon et al., 2021d; Wang et al., 2016). For instance, Xue et al. (2019) noted about 32.5% reduction in the national population-weighed $PM_{2.5}$ annual mean between 2013 and 2017. However, high $PM_{2.5}$ concentrations are still observed in most cities, with annual averages violating the annual Grade I (15 μg/m^3) and Grade II (35 μg/m^3) Chinese Ambient Air Quality Standards (CAAQS), and much higher than the WHO (5 μg/m^3) recommended limit or the USEPA (12 μg/m^3) standard.

The Beijing-Tianjin-Hebei (BTH) region that includes Beijing and Tianjin, and Hebei Province, is one of the most economically developed regions in China. The region has been suffering from severe $PM_{2.5}$ pollution over the past two decades (Chang et al., 2018; Dai et al., 2021a), particularly during the winter season. During past international events (e.g. 2008 Olympic Games, 2014 Asia-Pacific Economic Cooperation, and the 2015 Military Parade), Chinese authorities implemented major emissions reductions measures in the BTH region to improve air quality. The effectiveness and success of the emissions reduction policies have been assessed (Wang et al., 2016; Xu et al., 2017; Yang et al., 2016).

In December 2019, an outbreak of coronavirus disease (COVID-19) occurred in Wuhan (Zhu et al., 2020) and spread across China and many other countries within a short time. As one of the measures to curtail the spread of COVID-19 pandemic in China, a nationwide lockdown was implemented by the Chinese authorities, leading to significant reductions in anthropogenic emissions and $PM_{2.5}$ concentrations across China (Sulaymon et al., 2021a, 2021c; Wang et al., 2020; Zhao et al., 2020; Zhao et al., 2021). However, the BTH region still experienced high $PM_{2.5}$ pollution episodes during the lockdown (Sulaymon, et al., 2021a; Zhang et al., 2021). Compared to the past international events held in Beijing during the summer and autumn seasons (with no or few pollution episodes), the COVID-19 pandemic occurred in winter, a period with frequent severe pollution events especially in the BTH region. In addition, the COVID-19 lockdown had a longer period with very strict measures than the duration of the past three events.

Previous studies have assessed the impacts of COVID-19 lockdown on air quality as well as the relationships between air quality and meteorological conditions during lockdown in BTH region (Cui et al., 2020; Dai et al., 2020; 2021b; Sulaymon et al., 2021a;

Zhang et al., 2021; Zhao et al., 2021), other regions in China (Gao et al., 2021; Liu et al., 2020; Shen et al., 2021a, 2021b; Sulaymon, et al., 2021c; Wang et al., 2020; Wu et al., 2021; Xing et al., 2020), and outside mainland China (Bashir et al., 2020; Chauhan and Singh, 2020, 2021; Mishra et al., 2021; Muhammad et al., 2020; Orak and Ozdemir, 2021; Querol et al., 2021; Sharma et al., 2020; Singh and Chauhan, 2020; Srivastava, 2021; Ye et al., 2022). A few studies have also been performed on the regional source apportionment of $PM_{2.5}$ during the lockdown (Li et al., 2020; Ma et al., 2021). Li et al. (2020) reported that industry (32.2-61.1%) and residential (2.1-28.5%) were the two highest sources contributing to $PM_{2.5}$ in the Yangtze River Delta (YRD) region, while about 14.0-28.6% contribution was due to long-range transport from northern China. In the BTH region, a few studies have also investigated the source apportionment of $PM_{2.5}$ during lockdown (Cui et al., 2020; Dai et al., 2020). For example, Dai et al. (2020) used Positive Matrix Factorization (PMF) to investigate the sources of $PM_{2.5}$ in Tianjin. Their results showed that secondary inorganic aerosols (SIA) (50.5%), fireworks and residential burning (32.0%), and primary coal combustion emissions (13.3%) were the three dominant sources contributing to $PM_{2.5}$ during the lockdown. Overall, previous studies have reported persistent haze episodes in the BTH region during lockdown despite the emission reductions, and have generally attributed them to unfavorable meteorological conditions (Cui et al., 2020; Dai et al., 2020; 2021b; Sulaymon et al., 2021a; Zhang et al., 2021; Zhao et al., 2021). However, the formation of air pollutants involves various physical processes (such as emissions, condensation, advection, diffusion, deposition, etc.) as well as oxidative chemical process (Huang et al., 2005; Wang et al., 2014; Ye et al., 2022).

The process analysis (PA) tool in the Community Multiscale Air Quality (CMAQ) chemical transport model can provide quantitative analysis of the individual contributions of various physical and chemical processes to the observed air pollution (Liu et al., 2010; Liu and Zhang, 2011; Xing et al., 2011; Ye et al., 2022). Liu and Zhang (2011) employed the PA tool to analyze a regional $PM_{2.5}$ pollution episode in the U.S. They found that emissions and aerosol processes such as homogeneous nucleation, heterogeneous nucleation, and condensation were the dominant contributors to increased $PM_{2.5}$ concentrations, while horizontal and vertical transport and dry deposition were the primary loss mechanisms. Liu et al. (2010) utilized the PA to explore the contributions of various atmospheric processes on ozone and PM_{10} concentrations in China during four seasons. The results showed that emissions and aerosol processes were the main contributors to PM_{10} concentrations, while horizontal transport was the major removal pathway. Xing et al. (2011) used CMAQ-PA tool to quantify the air quality benefits from emissions reductions and meteorological variations during the 2008 Beijing Olympics. The results indicated that aerosol and emission processes acted as the major $PM_{2.5}$ pathways, while vertical transport was the major $PM_{2.5}$ sink at the surface.

Therefore, analyzing the air quality during the unique lockdown period to provide additional understanding of the underlying causes of high pollution episodes even during periods of substantially reduced anthropogenic activity is important for providing approaches to future air quality management strategies. The present study is the first that elucidated the contributions of various atmospheric processes to $PM_{2.5}$ pollution episodes during the lockdown in the BTH region. The results provide new insights into $PM_{2.5}$ formation of the three pollution episodes during lockdown. Thus, it provides a valuable example of how to use opportunities like the lockdown period to better understand the causal factors of episodes in other areas of the world, which can then be applied to develop more effective control strategies that would reduce the magnitude of these episodes and better protect public health.

2. Methodology

2.1. Model set-up and configurations

The Community Multiscale Air Quality model version 5.2 (CMAQv5.2) was applied to simulate the air quality in the BTH region during the COVID-19 lockdown period (January 24-February 29, 2020). The photochemical mechanism and the aerosol module used in configuring the model were the State-wide Air Pollution Research Center version 07 (SAPRC07tic) and AERO6i, respectively (Liu et al., 2020; Sulaymon et al., 2021a, 2021b). Two nested domains with horizontal resolutions of 36 and 12 km were used (Fig. S1). The outer domain (36 km) covers China and the surrounding regions (137 x 107 grids), and the inner domain (12 km) covers the study area, the BTH region (127 x 202 grids). Each of the two domains had 18 vertical layers, emanating from the surface to a height of about 20 km above the ground level. The initial and boundary conditions (IC/BC) used in the 36 km domain were based on the default profiles provided by the CMAQ model, while the IC/BC used for the 12 km domain were generated from the results of the 36 km simulations. As a way of reducing the impact of initial conditions on $PM_{2.5}$ predictions, the simulations began on January 19, and the results of the first 5 days (January 19-23, 2020) were excluded from the model analysis, thus serving as a spin-up of the model. The meteorological inputs were simulated by the Weather Research and Forecasting (WRF v4.0) model with the FNL reanalysis data serving as the IC/BC. The detailed settings and configurations, including the major physics schemes used in this study are listed in Table S1, while other settings could be found in previous studies where the WRF model was applied (Hu et al., 2015, 2016; Wang et al., 2021).

In this study, the Multi-resolution Emission Inventory for China (MEIC) of year 2016 (http://www.meicmodel.org) served as the anthropogenic emissions from China. In addition, the anthropogenic emissions from adjacent countries and regions were processed based on the Regional Emission inventory in ASia version 2 (REAS2) (Kurokawa et al., 2013). Biogenic emissions were estimated with the Model of Emissions of Gases and Aerosols from Nature (MEGAN) version 2.1. Open burning emissions were generated based on the data obtained from the Fire INventory from NCAR (FINN) (Wiedinmyer et al., 2011). Sea salt and windblown emissions were generated inline (Sulaymon et al., 2021a, 2021b). Further details regarding the emission processing can be found in Hu et al. (2016) and Qiao et al. (2015).

To evaluate the impacts of the emissions reductions on air quality, two scenarios (referred to as Cases 1 and 2) were simulated as presented in Table S2. The first scenario (Case 1) used the original MEIC16 emission inventory. In the second scenario (Case 2), emissions from transportation, industry, and power sectors were reduced (Table S2) during the lockdown period, while those of residential and agriculture were similar to Case 1. The basis for adopting the emission reduction factors has been previously presented (Sulaymon et al., 2021a; Wang et al., 2020), and has also been detailed in the Supplementary Material (Text S1). The differences between the results of Cases 1 and 2 represent the impact of emissions reductions on air quality during the lockdown.

2.2. *Process analysis*

The process analysis (PA) tool embedded in the CMAQ model has been described as a versatile analytical tool for quantifying the contributions of individual atmospheric processes and chemical reactions to a pollutant (Fu et al., 2020; Ye et al., 2022). PA is comprised of two components; the integrated process rate (IPR) and integrated reaction rate (IRR) analysis. The IPR involves the changes in the hourly concentrations of pollutants due to individual atmospheric processes such as gas-phase chemistry, emissions, aerosol processes, dry deposition, cloud processes, and vertical and horizontal transport at each grid cell in the model domain. The IPR analysis has been extensively used in quantifying the contributions individual atmospheric processes to air pollutants (Fan et al., 2015; Fu et al., 2020; Li et al., 2012; Wang et al., 2010; Xing et al., 2011; Ye et al., 2022), hence, detailed information about IPR can be found in these referenced studies.

In this study, the IPR module in CMAQv5.2 was employed to resolve both physical and chemical processes involved in the formation of $PM_{2.5}$ during the lockdown period in the BTH region. The IPR results were subsequently used to analyze the individual processes involved in $PM_{2.5}$ formation in the surface layer and full planetary boundary layer (PBL), respectively. For this purpose, the processes considered were the chemistry (gas-phase), emissions, aerosol processes (SOA formation, nucleation, condensation, coagulation, heterogeneous chemistry, mode merging, and aerosol thermodynamics), cloud processes, dry deposition, vertical transport (sum of vertical advection and diffusion), and horizontal transport (sum of horizontal advection and diffusion). Based on their contributions to $PM_{2.5}$ concentrations, atmospheric processes can be grouped into two; source process (concentration increases) and sink process (concentration decreases). Dry deposition and emission belong to the sink and source process, respectively. The IPR of other processes can either be source (positive) or sink (negative). The contributions of individual atmospheric processes to the formation of $PM_{2.5}$ were estimated using the approach of Ye et al. (2022):

$$SOURCE_p = \frac{\sum_t IPR_{p,t}}{\sum_p \sum_t IPR_{p,t}} \times 100\% \quad (IPR_{p,t} > 0) \qquad (1)$$

$$SINK_p = \frac{\sum_t IPR_{p,t}}{\sum_p \sum_t IPR_{p,t}} \times 100\% \quad (IPR_{p,t} < 0) \qquad (2)$$

where p is the atmospheric process, and t is the time (in hour). $SOURCE_p$ and $SINK_p$ are the proportions of the atmospheric process p in all source and sink processes, respectively. Both source and sink categories are used to reveal how important an atmospheric process is in influencing the changes in $PM_{2.5}$ concentrations.

3. Results and discussion

3.1. WRF model performance

Meteorological parameters play an important role in the formation and transportation of air pollution (Hu et al., 2016; Sulaymon et al., 2021a, 2021b; Wang et al., 2021). In addition, the influences of meteorological parameters on the air quality simulations using chemical transport model have also been established (Hu et al., 2016; Sulaymon et al., 2021a; Wang et al., 2021). To evaluate the WRF model performance, the predicted temperature (T2) and relative humidity (RH) at 2 m above ground level, and wind speeds (WS) and wind directions (WD) at 10 m above surface were compared to the observational data downloaded from the official website of the Chinese Meteorological Agency (http://data.cma.cn/en, last access: January 2023). Table S3 shows the summary statistics including the mean observation (OBS), mean prediction (PRE), mean bias (MB), mean error (ME), and the root mean square error (RMSE). In addition to the BTH region as a whole, four representative cities including Beijing (BJ), Tianjin (TJ), Shijiazhuang (SJZ), and Baoding (BD) were evaluated. Generally, T2 (Table S3) was slightly over-predicted in the BTH and the four representative cities during the lockdown. The MB and ME of T2 in BTH were 0.4 and 1.7, respectively, which fell below the suggested benchmarks (MB≤±0.5; and ME≤2.0) (Emery et al., 2001). These are consistent with a previous study over BTH region (Chang et al., 2019). Except in Tianjin (MB:0.5), the MB values in other three cities (Beijing:2.2; Shijiazhuang:0.6; and Baoding:1.3) exceeded the benchmark. Except in Beijing (ME:2.3), the ME values in all the cities were within the benchmark range. Although there were no suggested benchmarks for the MB and ME indices of RH, however, RH (Table S3) was underpredicted in BTH region and the four representative cities (Ma et al., 2021). Similar results had been reported by previous studies over BTH region (Chang et al., 2018; Li et al., 2021b; Sulaymon et al., 2021a; Zhao et al., 2021) and China as a whole (Hu et al., 2016; Sulaymon et al., 2021b; Wang et al., 2021). Bhati and Mohan (2018) obtained a similar result and attributed it to the influence of the boundary layer parameterization on the weather prediction. The mean observed WS across the cities and BTH ranged from 1.8 to 2.3 m/s, an illustration of relatively calm conditions during the lockdown. Generally, WS (Table S3) was over-predicted (Ma et al., 2021). However, based on the ME, MB, and RMSE indices, the predictions reasonably captured the observations across the four cities and BTH (Li et al., 2021b; Sulaymon et al., 2021a; Zhao et al., 2021). The over-predictions of WS might be due to unresolved topography within the WRF model (Li et al., 2014). The MB values met the suggested benchmark

(≤±0.5) in BTH and three cities except Shijiazhuang (0.7). During the lockdown, the ME and RMSE values ranged between 0.6-0.9 and 0.7-1.2, respectively, with both indices falling below the recommended benchmarks (≤2.0). WD (Table S3) was generally under-predicted except in Shijiazhuang where the PRE was slightly higher than the OBS. Overall, the MB values were above the suggested criterion range (≤±10) except in Baoding (MB: -0.8), Shijiazhuang (MB:2.3), and BTH (MB: -9.6). Also, the ME values in the four cities and BTH region greatly exceeded the benchmark (≤±30), especially in Shijiazhuang (ME:101.5), Beijing (ME:78.4), and BTH region (ME:70.5). Similar model performance of WD had been reported (Hu et al., 2016; Sulaymon et al., 2021a, 2021b; Wang et al., 2021). Generally, in this study, the WRF model exhibited better performance when compared to previous studies in BTH region (Chang et al., 2019; Li et al., 2021b; Sulaymon et al., 2021a; Zhang et al., 2021; Zhao et al., 2021) and China as a country (Ma et al., 2021; Sulaymon et al., 2021b; Wang et al., 2021). Since the simulated meteorological parameters were robust, they were used in driving the air quality simulations.

3.2. CMAQ model performance

In evaluating the performance of CMAQ model in predicting $PM_{2.5}$, statistical indices, which include the mean observations (OBS), mean predictions (PRE), mean fractional bias (MFB), mean fractional error (MFE), mean normalized bias (MNB), and mean normalized error (MNE) were calculated. The performance of CMAQ model for $PM_{2.5}$ over the BTH and at four representative cities during the lockdown period based on the two cases are shown in Table S4. Generally, the simulated $PM_{2.5}$ concentrations exhibited good agreement with the observed data with the model performance indices falling within the recommended benchmarks for $PM_{2.5}$ (MFB $\leq \pm 0.60$ and MFE $\leq$ 0.75) (Boylan and Russel, 2006) in BTH and the four cities for the two cases. For Case 1, $PM_{2.5}$ was over-estimated in BTH (0.10), Beijing (0.31), and Tianjin (0.41), while it was under-predicted in Shijiazhuang (-0.05) and Baoding (-0.19). Considering Case 2, all of the MFB values were negative except in Tianjin (0.32), an indication that CMAQ under-predicted the total $PM_{2.5}$ concentrations in BTH and the other three cities. Chang et al. (2019) had reported an under-estimation of $PM_{2.5}$ by CMAQ in Beijing and Shijiazhuang, which is consistent with this study for Case 2. Also, the model performances for Case 2 are in line with the findings of Sulaymon et al. (2021a) In addition, under-predictions of $PM_{2.5}$ in all of the prefectural-level cities of BTH region were reported by Jiang et al. (2021). The MFE values for the two cases ranged between 0.40-0.51, which were within the recommended benchmark (MFE$\leq$ 0.75). Overall, the CMAQ model has shown better performance in this study when compared to previous studies across the BTH region (Chang et al., 2019; Jiang et al., 2021; Li et al., 2021b; Sulaymon et al., 2021a; Zhang et al., 2021; Zhao et al., 2021). Thus, the model results were deemed acceptable for further analyses, including the IPR analysis.

3.3. IPR analysis of $PM_{2.5}$ formation at the surface layer

The hourly concentrations of $PM_{2.5}$ as well as the contributions of the individual atmospheric processes to the evolution of $PM_{2.5}$ at the surface layer in the BTH region and four representative cities for the two cases during the lockdown period are illustrated in Fig. 1. In the BTH region as a whole, the emissions (EMIS), horizontal transport (HTRA), and aerosol processes (AERO) were the major positive contributors (sources) to the net surface $PM_{2.5}$.

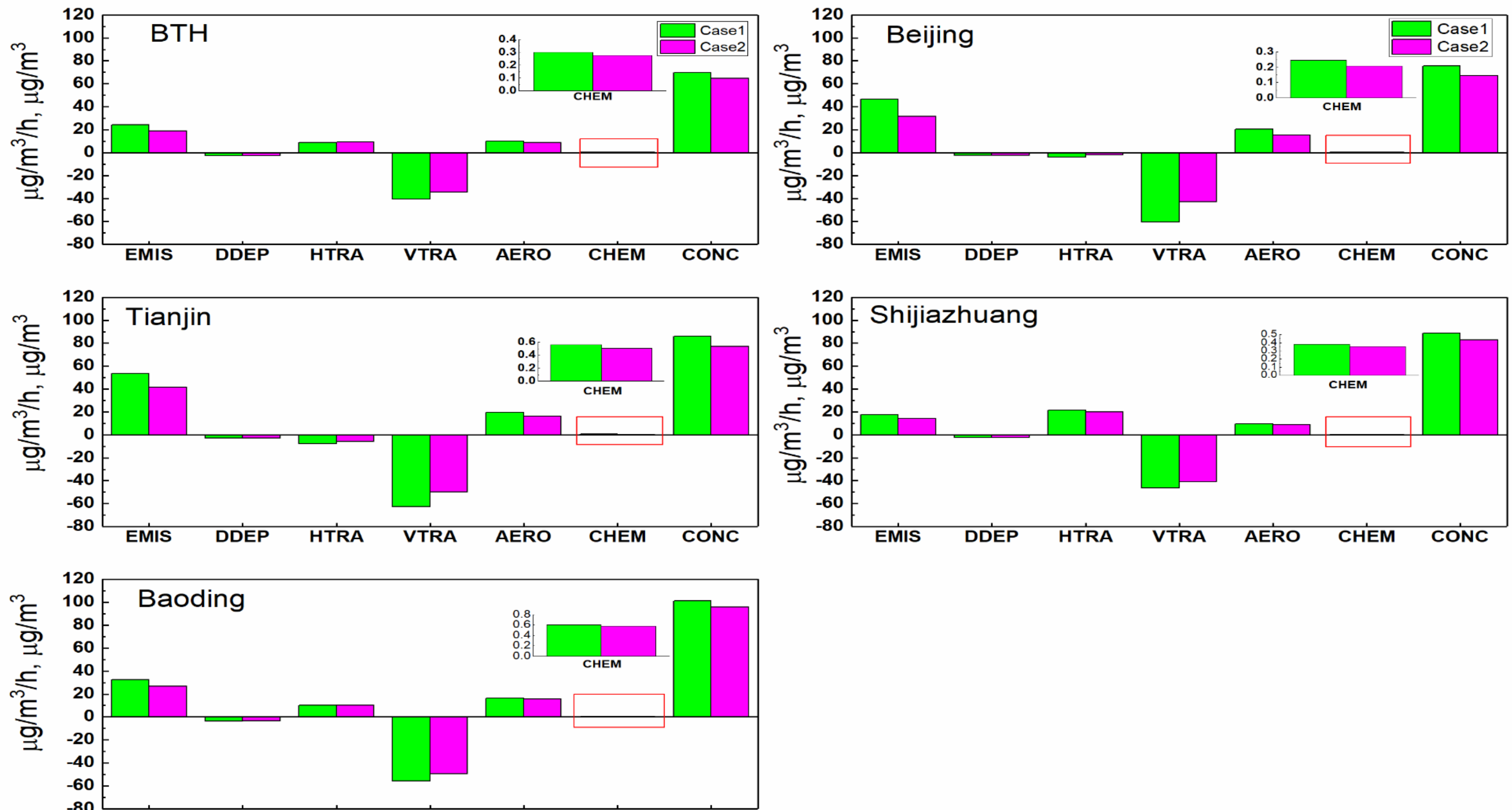

Fig. 1. Contributions of the individual processes to the concentrations of $PM_{2.5}$ at the surface layer in Cases 1 and 2 during the lockdown period. EMIS represents $PM_{2.5}$ input by emissions, DDEP represents $PM_{2.5}$ decrease by dry deposition; HTRA and VTRA represent $PM_{2.5}$ change by horizontal and vertical transport, respectively; AERO represents $PM_{2.5}$ change by the aerosol; and CHEM represents $PM_{2.5}$ change by gas-phase chemistry. The unit of the processes is μg/m^3/h. CONC is the hourly $PM_{2.5}$ concentrations in μg/m^3.

For Case 2, the contributions of EMIS, HTRA, and AERO to $PM_{2.5}$ formation were 42.4, 32.5, and 20.9% (Fig. 2b), respectively, while their contributions in the same order for Case 1 were 46.7, 29.4, and 20.3% (Fig. 2a), respectively. The reduction in the surface layer's $PM_{2.5}$ for the two cases was primarily attributed to the vertical transport (VTRA), while slight removal was also due to dry deposition (DDEP). In Beijing and Tianjin, EMIS and AERO were the predominant processes that contributed to the net surface $PM_{2.5}$ formation (Fig. 1) for both cases. The total contribution ratios of EMIS and AERO in Case 2 were 86.2% and 92.9% for Beijing and Tianjin (Fig. 2b), respectively. The reduction of surface $PM_{2.5}$ in Beijing and Tianjin for the two cases was associated with the VTRA, HTRA, and DDEP processes, with VTRA being the highest sink, with negative contributions of 79.0-81.3% (Beijing) and 80.2-81.0% (Tianjin). The results of the present study are consistent with those reported by Ye et al. (2022) in the coastal city of Kannur, India, where the EMIS, HTRA, and AERO were the dominant processes that positively contributed to $PM_{2.5}$ evolution, while VTRA and DDEP were responsible for surface $PM_{2.5}$ removal during the three periods considered in the study. Also, Fan et al. (2015) reported EMIS and VTRA as the two major processes that influenced $PM_{2.5}$ at the surface layer in the Pearl River Delta (PRD) region of China. Furthermore, Liu et al. (2010) and Xing et al. (2011) had earlier reported EMIS and AERO as the major $PM_{2.5}$ sources in both surface layer and the PBL in Beijing, while Xing et al. (2011) found VTRA as the major $PM_{2.5}$ sink in the surface layer. The $PM_{2.5}$ removal due to HTRA and DDEP in both cases were relatively the same in both Beijing and Tianjin. Considering Shijiazhuang and Baoding, similar trends were obtained regarding the contributions of individual processes to $PM_{2.5}$ formation.

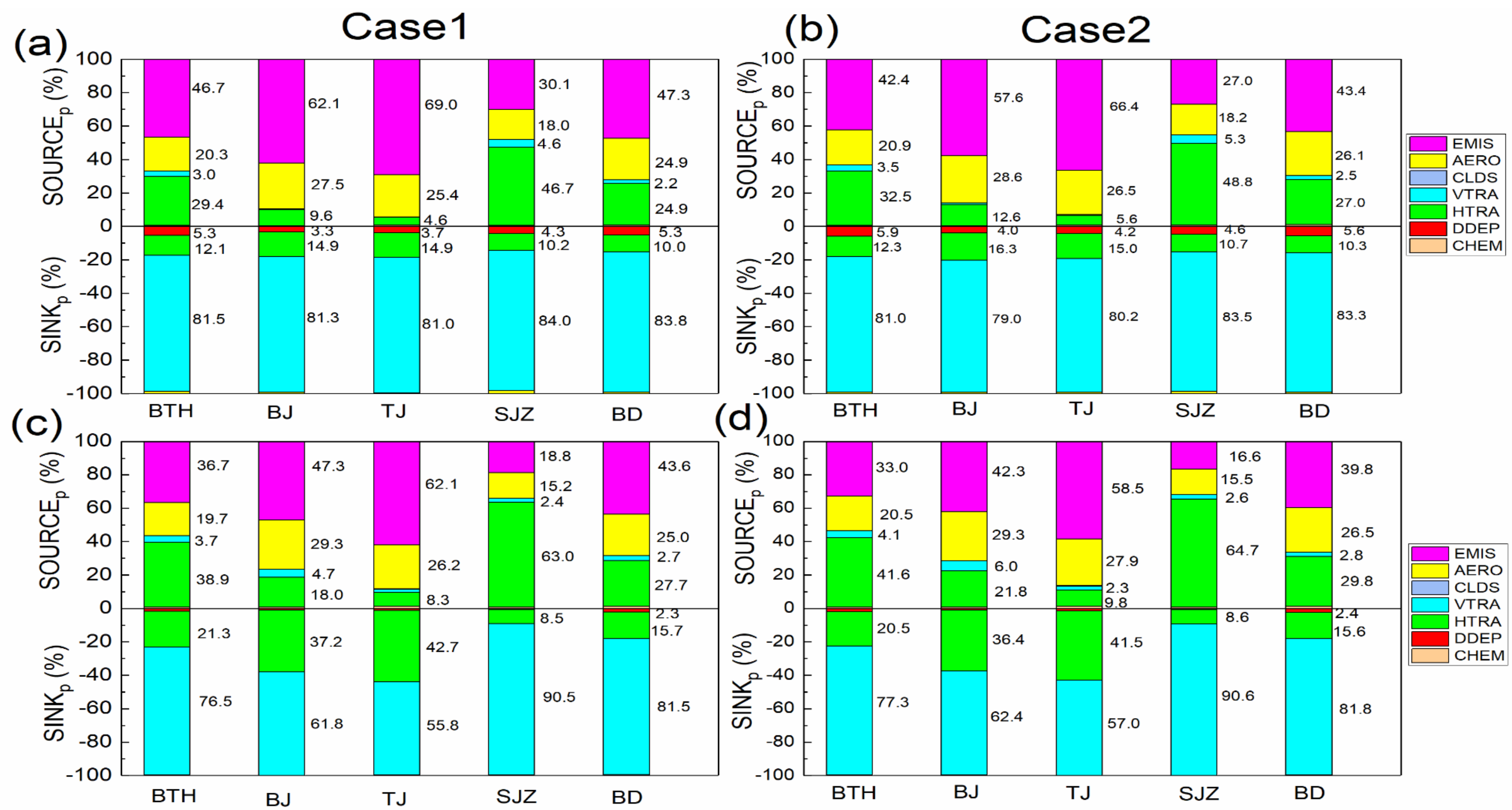

Fig. 2. Positive and negative contribution ratios of the individual processes to $PM_{2.5}$ concentrations (a,b) at the surface layer and (c,d) in the planetary boundary layer in Cases 1 and 2 during the lockdown period. EMIS, AERO, CLDS, VTRA, HTRA, DDEP, and CHEM represent the contributions of the emissions, aerosol, clouds, vertical transport, horizontal transport, dry deposition, and gas-phase chemistry, respectively to $PM_{2.5}$ formation.

The EMIS, AERO, and HTRA processes dominated the positive contributions to the net surface $PM_{2.5}$ in the two cities (Fig. 1), accounting for a total of 94.0 and 96.5% in Shijiazhuang and Baoding, respectively in Case 2 (Fig. 2b), while similar contributions were obtained in Case 1 (Fig. 2a). In addition to EMIS and AERO processes, the horizontal import of $PM_{2.5}$ to the surface layer via HTRA contributed to the elevated $PM_{2.5}$ concentrations in both Shijiazhuang and Baoding relative to Beijing and Tianjin. VTRA dominated the removal of $PM_{2.5}$ from the surface layer to upper layers in both cities, with higher rates in Case 1 relative to Case 2. DDEP process also had negative effects on $PM_{2.5}$ formation in the two cities, with very low contributions, especially in Shijiazhuang. The photochemistry (CHEM) process had positive net impacts on $PM_{2.5}$ evolution for the two cases across the BTH region and the four representative cities, however, the contributions were extremely low and negligible (Fan et al., 2015). This is contrary to what was reported in Kannur (Ye et al., 2022), as CHEM had negative effects on $PM_{2.5}$ in the city. Due to the negligible contributions of cloud (CLDS) processes to $PM_{2.5}$, it was not discussed in this study. It should be noted that the $PM_{2.5}$ concentrations in BTH region and the four cities in Case 2 were relatively low compared to Case 1. This could be attributed to low $PM_{2.5}$ formation from EMIS in Case 2. However, there was no substantive decrease in $PM_{2.5}$ concentrations in Case 2 despite reductions in anthropogenic emissions. This could be explained by the reduced $PM_{2.5}$ export from the surface layer to the upper layers due to low VTRA rates in Case 2 (compared to Case 1), leading to the accumulation of $PM_{2.5}$ in the surface layer, which subsequently led to high $PM_{2.5}$ pollution during the lockdown period.

3.4. IPR analysis of $PM_{2.5}$ formation in the PBL

Fig. S2 shows the mean hourly change rates attributed to individual atmospheric processes to $PM_{2.5}$ production and the concentrations of $PM_{2.5}$ in the PBL during the lockdown. The contributions of the various processes to $PM_{2.5}$ formation within the PBL in BTH and the four cities followed the similar trends as found in the surface layer. However, the contributions of the individual processes to $PM_{2.5}$ were smaller in the PBL compared to the surface layer, as $PM_{2.5}$ concentrations decrease as vertical layers increase (Fan et al., 2015). Generally, the contributions of EMIS and VTRA to the net $PM_{2.5}$ (Case 2) were low in the PBL compared to the surface layer. For instance, relative to what was obtained to the surface layer, the rates due to EMIS and VTRA in the PBL decreased by half in BTH region and all of the representative cities. Similar to the surface layer, the EMIS, HTRA, and AERO were the predominant contributors to the net $PM_{2.5}$ in the whole BTH region and Baoding, while only EMIS and AERO processes contributed substantially to the net $PM_{2.5}$ in Beijing and Tianjin. In Shijiazhuang, however, HTRA was the dominant contributor to $PM_{2.5}$ formation. Compared to other processes, the contributions of CHEM process were extremely low and negligible (Fan et al., 2015; Ye et al., 2022). In addition to VTRA as the major process responsible for the removal of $PM_{2.5}$ across the study areas, $PM_{2.5}$ removal in Beijing and Tianjin was also associated with HTRA. In all of the study areas, slight removal of $PM_{2.5}$ was also attributed to DDEP process. It could be noted that the VTRA and HTRA effects within the PBL were opposite to those to the surface layer. As illustrated in Fig. 2(d), the negative contributions (sinks) due to VTRA in the entire PBL substantially reduced in all of the study areas except Shijiazhuang (increased) when compared to the surface layer. Contrary to the surface layer, the sinks ($PM_{2.5}$ removal) due to HTRA within the PBL increased in all of the study areas except Shijiazhuang (decreased). It is worth noting that despite the decreases in EMIS rates by half (which might have adversely influenced $PM_{2.5}$ formation within the PBL) in comparison to the surface layer, the absolute difference in $PM_{2.5}$ concentrations between the surface layer and PBL was not significant, and ranged between 5.7-9.1 μg/m^3 across the study areas. This could be attributed to reduced $PM_{2.5}$ export due to low VTRA rates, leading to the accumulation of $PM_{2.5}$ within the PBL, and subsequently resulted to high $PM_{2.5}$ concentrations. Overall, in the PBL, EMIS and VTRA served as the two dominant processes that impacted $PM_{2.5}$ in BTH, Beijing, Tianjin, and Baoding, while VTRA and HTRA were the two major processes that influenced $PM_{2.5}$ formation in Shijiazhuang.

3.5. Vertical profiles of the atmospheric processes contributing to $PM_{2.5}$

The mean hourly $PM_{2.5}$ change rates attributed to individual atmospheric processes for the first ten layers (layers 1-10), as well as the vertical profiles of $PM_{2.5}$ evolution for Case 2 during the lockdown period are illustrated in Fig. 3, while that of Case 1 are shown in Fig. S3. As earlier stated in section 3.4, the characteristics of $PM_{2.5}$ concentrations at upper layers (layer 4 and above) were different from near-surface layers, hence, the contributions of emissions sources at upper layers were negligible (Fan et al., 2015). Across the study areas, the contributions from EMIS sources were only found within layers 1-3 (Fig. 3a-e) (Fan et al., 2015; Ye et al., 2022), and this was associated with the height of the emissions sources (Fan et al., 2015; Ye et al., 2022). The highest and lowest contributions of EMIS were found in Tianjin and Shijiazhuang, respectively, and the contribution decreased as the vertical layer increased. Within the first three layers, AERO process was another major source of $PM_{2.5}$ in all of the study areas, and the formation rate of $PM_{2.5}$

through the AERO process decreased as the vertical layer increased. Furthermore, VTRA contributed negatively and served as the predominant sink for removing the near-surface $PM_{2.5}$ at the lower layers in Beijing (layers 1-3), Shijiazhuang (layers 1-4), Tianjin and Baoding (layers 1-2), while it slightly contributed positively (acted as source) at the upper layers. This is consistent with the results of Fan et al. (2015), in which VTRA was reported as a sink in the near-surface layers and a source in the upper layers (layer 4 and above). In Beijing (Fig. 3b) and Tianjin (Fig. 3c), HTRA served as another sink for $PM_{2.5}$ across the vertical layers, and the rate initially increased between layers 1 and 2, but continuously decreased as the vertical layer increased. In Shijiazhuang (Fig. 3d), HTRA contributed positively at the lower layers (layers 1-3) and negatively at the upper layers. Considering Baoding (Fig. 3e), HTRA only acted as the source at the first layer, while it behaved as the sink from the second layer upward. It could be deduced that there were vertical and horizontal exports of $PM_{2.5}$ in Beijing and Tianjin at the surface layer, while Shijiazhuang, Baoding, and the whole BTH region witnessed vertical export and horizontal import of $PM_{2.5}$ in the surface layer. DDEP acted as another sink of $PM_{2.5}$, and only existed at the first layer across the study areas (Fan et al., 2015; Ye et al., 2022). DDEP contributions were only found in the first layer because dry deposition was treated as a bivariate variable by the CMAQ model, and integrated it over the whole atmospheric column (Fan et al., 2015). As shown in Fig. 3(f-j), the highest $PM_{2.5}$ concentration was found in the surface layer, and decreased with increases in vertical layer height (Fan et al., 2015). This result could be attributed to the contributions of EMIS and AERO processes, as well as the decreasing trends of the two processes as the vertical layer increased.

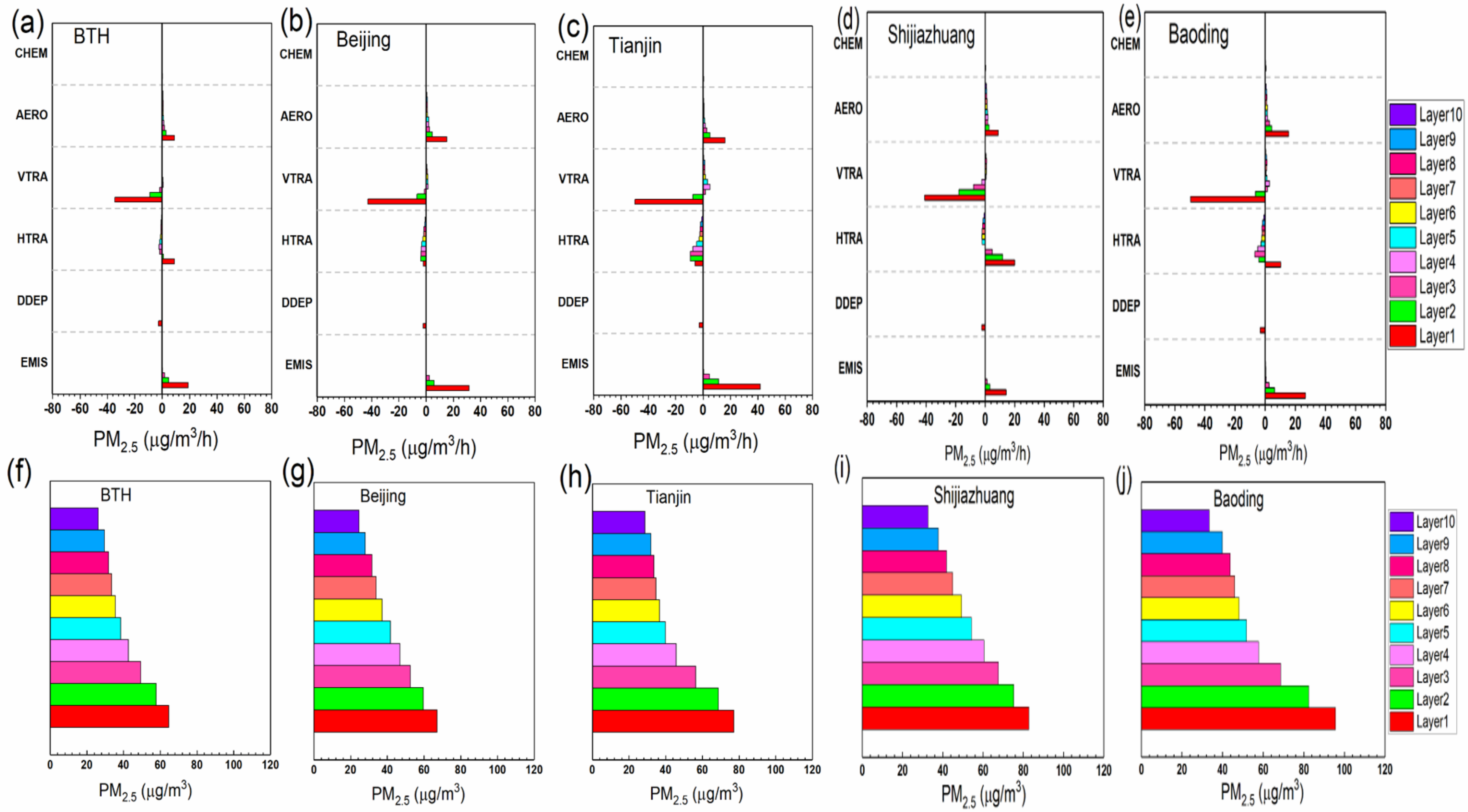

Fig. 3. Hourly $PM_{2.5}$ change rates due to individual atmospheric processes for layers 1-10 (a-e) and evolution of hourly $PM_{2.5}$ vertical profiles (f-j) in Case 2 during the lockdown period. Abbreviations used in this figure are the same as in Fig. 1.

3.6 IPR analysis of $PM_{2.5}$ pollution episodes during lockdown

During the lockdown period, the predicted $PM_{2.5}$ concentrations (in Case 2) (Fig.4; Tables S5-S6) indicated that persistent $PM_{2.5}$ pollution episodes could not be avoided in the BTH region despite reductions in anthropogenic emissions (Sulaymon et al., 2021a). Fig. S6 illustrates the spatial distributions of $PM_{2.5}$ in the BTH region during the lockdown for the two cases. Fig. S6(b) shows that the $PM_{2.5}$ concentrations during the lockdown were higher ($PM_{2.5} \geq 75$ μg/m^3, level II of Chinese air quality standard) in Tianjin and southern Hebei Province, while the northern Hebei was characterized with low concentrations ($PM_{2.5} \leq 50$ μg/m^3). In the prefectural-level cities of BTH region, three severe $PM_{2.5}$ pollution episodes (EPs) (Fig. 4) occurred during the lockdown (Case 2). They are represented as EP1 (January 24-31, 2020), EP2 (February 7-13), and EP3 (February 19-21). It should be noted that EP1 and EP2 coincided with the 2020 Spring (January 25) and Lantern (February 8) festivals, respectively. The statistics for all the EPs in each city are enumerated in Tables S5-S6. For the purpose of process analysis of $PM_{2.5}$ during the EPs, Beijing, Tianjin, Shijiazhuang, and Baoding were selected as the representative cities. As illustrated in Fig. 5, Beijing and Tianjin had the highest $PM_{2.5}$ concentrations during EP2, while Shijiazhuang and Baoding recorded their highest $PM_{2.5}$ concentrations during EP1. Also, during EP2 and EP3, Baoding experienced severe pollution with elevated $PM_{2.5}$ concentrations. This indicates that the region suffered severe pollution episodes during the lockdown. Dai et al. (2021) and Sulaymon et al. (2021a) had previously reported severe haze episodes in the BTH region during the lockdown. Therefore, it becomes pertinent to elucidate the major atmospheric processes responsible for the formation of the EPs.

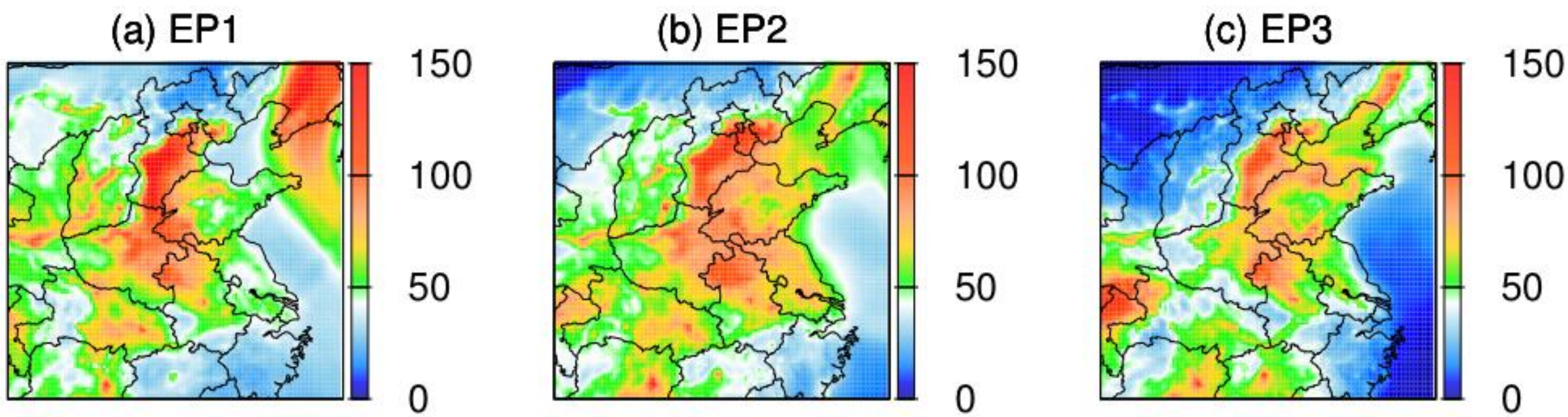

Fig. 4. Spatial distributions of predicted $PM_{2.5}$ (Case 2) during (a) EP1, (b) EP2, and (c) EP3 in the BTH region. Units are μg/m^3.

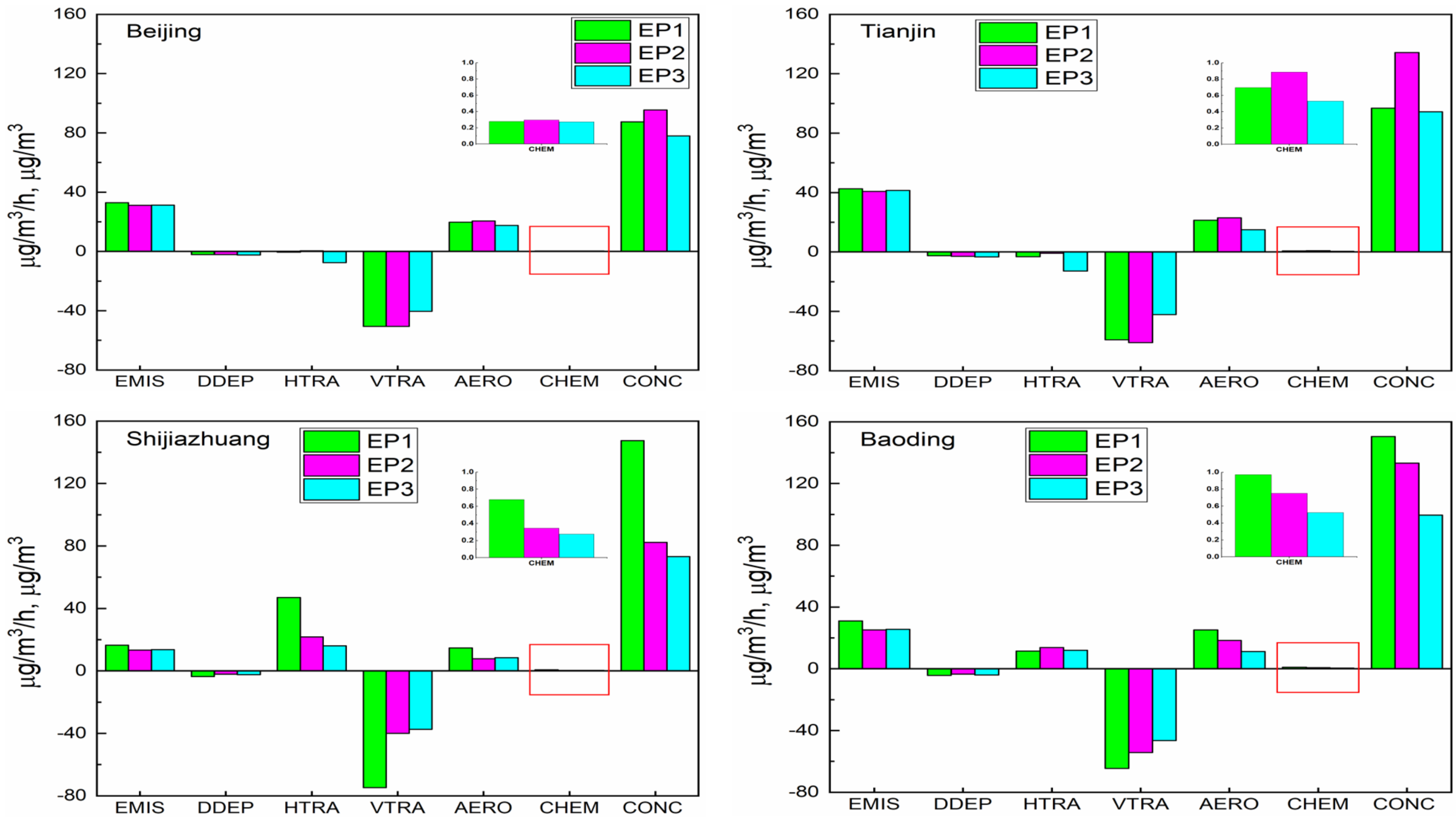

Fig. 5. Contributions of the individual processes to the concentrations of $PM_{2.5}$ (Case 2) at the surface layer during the three pollution episodes in the four representative cities. Abbreviations used in this figure are the same as in Fig. 1.

The contributions of different atmospheric processes to $PM_{2.5}$ formation (in Case 2) during the three EPs in the four representative cities were analyzed. Table S7 shows the average planetary boundary layer height (PBLH) and wind speed for the four cities during the three EPs. The PBLH during the third pollution episode (EP3; PBLH>400 m) was higher than the PBLH during the first two pollution episodes (EP1 and EP2; PBLH<370 m) across the study areas. A thinner boundary layer is more conducive for the accumulation of locally-emitted particles, leading to increased $PM_{2.5}$ concentrations and results in haze events (Fan et al., 2015). As illustrated in Fig. 5, the three pollution episodes in Beijing and Tianjin were principally caused by local emissions (EMIS), while the pollution events in Shijiazhuang and Baoding could be attributed to both local emissions (EMIS) and regional transport (HTRA).

Fig. 5 shows that emissions sources and aerosols were the major positive contributors to $PM_{2.5}$ pollution in Beijing, Tianjin, and Baoding, while horizontal transport was the most significant positive contributor to pollution level in Shijiazhuang, followed by emissions and aerosols. In Baoding, however, HTRA also contributed positively towards $PM_{2.5}$ concentrations throughout the three episodes. There were no significant differences between emissions sources among the three episodes in all of the study areas, and the average total emissions ranged between 13.3-42.6 $\mu g/m^3/h$ across the EPs in the cities. During the three episodes across the four cities, $PM_{2.5}$ was released into the atmosphere through EMIS and AERO processes, and fell back to the surface layer via DDEP process (Fan et al., 2015), with very low rates of dry deposition (ranged between -2.1 $\mu g/m^3/h$ and -4.3 $\mu g/m^3/h$). Also, $PM_{2.5}$ was transported and diffused through VTRA and HTRA processes. In Beijing and Tianjin, there were negligible differences between the contributions from VTRA during the first two episodes, and the total rates were approximately -51 μg/m^3/h and -60 μg/m^3/h in Beijing and Tianjin, respectively. During EP3 in the two cities, the contributions by VTRA (-40 μg/m^3/h in Beijing; and -42 μg/m^3/h in Tianjin) were low relative to the first two episodes. The VTRA contributions in Shijiazhuang (-75 μg/m^3/h) and Baoding (-65 μg/m^3/h) during EP1 were greater than those contributed in Beijing and Tianjin during the same period, and this was due to lower PBLH values (Table S7) in Shijiazhuang and Baoding relative to Beijing and Tianjin. The difference in the VTRA rates between the first two episodes and the third episode in Beijing and Tianjin could be explained by the accumulation of particulates on near-surface layers due to the nature of boundary layer (thinner) (Fan et al., 2015) being exhibited during the first two pollution episodes. Therefore, VTRA had a greater clearing impact for $PM_{2.5}$ during the first two episodes in the two cities. Contrarily, during the third episode in the two cities, a more uniform vertical mixing of $PM_{2.5}$ was achieved, and this was due to the thicker PBLHs during EP3 (Table S7). Hence, the clearing effect of VTRA during EP3 was low compared to EP1 and EP2. In addition, due to higher wind speed during EP3 (Table S7), the negative contributions due to HTRA were higher in Beijing (-8 μg/m^3/h) and Tianjin (-13 μg/m^3/h) during EP3 compared to EP1 and EP2, and this subsequently reduced the contributions from VTRA during EP3. In Shijiazhuang, VTRA also exhibited a very greater clearing effect during EP1 than EP2 and EP3, and similar scenario also occurred in Baoding. In Shijiazhuang, HTRA was the dominant positive contributor to $PM_{2.5}$ throughout the episodes, with the highest contribution rate during EP1. In Baoding, however, there was negligible difference between the contributions from HTRA to $PM_{2.5}$ pollution during the three episodes. Due to availability of several emissions sources in

Beijing and Tianjin, which result to a large quantity of local emissions, $PM_{2.5}$ concentrations were generally higher in the two cities. Hence, the effects of both VTRA and HTRA on pollution levels were negative during the three pollution episodes, and both mainly provided dilution and clearing effects in the two cities (Fan et al., 2015). On the other hand, in both Shijiazhuang and Baoding, horizontal transport contributed positively and significantly increased $PM_{2.5}$ concentrations during the three episodes. It is also worthy to mention that $PM_{2.5}$ concentrations during the three episodes in the four cities were greatly and positively influenced by the planetary boundary layer height, as the episode with the lowest PBLH had the highest $PM_{2.5}$ concentration in a city. The results of the present study are consistent with those reported by Fan et al. (2015) during three pollution episodes over the PRD region. Fan et al. (2015) had reported surface emissions, aerosol processes, and horizontal transport as the major contributors to air pollution episodes over the PRD. In the PBL (Fig. S7), EMIS and AERO were also the dominant contributors to $PM_{2.5}$ concentrations in Beijing and Tianjin, HTRA was the most important source in Shijiazhuang, and EMIS, AERO, and HTRA actively contributed to $PM_{2.5}$ formation in Baoding during the EPs. VTRA was the major removal pathway. However, the contribution and removal rates were low in the PBL relative to the surface layer.

To better understand the roles of the atmospheric processes towards the pollution episodes, $PM_{2.5}$ formation and removal within the PBL (layers 1-10) were analyzed in Tianjin (Fig. 6), while those of other three cities are illustrated in Figs S8-S10. Considering the three EPs in Tianjin, the positive contributions of EMIS and AERO processes to the hourly $PM_{2.5}$ significantly occurred within layers 1-3 (Fig. 6a-c), while they both contributed less at upper layers. Also, there were vertical imports of $PM_{2.5}$ (although very low) at upper layers (layers 3-10 for EP1 and EP2; and layers 3-6 for EP3). Conversely, VTRA (layers 1-2) and HTRA (layers 1-10) served as the predominant sinks and $PM_{2.5}$ removal pathways. DDEP process also acted as another sink for $PM_{2.5}$ during the EPs, and only existed at the first layer (Fan et al., 2015). The contributions by CHEM process were negligible across the vertical layers (Fan et al., 2015; Ye et al., 2022). As shown in Fig. 6(d-f), EP2 was characterized with the highest $PM_{2.5}$ concentrations, followed by EP1 and EP3. Furthermore, the $PM_{2.5}$ formation processes in the surface layer during the EPs were compared. Fig. 7 illustrates the percentage contributions of the atmospheric processes to $PM_{2.5}$ formation/removal during the EPs in the four cities. The total contributions of EMIS and AERO (EMIS+AERO) during the EPs ranged between 80-89% and 88-97% in Beijing (Fig. 7a) and Tianjin (Fig. 7b), respectively. In Shijiazhuang (Fig. 7c), the contributions due to HTRA during the episodes ranged between 44-61%, making it the major $PM_{2.5}$ source. As earlier revealed in Fig. 5, $PM_{2.5}$ formation during the episodes in Baoding (Fig. 7d) was attributed to the contributions of EMIS, AERO, and HTRA, with total contributions of 93-98% during the EPs. In the four cities, $PM_{2.5}$ removal was dominantly influenced by VTRA during the EPs.

Furthermore, the diel variations of the contributions of various atmospheric processes to the formation of $PM_{2.5}$ as well as the hourly variations of $PM_{2.5}$ concentrations at the surface layer during the three episodes are illustrated in Fig. 8. In Beijing, EMIS and AERO processes were the major $PM_{2.5}$ sources, and showed two peaks (07:00 LT and 20:00 LT) during the three episodes.

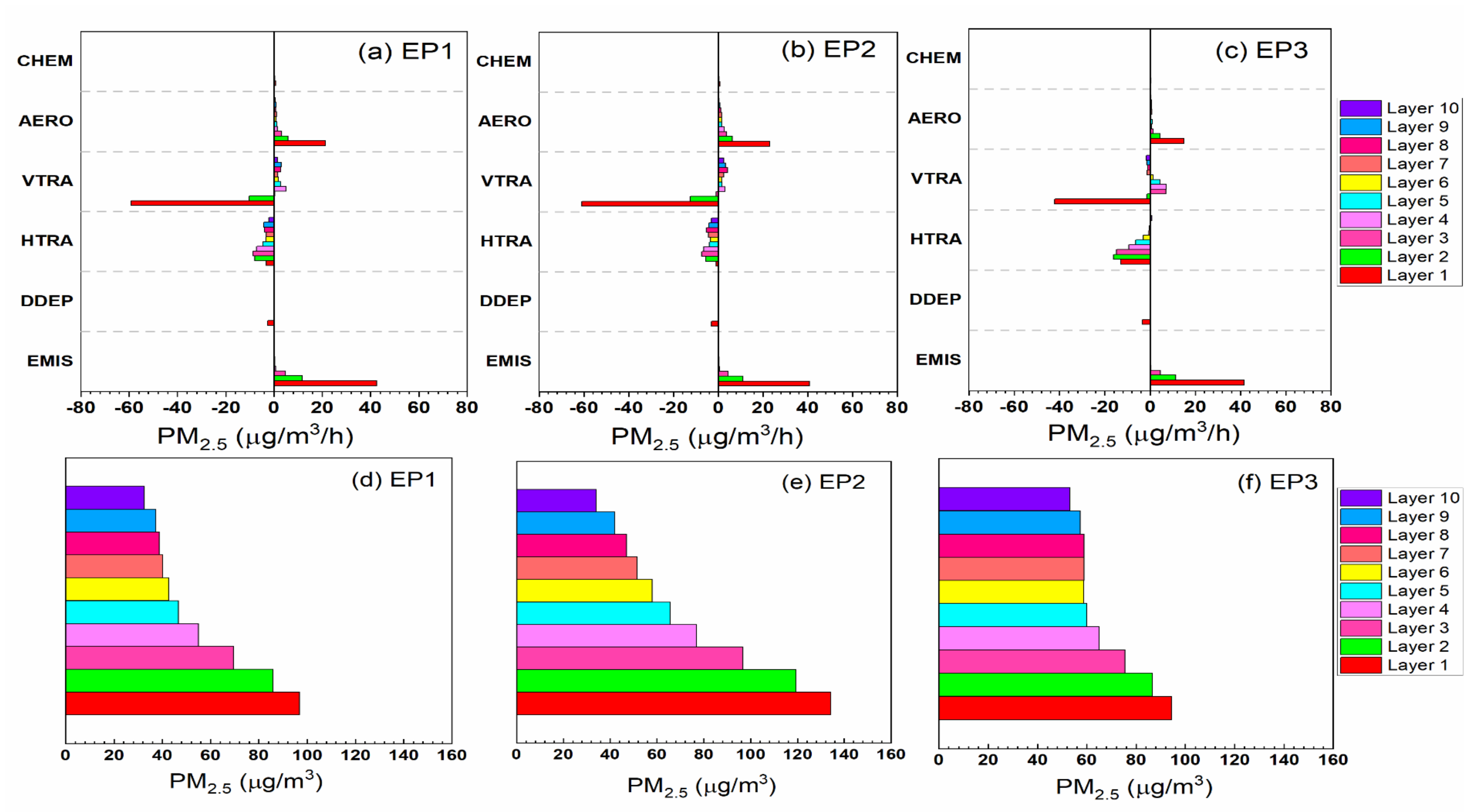

Fig. 6. Hourly $PM_{2.5}$ change rates (Case 2) due to individual atmospheric processes for layers 1-10 (a-c) and evolution of hourly $PM_{2.5}$ vertical profiles (d-f) during the three pollution episodes in Tianjin. Abbreviations used in this figure are the same as in Fig. 1.

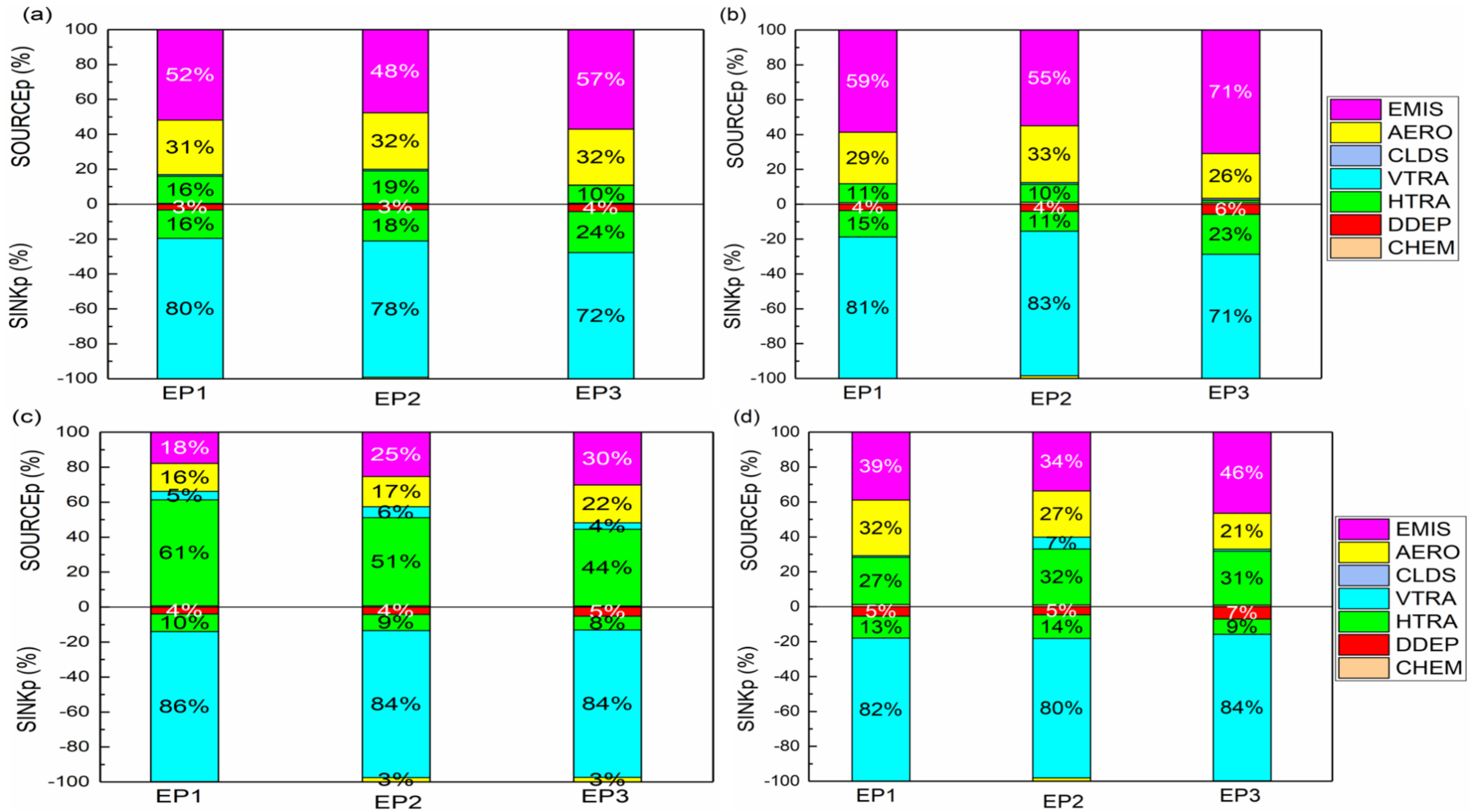

Fig. 7. Positive and negative contribution ratios of the individual processes to $PM_{2.5}$ concentrations (Case 2) at the surface layer in (a) Beijing, (b) Tianjin, (c) Shijiazhuang, and (d) Baoding during the three pollution episodes. Abbreviations used in this figure are the same as in Fig. 2.

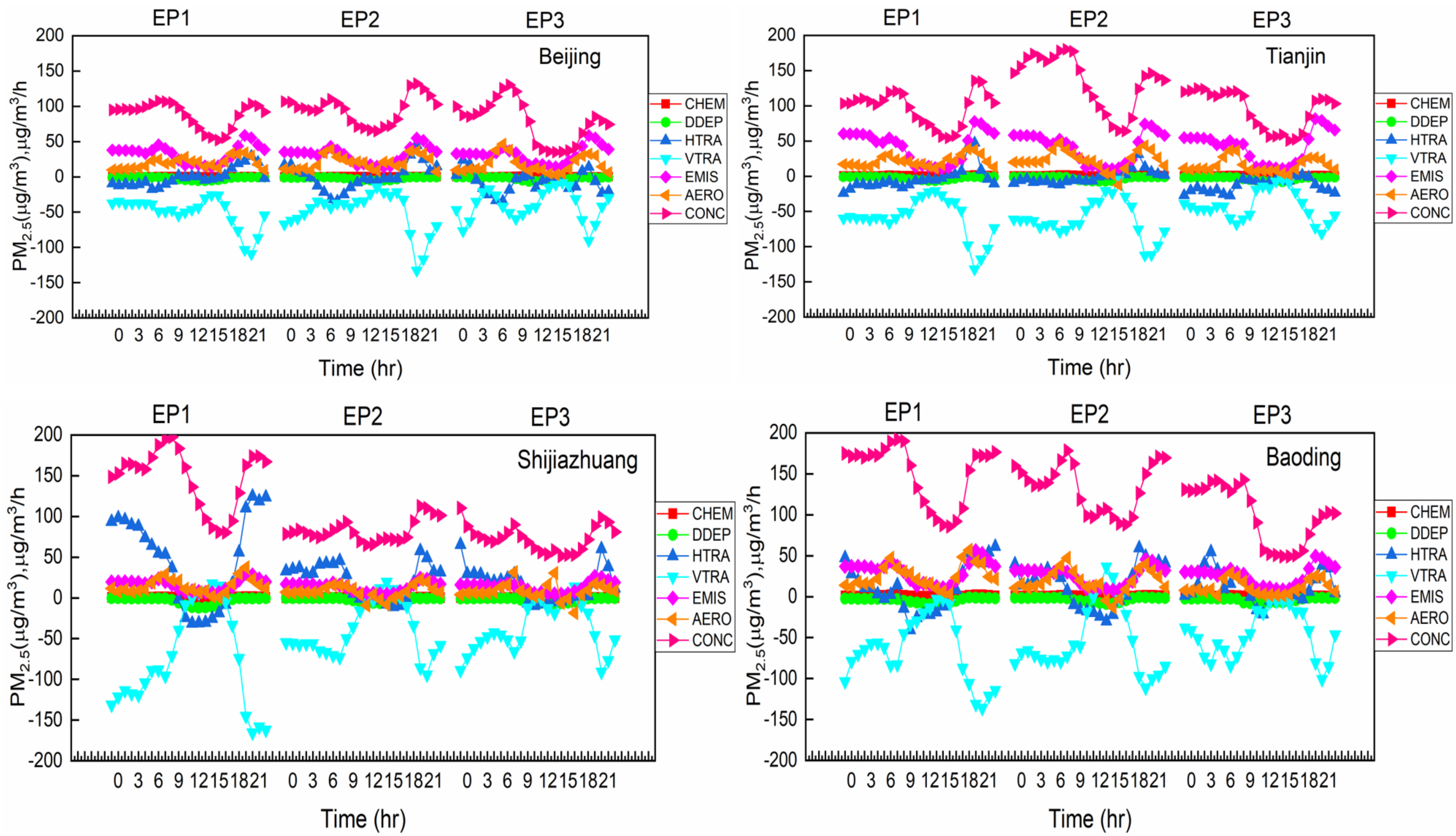

Fig. 8. Diel variations of contributions of individual processes to $PM_{2.5}$ formation (Case 2) at the surface layer during the three pollution episodes in the four representative cities. Abbreviations used in this figure are the same as in Fig. 1.

The highest rates of EMIS during the EPs ranged between 54.8-58.6 μg/m^3/h, all occurred at 20:00 LT. The VTRA dominated the $PM_{2.5}$ removal, with the highest removal rates of -109.3 μg/m^3/h (at 21:00 LT), -132.6 μg/m^3/h (at 20:00 LT), and -90.7 μg/m^3/h (at 20:00 LT) during EP1, EP2, and EP3, respectively. In addition, HTRA was another major $PM_{2.5}$ removal pathway during the EPs. However, HTRA later acted as another $PM_{2.5}$ source during EP1 (17:00-22:00 LT; with maximum rate of 29.6 μg/m^3/h at 21:00 LT), EP2 (00:00-03:00 and 18:00-23:00 LT; with maximum rate of 44.7 μg/m^3/h at 20:00 LT), and EP3 (00:00-02:00 and 19:00-20:00 LT; with highest rate of 24.0 μg/m^3/h at 01:00 LT), leading to the horizontal import of $PM_{2.5}$ during the periods. Considering Tianjin, EMIS process was the dominant $PM_{2.5}$ source and exhibited two distinct peaks (00:00 LT and 20:00 LT) during the three episodes. The highest contributions of EMIS during EP1, EP2, and EP3 were 77.7 μg/m^3/h, 74.1 μg/m^3/h, and 81.7 μg/m^3/h, respectively, all occurred at 20:00 LT. AERO process was another $PM_{2.5}$ source with two peaks during EP1 (07:00 LT and 19:00 LT), EP2 and EP3 (07:00 LT and 20:00 LT). The negative contributions of VTRA made it the dominant $PM_{2.5}$ sink throughout the 24hrs period, with the maximum removal rates of -132.1 μg/m^3/h (at 20:00 LT), -112.5 μg/m^3/h (at 20:00 LT), and -81.3 μg/m^3/h (at 21:00 LT) during EP1, EP2, and EP3, respectively. Besides VTRA, HTRA served as the second major $PM_{2.5}$ sink during the three EPs. However, HTRA later became another $PM_{2.5}$ source during EP1 (16:00-21:00 LT; with maximum rate of 47.5 μg/m^3/h), EP2 (14:00-23:00; with maximum rate of 31.1 μg/m^3/h), and EP3 (17:00-18:00 LT; with very low rates). In Shijiazhuang, HTRA was the major $PM_{2.5}$ contributor, and showed two peaks during EP1 (98.3 μg/m^3/h at 01:00 LT and 124.8 μg/m^3/h at 21:00 LT), EP2 (45.8 μg/m^3/h at 08:00 LT and 57.8 μg/m^3/h at 20:00 LT), and EP3 (65.2 μg/m^3/h at 00:00 LT and 60.3 μg/m^3/h at 21:00 LT). The VTRA was the dominant $PM_{2.5}$ removal pathway, with the highest rates of -165.6 μg/m^3/h, -94.5 μg/m^3/h, and -91.0 μg/m^3/h during EP1, EP2, and EP3, respectively, all at 21:00 LT. However, VTRA later became positive and served as another $PM_{2.5}$ source during EP1 (13:00-16:00 LT; with maximum rate of 17.4 μg/m^3/h at 15:00 LT), EP2 (14:00-17:00 with maximum rate of 19.4 μg/m^3/h at 15:00 LT), and EP3 (15:00-17:00 with highest rate of 13.6 μg/m^3/h at 17:00 LT), resulting to the vertical import of $PM_{2.5}$ during the periods. In Baoding, EMIS, AERO, and HTRA were the major $PM_{2.5}$ formation pathways during nighttime, while EMIS and AERO were the dominant sources during daytime. Being the major $PM_{2.5}$ removal pathway, VTRA had the highest rates of -136.3 μg/m^3/h (21:00 LT), -111.4 μg/m^3/h (20:00 LT), and -101.1 μg/m^3/h (21:00 LT) during EP1, EP2, and EP3, respectively. During EP2, VTRA shortly behaved as another $PM_{2.5}$ source (13:00-15:00 LT, with highest rate of 36.5 μg/m^3/h. With very low rates during the episodes, DDEP and CHEM processes served as $PM_{2.5}$ sink and source, respectively across the four cities. The $PM_{2.5}$ concentrations peaked in Beijing (EP1: 107.8 μg/m^3 at 07:00 LT; EP2: 132.1 μg/m^3 at 20:00 LT; EP3: 130.3 μg/m^3 at 08:00 LT), Tianjin (EP1: 135.7 μg/m^3 at 20:00 LT; EP2: 180.1 μg/m^3 at 08:00 LT; EP3: 124.6 μg/m^3 at 02:00 LT), Shijiazhuang (EP1: 197.6 μg/m^3 at 09:00 LT; EP2: 112.6 μg/m^3 at 20:00 LT; EP3: 110.3 μg/m^3 at 00:00 LT), and Baoding (EP1: 192.0 μg/m^3 at 08:00 LT; EP2: 178.2 μg/m^3 at 08:00 LT; EP3: 142.8 μg/m^3 at 09:00 LT).

4. Conclusions

This study employed the PA tool in the CMAQ model to identify and quantify the contributions of individual atmospheric processes and meteorology to the three $PM_{2.5}$ pollution episodes that occurred during the COVID-19 lockdown in the BTH region even with the required reductions in human activities. Due to emission reductions, the total $PM_{2.5}$ concentrations across the BTH decreased by 6.2-11.0%. However, the region still experienced three $PM_{2.5}$ pollution episodes during the lockdown. The IPR results showed that the EMIS and AERO processes were the dominant positive contributors to the net surface $PM_{2.5}$ in Beijing and Tianjin, while the EMIS, HTRA, and AERO pathways dominated the net surface $PM_{2.5}$ formation in Shijiazhuang and Baoding. In Case 2, the decrease in surface $PM_{2.5}$ concentrations across the BTH was primarily attributed to the reduced EMIS and AERO processes, which shows the reduction in the primary source of $PM_{2.5}$ as well as decrease in the formation of secondary aerosol through gas-to-particle conversion. Both vertical and horizontal transport had significant impacts on the changes in surface $PM_{2.5}$. Elevated $PM_{2.5}$ concentrations (in Case 2) in the BTH region during the lockdown could be attributed to a low vertical transport rate of $PM_{2.5}$ from the surface layer to the upper layers. Furthermore, during the three pollution episodes, EMIS and AERO processes were the dominant sources of $PM_{2.5}$ formation in Beijing, Tianjin, and Baoding, while HTRA was the major source in Shijiazhuang. In all of the four cities, vertical transport served as the major $PM_{2.5}$ sink throughout the episodes, with differences in vertical rates between the episodes in each city. The pollution levels in the four cities were greatly and positively influenced by the PBLH, as the episode with the lowest PBLH had the highest $PM_{2.5}$ concentration in a city. This study reveals the various atmospheric processes and meteorological factors governing the $PM_{2.5}$ formation during the severe pollution episodes in the BTH region, as well as the changes in the individual atmospheric processes and $PM_{2.5}$ concentrations due to the lockdown measures, and shows that the existing emissions control strategies could not prevent pollution episodes in the region, especially during the winter period. Since it is not possible to control the aerosol and transport processes, only further changes in emissions will reduce the severity of the episodes. Thus, better forecasting of the conditions that would foment such episodes combined with more effective emissions control strategies are urgently required to be able to mitigate such future severe pollution episodes in the BTH region.

Acknowledgements

This work was supported by the National Natural Science Foundation of China (42007187).

Conflict of Interest

The authors declare that they have no conflict of interest.

Open Research

The simulated and the observation data ($PM_{2.5}$ and meteorological variables) used in this study for model evaluation and postprocessing (Figures and Tables) can be found in Sulaymon et al. (2023).

References

Ambient air pollution (2021). Retrieved 28 October 2021, from https://www.who.int/airpollution/ambient/health-impacts/en

Bashir, M. F., MA, B. J., Bilal, Komal, B., Bashir, M. A., Farooq, T. H., Iqbal, N., & Bashir, M. (2020). Correlation between environmental pollution indicators and COVID-19 pandemic: A brief study in Californian context. Environmental Research, 187. https://doi.org/10.1016/j.envres.2020.109652

Bhati, S., & Mohan, M. (2018). WRF-urban canopy model evaluation for the assessment of heat island and thermal comfort over an urban airshed in India under varying land use/land cover conditions. Geoscience Letters, 5(1). https://doi.org/10.1186/s40562-018-0126-7

Boylan, J. W., & Russel, A. G. (2006). PM and light extinction model performance metrics, goals, and criteria for three-dimensional air quality models. Atmospheric Environment, 40, 4946-4959. https://doi.org/10.1016/j.atmosenv.2005.09.087

Chang, X., Wang, S., Zhao, B., Cai, S., & Hao, J. (2018). Assessment of inter-city transport of particulate matter in the Beijing-Tianjin-Hebei region. Atmospheric Chemistry and Physics, 18(7), 4843-4858. https://doi.org/10.5194/acp-18-4843-2018

Chang, X., Wang, S., Zhao, B., Xing, J., Liu, X., Wei, L., Song, Y., Wu, W., Cai, S., Zheng, H., Ding, D., & Zheng, M. (2019). Contributions of inter-city and regional transport to $PM_{2.5}$ concentrations in the Beijing-Tianjin-Hebei region and its implications on regional joint air pollution control. Science of the Total Environment, 660, 1191-1200. https://doi.org/10.1016/j.scitotenv.2018.12.474

Chauhan A., & Singh, R.P. (2020). Decline in $PM_{2.5}$ concentrations over major cities around the world associated with COVID-19. Environ. Res. 187, 109634. 10.1016/j.envres.2020.109634

Chauhan, A.K., & Singh, R.P. (2021). Effect of lockdown on HCHO and trace gases over India during March 2020. AAQR, Volume 21, Issue 4, Article Number 200445. 10.4209/aaqr.2020.07.0445.

Chen, D., Xia, L., Guo, X., Lang, J., Zhou, Y., Wei, L., & Fu, X. (2021). Impact of inter-annual meteorological variation from 2001 to 2015 on the contribution of regional transport to PM2.5 in Beijing, China. Atmospheric Environment, 260. https://doi.org/10.1016/j.atmosenv.2021.118545

Chen, L., Shi, M., Gao, S., Li, S., Mao, J., Zhang, H., Sun, Y., Bai, Z., & Wang, Z. (2017). Assessment of population exposure to $PM_{2.5}$ for mortality in China and its public health benefit based on BenMAP. Environmental Pollution, 221, 311-317. https://doi.org/10.1016/j.envpol.2016.11.080

Croft, D. P., Zhang, W., Lin, S., Thurston, S. W., Hopke, P. K., Masiol, M., Squizzato, S., van Wijngaarden, E., Utell, M. J., & Rich, D. Q. (2019). The association between respiratory infection and air pollution in the setting of air quality policy and economic change. Annals of the American Thoracic Society, 16(3), 321-330. https://doi.org/10.1513/AnnalsATS.201810-691OC

Cui, Y., Ji, D., Maenhaut, W., Gao, W., Zhang, R., & Wang, Y. (2020). Levels and sources of hourly PM2.5-related elements during the control period of the COVID-19 pandemic at a rural site between Beijing and Tianjin. Science of the Total Environment, 744. https://doi.org/10.1016/j.scitotenv.2020.140840

Dai, Q., Ding, J., Hou, L., Li, L., Cai, Z., Liu, B., Song, C., Bi, X., Wu, J., Zhang, Y., Feng, Y., & Hopke, P. K. (2021). Haze episodes before and during the COVID-19 shutdown in Tianjin, China: Contribution of fireworks and residential burning. Environmental Pollution, 286. https://doi.org/10.1016/j.envpol.2021.117252

Dai, Q., Ding, J., Song, C., Liu, B., Bi, X., Wu, J., Zhang, Y., Feng, Y., & Hopke, P. K. (2021). Changes in source contributions to particle number concentrations after the COVID-19 outbreak: Insights from a dispersion normalized PMF. Science of the Total Environment, 759. https://doi.org/10.1016/j.scitotenv.2020.143548

Dai, Q., Liu, B., Bi, X., Wu, J., Liang, D., Zhang, Y., Feng, Y., & Hopke, P. K. (2020). Dispersion normalized PMF provides insights into the significant changes in source contributions to $PM_{2.5}$ after the CoviD-19 outbreak. Environmental Science and Technology, 54(16), 9917-9927. https://doi.org/10.1021/acs.est.0c02776

Emery, C., Tai, E., & Yarwood, G. (2001). Enhanced Meteorological Modeling and Performance Evaluation for Two Texas Ozone Episodes, Prepared for the Texas Natural Resource Conservation Commission. Environ International Corporation, Novato, CA.

Fan, Q., Lan, J., Liu, Y., Wang, X., Chan, P., Hong, Y., Feng, Y., Liu, Y., Zeng, Y., & Liang, G. (2015). Process analysis of regional aerosol pollution during spring in the Pearl River Delta region, China. Atmos. Environ. 122, 829-838.

Fan, H., Zhao, C., & Yang, Y. (2020). A comprehensive analysis of the spatio-temporal variation of urban air pollution in China during 2014-2018. Atmospheric Environment, 220. https://doi.org/10.1016/j.atmosenv.2019.117066

Fu, X.,Wang, T., Gao, J., Wang, P., Liu, Y., Wang, S., Zhao, B., & Xue, L. (2020). Persistent heavy winter nitrate pollution by increased photochemical oxidants in Northern China. Environ. Sci. Technol., 54, 3881-3889.

Gao, C., Li, S., Liu, M., Zhang, F., Achal, V., Tu, Y., Zhang, S., & Cai, C. (2021). Impact of the COVID-19 pandemic on air pollution in Chinese megacities from the perspective of traffic volume and meteorological factors. Science of the Total Environment, 773. https://doi.org/10.1016/j.scitotenv.2021.145545

Hopke, P. K., Croft, D., Zhang, W., Lin, S., Masiol, M., Squizzato, S., Thurston, S. W., van Wijngaarden, E., Utell, M. J., & Rich, D. Q. (2019). Changes in the acute response of respiratory diseases to PM 2.5 in New York State from 2005 to 2016. Science of the Total Environment, 677, 328-339. https://doi.org/10.1016/j.scitotenv.2019.04.357

Hu, J., Chen, J., Ying, Q., & Zhang, H. (2016). One-year simulation of ozone and particulate matter in China using WRF/CMAQ modeling system. Atmospheric Chemistry and Physics, 16(16), 10333-10350. https://doi.org/10.5194/acp- 16-10333-2016

Hu, J., Wu, L., Zheng, B., Zhang, Q., He, K., Chang, Q., Li, X., Yang, F., Ying, Q., & Zhang, H. (2015). Source contributions and regional transport of primary particulate matter in China. Environmental Pollution, 207, 31-42. https://doi.org/10.1016/j.envpol.2015.08.037

Hua, J., Zhang, Y., de Foy, B., Shang, J., Schauer, J. J., Mei, X., Sulaymon, I. D., & Han, T. (2021). Quantitative estimation of meteorological impacts and the COVID-19 lockdown reductions on NO2 and PM2.5 over the Beijing area using Generalized Additive Models (GAM). Journal of Environmental Management, 291. https://doi.org/10.1016/j.jenvman.2021.112676

Huang, J.P., Fung, J.C.H., Lau, A.K.H., & Qin, Y. (2005). Numerical Simulation and Process Analysis of Typhoon-Related Ozone Episodes in Hong Kong, p. 110.

Jiang, Y., Xing, J., Wang, S., Chang, X., Liu, S., Shi, A., Liu, B., & Sahu, S. K. (2021). Understand the local and regional contributions on air pollution from the view of human health impacts. Frontiers of Environmental Science and Engineering, 15(5). https://doi.org/10.1007/s11783-020-1382-2

Kwok, R. H. F., Napelenok, S. L., & Baker, K. R. (2013). Implementation and evaluation of $PM_{2.5}$ source contribution analysis in a photochemical model. Atmospheric Environment, 80, 398-407. https://doi.org/10.1016/j.atmosenv.2013.08.017

Li, L., Chen, C.H., Huang, C., Huang, H.Y., Zhang, G.F., Wang, Y.J., Wang, H.L., Lou, S.R., Qiao, L.P., Zhou, M., Chen, M.H., Chen, Y.R., Streets, D.G., Fu, J.S., & Jang, C.J. (2012). Process analysis of regional ozone formation over the Yangtze River Delta, China using the Community Multi-scale Air Quality modeling system. Atmos. Chem. Phys. 12, 10971-10987.

Li, L., Li, Q., Huang, L., Wang, Q., Zhu, A., Xu, J., Liu, Z., Li, H., Shi, L., Li, R., Azari, M., Wang, Y., Zhang, X., Liu, Z., Zhu, Y., Zhang, K., Xue, S., Ooi, M. C. G., Zhang, D., & Chan, A. (2020). Air quality changes during the COVID-19 lockdown over the Yangtze River Delta Region: An insight into the impact of human activity pattern changes on air pollution variation. Science of the Total Environment, 732. https://doi.org/10.1016/j.scitotenv.2020.139282

Li, M., Song, Y., Huang, X., Li, J., Mao, Y., Zhu, T., Cai, X., & Liu, B. (2014). Improving mesoscale modeling using satellite-derived land surface parameters in the Pearl River Delta region, China. Journal of Geophysical Research, 119(11), 6325-6346. https://doi.org/10.1002/2014JD021871

Li, M., Zhang, Z., Yao, Q., Wang, T., Xie, M., Li, S., Zhuang, B., & Han, Y. (2021). Nonlinear responses of particulate nitrate to NOx emission controls in the megalopolises of China. Atmospheric Chemistry and Physics, 21(19), 15135-15152. https://doi.org/10.5194/acp-21-15135-2021

Li, X., Huang, L., Li, J., Shi, Z., Wang, Y., Zhang, H., Ying, Q., Yu, X., Liao, H., & Hu, J. (2019). Source contributions to poor atmospheric visibility in China. Resources, Conservation & Recycling, 143: 167-177.

Liu, J., Mauzerall, D. L., Chen, Q., Zhang, Q., Song, Y., Peng, W., Klimont, Z., Qiu, X. H., Zhang, S. Q., Hu, M., Lin, W. L., Smith, K. R., & Zhu, T. (2016) Air pollutant emissions from Chinese households: A major and underappreciated ambient pollution source. P. Natl. Acad. Sci. USA, 113, 7756-7761.

Liu, P., & Zhang, Y. (2011). Use of a process analysis tool for diagnostic study on fine particulate matter predictions in the U.S. Part II: analyses and sensitivity simulations. Atmos. Poll. Res. 2, 61-71.

Liu, T., Wang, X., Hu, J., Wang, Q., An, J., Gong, K., Sun, J., Li, L., Qin, M., Li, J., Tian, J., Huang, Y., Liao, H., Zhou, M., Hu, Q., Yan, R., Wang, H., & Huang, C. (2020). Driving Forces of Changes in Air Quality during the COVID-19 Lockdown Period in the Yangtze River Delta Region, China. Environmental Science and Technology Letters, 7(11), 779-786. https://doi.org/10.1021/acs.estlett.0c00511

Liu, X.H., Zhang, Y., Xing, J., Zhang, Q., Wang, K., Streets, D.G., Jang, C., Wang, W.X., & Hao, J.M. (2010). Understanding of regional air pollution over China using CMAQ. Part II: process analysis and sensitivity of ozone and particulate matter to precursor emissions. Atmos. Environ. 44, 3719-3727.

Ma, J., Shen, J., Wang, P., Zhu, S., Wang, Y., Wang, P., Wang, G., Chen, J., & Zhang, H. (2021). Modeled changes in source contributions of particulate matter during the COVID-19 pandemic in the Yangtze River Delta, China. Atmospheric Chemistry and Physics, 21(9), 7343-7355. https://doi.org/10.5194/acp-21-7343-2021

Mishra, R., Mishra, N.C., Singh, R., & Mishra, R. (2021). Improvement of atmospheric pollution in the capital cities of US during COVID-19, https://doi.org/10.1002/essoar.10505250.2

Muhammad, S., Long, X., & Salman, M. (2020). COVID-19 pandemic and environmental pollution: A blessing in disguise? Science of the Total Environment, 728. https://doi.org/10.1016/j.scitotenv.2020.138820

Orak, N. H., & Ozdemir, O. (2021). The impacts of COVID-19 lockdown on PM_{10} and SO_2 concentrations and association with human mobility across Turkey. Environmental Research, 197. https://doi.org/10.1016/j.envres.2021.111018.

Qiao, X., Tang, Y., Hu, J., Zhang, S., Li, J., Kota, S. H., Wu, L., Gao, H., Zhang, H., & Ying, Q. (2015). Modeling dry and wet deposition of sulfate, nitrate, and ammonium ions in Jiuzhaigou National Nature Reserve, China using a source-oriented CMAQ model: Part I. Base case model results. Science of the Total Environment, 532, 831-839. https://doi.org/10.1016/j.scitotenv.2015.05.108

Querol, X., Massagué, J., Alastuey, A., Moreno, T., Gangoiti, G., Mantilla, E., Duéguez, J. J., Escudero, M., Monfort, E., Pérez García-Pando, C., Petetin, H., Jorba, O., Vázquez, V., de la Rosa, J., Campos, A., Muñóz, M., Monge, S., Hervás, M., Javato, R., & Cornide, M. J. (2021). Lessons from the COVID-19 air pollution decrease in Spain: Now what? Science of the Total Environment, 779. https://doi.org/10.1016/j.scitotenv.2021.146380

Shang, X., Zhang, K., Meng, F., Wang, S., Lee, M., Suh, I., Kim, D., Jeon, K., Park, H., Wang, X., & Zhao, Y. (2018). Characteristics and source apportionment of fine haze aerosol in Beijing during the winter of 2013. Atmospheric Chemistry and Physics, 18(4), 2573-2584. https://doi.org/10.5194/acp-18-2573-2018

Sharma, S., Zhang, M., Anshika, Gao, J., Zhang, H., & Kota, S. H. (2020). Effect of restricted emissions during COVID-19 on air quality in India. Science of the Total Environment, 728. https://doi.org/10.1016/j.scitotenv.2020.138878

Shen, J., Zhao, Q., Cheng, Z., Huo, J., Zhu, W., Zhang, Y., Duan, Y., Wang, X., Antony Chen, L. W., & Fu, Q. (2020). Evolution of source contributions during heavy fine particulate matter (PM2.5) pollution episodes in eastern China through online measurements. Atmospheric Environment, 232. https://doi.org/10.1016/j.atmosenv.2020.117569

Shen, L., Wang, H., Zhu, B., Zhao, T., Liu, A., Lu, W., Kang, H., & Wang, Y. (2021). Impact of urbanization on air quality in the Yangtze River Delta during the COVID-19 lockdown in China. Journal of Cleaner Production, 296. https://doi.org/10.1016/j.jclepro.2021.126561

Shen, L., Zhao, T., Wang, H., Liu, J., Bai, Y., Kong, S., Zheng, H., Zhu, Y., & Shu, Z. (2021). Importance of meteorology in air pollution events during the city lockdown for COVID-19 in Hubei Province, Central China. Science of the Total Environment, 754. https://doi.org/10.1016/j.scitotenv.2020.142227

Shi, Z., Huang, L., Li, J., Ying, Q., Zhang, H., & Hu, J. (2020). Sensitivity analysis of the surface ozone and fine particulate matter to meteorological parameters in China. Atmospheric Chemistry and Physics, 20(21), 13455-13466. https://doi.org/10.5194/acp-20-13455-2020

Shi, Z., Li, J., Huang, L., Wang, P., Wu, L., Ying, Q., Zhang, H., Lu, L., Liu, X., Liao, H., & Hu, J. (2017). Source apportionment of fine particulate matter in China in 2013 using a source-oriented chemical transport model. Science of the Total Environment, 1476-1487. https://doi.org/10.1016/j.scitotenv.2017.06.019

Singh, R.P., & Chauhan, A.K. (2020). Impact of lockdown on air quality in India during COVID-19 pandemic. Air Quality, Atmosphere and Health, Volume: 13, Issue: 8, 921-928.

Srivastava, A. (2021). COVID-19 and air pollution and meteorology-an intricate relationship: A review. In Chemosphere (Vol. 263). Elsevier Ltd. https://doi.org/10.1016/j.chemosphere.2020.128297

Sulaymon, I. D., Mei, X., Yang, S., Chen, S., Zhang, Y., Hopke, P. K., Schauer, J. J., & Zhang, Y. (2020). $PM_{2.5}$ in Abuja, Nigeria: Chemical characterization, source apportionment, temporal variations, transport pathways and the health risks assessment. Atmospheric Research, 237. https://doi.org/10.1016/j.atmosres.2019.104833

Sulaymon, I. D., Zhang, Y., Hopke, P. K., Hu, J., Zhang, Y., Li, L., Mei, X., Gong, K., Shi, Z., Zhao, B., & Zhao, F. (2021a). Persistent high PM2.5 pollution driven by unfavorable meteorological conditions during the COVID-19 lockdown period in the Beijing-Tianjin-Hebei region, China. Environmental Research, 198. https://doi.org/10.1016/j.envres.2021.111186

Sulaymon, I. D., Zhang, Y., Hu, J., Hopke, P. K., Zhang, Y., Zhao, B., Xing, J., Li, L., & Mei, X. (2021b). Evaluation of regional transport of PM2.5 during severe atmospheric pollution episodes in the western Yangtze River Delta, China. Journal of Environmental Management, 293. https://doi.org/10.1016/j.jenvman.2021.112827

Sulaymon, I. D., Zhang, Y., Hopke, P. K., Zhang, Y., Hua, J., & Mei, X. (2021c). COVID-19 pandemic in Wuhan: Ambient air quality and the relationships between criteria air pollutants and meteorological variables before, during, and after lockdown. Atmospheric Research, 250. https://doi.org/10.1016/j.atmosres.2020.105362

Sulaymon, I. D., Zhang, Y., Hopke, P. K., Hu, J., Rupakheti, D., Xie, X., Zhang, Y., Ajibade, F. O., Hua, J., & She, Y. (2021d). Influence of transboundary air pollution and meteorology on air quality in three major cities of Anhui Province, China. Journal of Cleaner Production, 129641. https://doi.org/10.1016/j.jclepro.2021.12964

Sulaymon, I.D., Zhang, Y., Hopke, P.K., Guo, S., Ye, F., Sun, J., Zhu, Y., & Hu, J. (2023). Quantifying the contributions of atmospheric processes and meteorology to severe $PM_{2.5}$ pollution episodes during the COVID-19 lockdown in the Beijing-Tianjin-Hebei, China. [Dataset]. Zenodo. https://doi.org/10.5281/zenodo.7711747

Tang, L., Shang, D., Fang, X., Wu, Z., Qiu, Y., Chen, S., Li, X., Zeng, L., Guo, S., & Hu, M. (2021). More significant impacts from new particle formation on haze formation during COVID-19 lockdown. *Geophysical Research Letters*, *48*, e2020GL091591. https://doi.org/10.1029/2020GL091591

Wang, B., Qiu, T., & Chen, B. (2014). Photochemical process modeling and analysis of ozone generation. Chin. J. Chem. Eng. 22, 721-729.

Wang, N., Lyu, X. P., Deng, X. J., Guo, H., Deng, T., Li, Y., Yin, C. Q., Li, F., & Wang, S. Q. (2016). Assessment of regional air quality resulting from emission control in the Pearl River Delta region, southern China. Science of the Total Environment, 573, 1554-1565. https://doi.org/10.1016/j.scitotenv.2016.09.013

Wang, P., Chen, K., Zhu, S., Wang, P., & Zhang, H. (2020). Severe air pollution events not avoided by reduced anthropogenic activities during COVID-19 outbreak.

Resources, Conservation and Recycling, 158. https://doi.org/10.1016/j.resconrec.2020.104814

Wang, P., Ying, Q., Zhang, H., Hu, J., Lin, Y., & Mao, H. (2018). Source apportionment of secondary organic aerosol in China using a regional source-oriented chemical transport model and two emission inventories. Environmental Pollution, 237, 756-766. https://doi.org/10.1016/j.envpol.2017.10.122

Wang, X., Li, L., Gong, K., Mao, J., Hu, J., Li, J., Liu, Z., Liao, H., Qiu, W., Yu, Y., Dong, H., Guo, S., Hu, M., Zeng, L., & Zhang, Y. (2021). Modelling air quality during the EXPLORE-YRD campaign - Part I. Model performance evaluation and impacts of meteorological inputs and grid resolutions. Atmospheric Environment, 246. https://doi.org/10.1016/j.atmosenv.2020.118131

Wang, X., Zhang, Y., Hu, Y., Zhou, W., Lu, K., Zhong, L., Zeng, L., Shao, M., Hu, M., & Russell, A.G. (2010). Process analysis and sensitivity study of regional ozone formation over the Pearl River Delta, China, during the PRIDE-PRD2004 campaign using the Community Multiscale Air Quality modeling system. Atmos. Chem. Phys. 10, 4423-4437.

Wu, C., Wang, H., Cai, W., He, H., Ni, A., & Peng, Z. (2021). Impact of the COVID-19 lockdown on roadside traffic related air pollution in Shanghai, China. Building and Environment, 194. https://doi.org/10.1016/j.buildenv.2021.107718

Xing, J., Zhang, Y., Wang, S.X., Liu, X.H., Cheng, S.H., & Zhang, Q. (2011). Modeling study on the air quality impacts from emission reductions and atypical meteorological conditions during the 2008 Beijing Olympics. Atmos. Environ. 45, 1786-1798.

Xing, J., Li, S., Jiang, Y., Wang, S., Ding, D., Dong, Z., Zhu, Y., & Hao, J. (2020). Quantifying the emission changes and associated air quality impacts during the COVID-19 pandemic on the North China Plain: A response modeling study. Atmospheric Chemistry and Physics, 20(22), 14347-14359. https://doi.org/10.5194/acp-20-14347-2020

Xue, T., Liu, J., Zhang, Q., Geng, G., Zheng, Y., Tong, D., Liu, Z., Guan, D., Bo, Y., Zhu, T., He, K., & Hao, J. (2019). Rapid improvement of PM2.5 pollution and associated health benefits in China during 2013-2017. Science China Earth Sciences, 62(12), 1847-1856. https://doi.org/10.1007/s11430-018-9348-2

Xu, W., Song, W., Zhang, Y., Liu, X., Zhang, L., Zhao, Y., Liu, D., Tang, A., Yang, D., Wang, D., Wen, Z., Pan, Y., Fowler, D., Collett, J. L., Willem Erisman, J., Goulding, K., Li, Y., & Zhang, F. (2017). Air quality improvement in a megacity: Implications from 2015 Beijing Parade Blue pollution control actions. Atmospheric Chemistry and Physics, 17(1), 31-46. https://doi.org/10.5194/acp-17-31-2017

Yan, D., Lei, Y., Shi, Y., Zhu, Q., Li, L., & Zhang, Z. (2018). Evolution of the spatiotemporal pattern of PM2.5 concentrations in China - A case study from the Beijing-Tianjin-Hebei region. Atmospheric Environment, 183, 225-233. https://doi.org/10.1016/j.atmosenv.2018.03.041

Ye, F., Rupakheti, D., Huang, L., T, Nishanth., MK, S.K., Li, L., KT, V., & Hu, J. (2022). Integrated process analysis retrieval of changes in ground-level ozone and fine particulate matter during the COVID-19 outbreak in the coastal city of Kannur, India. Environmental Pollution, 307. https://doi.org/10.1016/j.envpol.2022.119468

Yin, P., Brauer, M., Cohen, A.J., Wang, H., Li, J., Burnett, R.T., Stanaway, J.D., Causey, K., Larson, S., Godwin, W., Frostad, J., Marks, A., Wang, L., Zhou, M., & Murray, C.J.L. (2020). The effect of air pollution on deaths, disease burden, and life expectancy across China and its provinces, 1990-2017: an analysis for the Global Burden of Disease Study 2017. The Lancet Planetary Health 4, e386–e398.

Zhang, Y., Ma, Z., Gao, Y., & Zhang, M. (2021). Impacts of the meteorological condition versus emissions reduction on the PM2.5 concentration over Beijing-Tianjin-Hebei during the COVID-19 lockdown. Atmospheric and Oceanic Science Letters, 14(4). https://doi.org/10.1016/j.aosl.2020.100014

Zhao, N., Wang, G., Li, G., Lang, J., & Zhang, H. (2020). Air pollution episodes during the COVID-19 outbreak in the Beijing-Tianjin-Hebei region of China: An insight into the transport pathways and source distribution. Environmental Pollution, 267. https://doi.org/10.1016/j.envpol.2020.115617

Zhao, X., Wang, G., Wang, S., Zhao, N., Zhang, M., & Yue, W. (2021). Impacts of COVID-19 on air quality in mid-eastern China: An insight into meteorology and emissions. Atmospheric Environment, 266. https://doi.org/10.1016/j.atmosenv.2021.118750

Zheng, B., Zhang, Q., Geng, G., Chen, C., Shi, Q., Cui, M., Lei, Y., & He, K. (2021). Changes in China's anthropogenic emissions and air quality during the COVID-19 pandemic in 2020. Earth System Science Data, 13(6), 2895-2907. https://doi.org/10.5194/essd-13-2895-2021

Zheng, B., Zhang, Q., Geng, G., Shi, Q., Lei, Y., & He, K. (2020). Changes in China's anthropogenic emissions during the COVID-19 pandemic. Earth System Science Data Discussions, 1-20. https://doi.org/10.5194/essd-2020-355

Zhou, C., Zhou, H., Holsen, T. M., Hopke, P. K., Edgerton, E. S., & Schwab, J. J. (2019). Ambient Ammonia Concentrations Across New York State. Journal of Geophysical Research: Atmospheres, 124(14), 8287-8302. https://doi.org/10.1029/2019JD030380

Zhu, N., Zhang, D., Wang, W., Li, X., Yang, B., Song, J., Zhao, X., Huang, B., Shi, W., Lu, R., Niu, P., Zhan, F., Ma, X., Wang, D., Xu, W., Wu, G., Gao, G. F., & Tan, W. (2020). A Novel Coronavirus from Patients with Pneumonia in China, 2019. New England Journal of Medicine, 382(8), 727-733. https://doi.org/10.1056/nejmoa2001017

Quantifying the contributions of atmospheric processes and meteorology to severe $PM_{2.5}$ pollution episodes during the COVID-19 lockdown in the Beijing-Tianjin-Hebei, China

Ishaq Dimeji Sulaymon[a], Yuanxun Zhang[b,c], Philip K. Hopke[d,e], Song Guo[f], Fei Ye[a], Jinjin Sun[a], Yanhong Zhu[a], Jianlin Hu[a*]

[a] *Jiangsu Key Laboratory of Atmospheric Environment Monitoring and Pollution Control, Collaborative Innovation Center of Atmospheric Environment and Equipment Technology, School of Environmental Science and Engineering, Nanjing University of Information Science and Technology, Nanjing, 210044, China*

[b] *College of Resources and Environment, University of Chinese Academy of Sciences, Beijing 100049, China*

[c] *CAS Center for Excellence in Regional Atmospheric Environment, Chinese Academy of Sciences, Xiamen, 361021, China*

[d] *Center for Air Resources Engineering and Science, Clarkson University, Potsdam, NY 13699, USA*

[e] *Department of Public Health Sciences, University of Rochester School of Medicine and Dentistry, Rochester, NY 14642, USA*

[f] *State Key Joint Laboratory of Environmental Simulation and Pollution Control, College of Environmental Sciences and Engineering, Peking University, Beijing, 100871, China*

---

* Corresponding author. *E-mail address:* sulaymondimeji@nuist.edu.cn; jianlinhu@nuist.edu.cn

Key Points:

- Three severe $PM_{2.5}$ pollution episodes were identified in the Beijing-Tianjin-Hebei region during the COVID-19 lockdown.
- The $PM_{2.5}$ episodes were dominated by emissions and aerosol processes, and enhanced by unfavorable meteorological conditions.
- Designing more effective emissions control strategies with both chemistry and meteorology in thought could mitigate future $PM_{2.5}$ episodes.

Abstract

A major tool for curtailing the spread of COVID-19 pandemic in China was a nationwide lockdown, which led to significant reductions in anthropogenic emissions and fine particulate matter ($PM_{2.5}$). However, the lockdown measures did not prevent high $PM_{2.5}$ pollution episodes (EPs). Three severe EPs were identified in the Beijing-Tianjin-Hebei (BTH) region during the lockdown. The integrated process rate (IPR) analysis tool in the Community Multiscale Air Quality (CMAQ) model was employed to quantify the contributions of individual atmospheric processes to $PM_{2.5}$ formation during the lockdown in the BTH region. The IPR results showed that emissions and aerosol processes were the dominant sources of net surface $PM_{2.5}$ in Beijing and Tianjin, constituting a total of 86.2% and 92.9%, respectively, while emissions, horizontal transport, and aerosol processes dominated the net surface $PM_{2.5}$ in Shijiazhuang and Baoding. In addition, the EPs in Beijing and Tianjin were primarily driven by local emissions, while the EPs in Shijiazhuang and Baoding were attributed to combined local emissions and regional transport. The reductions in $PM_{2.5}$ in Case 2 relative to Case 1 were attributed to the weaker $PM_{2.5}$ formation from emissions and aerosol processes. However, the EPs were enhanced by low planetary boundary layer heights, low vertical export of $PM_{2.5}$ from the boundary layer to the free troposphere, and substantial horizontal import, especially in Shijiazhuang and Baoding. This study improves the understanding of buildup of $PM_{2.5}$ during the EPs, and the results provide insights for designing more effective emissions control strategies to mitigate future $PM_{2.5}$ episodes.

Keywords: Fine particulate matter; Pollution episodes; Process analysis; WRF-CMAQ; COVID-19 shutdown.

1. Introduction

For more than two decades, China has been suffering from severe haze pollution, attributed to its population growth, urbanization, fast industrialization, as well as economic advancement (Li et al., 2020; Shi et al., 2017; Zhao et al., 2021). The development of severe haze is caused by a combination of anthropogenic emissions (local and regional) (Sulaymon et al., 2020, 2021a) and adverse meteorological conditions (Chen et al., 2021; Hua et al., 2021; Hu et al., 2016; Shen, et al., 2021; Shi et al., 2020; Sulaymon et al., 2021a, 2021b). Severe air pollution causes reductions in visibility (Jiang et al., 2021; Li et al., 2019; Wang et al., 2018), changes in climate and ecosystem services (Jiang et al., 2021; Zhao et al., 2021), and adverse human health effects (Chen et al., 2017; Croft et al., 2019; Hopke et al., 2019; Shang et al., 2018; Shen et al., 2020; Yan et al., 2018). The global disease burden (GDB) has attributed about 2 million premature deaths per annum to severe air pollution exposure in China (Yin et al., 2020).

The issuance of the new ambient air quality standards (GB3095-2012) in 2012 and the subsequent implementation of the Air Pollution Prevention and Control Action Plan (APPCAP) in September 2013 by the Chinese authorities has led to reduction in the concentrations of fine particulate matter with aerodynamic diameters of ≤2.5 ($PM_{2.5}$) in Chinese cities (Fan et al., 2020; Sulaymon et al., 2021d; Wang et al., 2016). For instance, Xue et al. (2019) noted about 32.5% reduction in the national population-weighed $PM_{2.5}$ annual mean between 2013 and 2017. However, high $PM_{2.5}$ concentrations are still observed in most cities, with annual averages violating the annual Grade I (15 μg/m^3) and Grade II (35 μg/m^3) Chinese Ambient Air Quality Standards (CAAQS), and much higher than the WHO (5 μg/m^3) recommended limit or the USEPA (12 μg/m^3) standard.

The Beijing-Tianjin-Hebei (BTH) region that includes Beijing and Tianjin, and Hebei Province, is one of the most economically developed regions in China. The region has been suffering from severe $PM_{2.5}$ pollution over the past two decades (Chang et al., 2018; Dai et al., 2021a), particularly during the winter season. During past international events (e.g. 2008 Olympic Games, 2014 Asia-Pacific Economic Cooperation, and the 2015 Military Parade), Chinese authorities implemented major emissions reductions measures in the BTH region to improve air quality. The effectiveness and success of the emissions reduction policies have been assessed (Wang et al., 2016; Xu et al., 2017; Yang et al., 2016).

In December 2019, an outbreak of coronavirus disease (COVID-19) occurred in Wuhan (Zhu et al., 2020) and spread across China and many other countries within a short time. As one of the measures to curtail the spread of COVID-19 pandemic in China, a nationwide lockdown was implemented by the Chinese authorities, leading to significant reductions in anthropogenic emissions and $PM_{2.5}$ concentrations across China (Sulaymon et al., 2021a, 2021c; Wang et al., 2020; Zhao et al., 2020; Zhao et al., 2021). However, the BTH region still experienced high $PM_{2.5}$ pollution episodes during the lockdown (Sulaymon, et al., 2021a; Zhang et al., 2021). Compared to the past international events held in Beijing during the summer and autumn seasons (with no or few pollution episodes), the COVID-19 pandemic occurred in winter, a period with frequent severe pollution events especially in the BTH region. In addition, the COVID-19 lockdown had a longer period with very strict measures than the duration of the past three events.

Previous studies have assessed the impacts of COVID-19 lockdown on air quality as well as the relationships between air quality and meteorological conditions during lockdown in BTH region (Cui et al., 2020; Dai et al., 2020; 2021b; Sulaymon et al., 2021a;

Zhang et al., 2021; Zhao et al., 2021), other regions in China (Gao et al., 2021; Liu et al., 2020; Shen et al., 2021a, 2021b; Sulaymon, et al., 2021c; Wang et al., 2020; Wu et al., 2021; Xing et al., 2020), and outside mainland China (Bashir et al., 2020; Chauhan and Singh, 2020, 2021; Mishra et al., 2021; Muhammad et al., 2020; Orak and Ozdemir, 2021; Querol et al., 2021; Sharma et al., 2020; Singh and Chauhan, 2020; Srivastava, 2021; Ye et al., 2022). A few studies have also been performed on the regional source apportionment of $PM_{2.5}$ during the lockdown (Li et al., 2020; Ma et al., 2021). Li et al. (2020) reported that industry (32.2-61.1%) and residential (2.1-28.5%) were the two highest sources contributing to $PM_{2.5}$ in the Yangtze River Delta (YRD) region, while about 14.0-28.6% contribution was due to long-range transport from northern China. In the BTH region, a few studies have also investigated the source apportionment of $PM_{2.5}$ during lockdown (Cui et al., 2020; Dai et al., 2020). For example, Dai et al. (2020) used Positive Matrix Factorization (PMF) to investigate the sources of $PM_{2.5}$ in Tianjin. Their results showed that secondary inorganic aerosols (SIA) (50.5%), fireworks and residential burning (32.0%), and primary coal combustion emissions (13.3%) were the three dominant sources contributing to $PM_{2.5}$ during the lockdown. Overall, previous studies have reported persistent haze episodes in the BTH region during lockdown despite the emission reductions, and have generally attributed them to unfavorable meteorological conditions (Cui et al., 2020; Dai et al., 2020; 2021b; Sulaymon et al., 2021a; Zhang et al., 2021; Zhao et al., 2021). However, the formation of air pollutants involves various physical processes (such as emissions, condensation, advection, diffusion, deposition, etc.) as well as oxidative chemical process (Huang et al., 2005; Wang et al., 2014; Ye et al., 2022).

The process analysis (PA) tool in the Community Multiscale Air Quality (CMAQ) chemical transport model can provide quantitative analysis of the individual contributions of various physical and chemical processes to the observed air pollution (Liu et al., 2010; Liu and Zhang, 2011; Xing et al., 2011; Ye et al., 2022). Liu and Zhang (2011) employed the PA tool to analyze a regional $PM_{2.5}$ pollution episode in the U.S. They found that emissions and aerosol processes such as homogeneous nucleation, heterogeneous nucleation, and condensation were the dominant contributors to increased $PM_{2.5}$ concentrations, while horizontal and vertical transport and dry deposition were the primary loss mechanisms. Liu et al. (2010) utilized the PA to explore the contributions of various atmospheric processes on ozone and PM_{10} concentrations in China during four seasons. The results showed that emissions and aerosol processes were the main contributors to PM_{10} concentrations, while horizontal transport was the major removal pathway. Xing et al. (2011) used CMAQ-PA tool to quantify the air quality benefits from emissions reductions and meteorological variations during the 2008 Beijing Olympics. The results indicated that aerosol and emission processes acted as the major $PM_{2.5}$ pathways, while vertical transport was the major $PM_{2.5}$ sink at the surface.

Therefore, analyzing the air quality during the unique lockdown period to provide additional understanding of the underlying causes of high pollution episodes even during periods of substantially reduced anthropogenic activity is important for providing approaches to future air quality management strategies. The present study is the first that elucidated the contributions of various atmospheric processes to $PM_{2.5}$ pollution episodes during the lockdown in the BTH region. The results provide new insights into $PM_{2.5}$ formation of the three pollution episodes during lockdown. Thus, it provides a valuable example of how to use opportunities like the lockdown period to better understand the causal factors of episodes in other areas of the world, which can then be applied to develop more effective control strategies that would reduce the magnitude of these episodes and better protect public health.

2. Methodology

2.1. Model set-up and configurations

The Community Multiscale Air Quality model version 5.2 (CMAQv5.2) was applied to simulate the air quality in the BTH region during the COVID-19 lockdown period (January 24-February 29, 2020). The photochemical mechanism and the aerosol module used in configuring the model were the State-wide Air Pollution Research Center version 07 (SAPRC07tic) and AERO6i, respectively (Liu et al., 2020; Sulaymon et al., 2021a, 2021b). Two nested domains with horizontal resolutions of 36 and 12 km were used (Fig. S1). The outer domain (36 km) covers China and the surrounding regions (137 x 107 grids), and the inner domain (12 km) covers the study area, the BTH region (127 x 202 grids). Each of the two domains had 18 vertical layers, emanating from the surface to a height of about 20 km above the ground level. The initial and boundary conditions (IC/BC) used in the 36 km domain were based on the default profiles provided by the CMAQ model, while the IC/BC used for the 12 km domain were generated from the results of the 36 km simulations. As a way of reducing the impact of initial conditions on $PM_{2.5}$ predictions, the simulations began on January 19, and the results of the first 5 days (January 19-23, 2020) were excluded from the model analysis, thus serving as a spin-up of the model. The meteorological inputs were simulated by the Weather Research and Forecasting (WRF v4.0) model with the FNL reanalysis data serving as the IC/BC. The detailed settings and configurations, including the major physics schemes used in this study are listed in Table S1, while other settings could be found in previous studies where the WRF model was applied (Hu et al., 2015, 2016; Wang et al., 2021).

In this study, the Multi-resolution Emission Inventory for China (MEIC) of year 2016 (http://www.meicmodel.org) served as the anthropogenic emissions from China. In addition, the anthropogenic emissions from adjacent countries and regions were processed based on the Regional Emission inventory in ASia version 2 (REAS2) (Kurokawa et al., 2013). Biogenic emissions were estimated with the Model of Emissions of Gases and Aerosols from Nature (MEGAN) version 2.1. Open burning emissions were generated based on the data obtained from the Fire INventory from NCAR (FINN) (Wiedinmyer et al., 2011). Sea salt and windblown emissions were generated inline (Sulaymon et al., 2021a, 2021b). Further details regarding the emission processing can be found in Hu et al. (2016) and Qiao et al. (2015).

To evaluate the impacts of the emissions reductions on air quality, two scenarios (referred to as Cases 1 and 2) were simulated as presented in Table S2. The first scenario (Case 1) used the original MEIC16 emission inventory. In the second scenario (Case 2), emissions from transportation, industry, and power sectors were reduced (Table S2) during the lockdown period, while those of residential and agriculture were similar to Case 1. The basis for adopting the emission reduction factors has been previously presented (Sulaymon et al., 2021a; Wang et al., 2020), and has also been detailed in the Supplementary Material (Text S1). The differences between the results of Cases 1 and 2 represent the impact of emissions reductions on air quality during the lockdown.

2.2. Process analysis

The process analysis (PA) tool embedded in the CMAQ model has been described as a versatile analytical tool for quantifying the contributions of individual atmospheric processes and chemical reactions to a pollutant (Fu et al., 2020; Ye et al., 2022). PA is comprised of two components; the integrated process rate (IPR) and integrated reaction rate (IRR) analysis. The IPR involves the changes in the hourly concentrations of pollutants due to individual atmospheric processes such as gas-phase chemistry, emissions, aerosol processes, dry deposition, cloud processes, and vertical and horizontal transport at each grid cell in the model domain. The IPR analysis has been extensively used in quantifying the contributions individual atmospheric processes to air pollutants (Fan et al., 2015; Fu et al., 2020; Li et al., 2012; Wang et al., 2010; Xing et al., 2011; Ye et al., 2022), hence, detailed information about IPR can be found in these referenced studies.

In this study, the IPR module in CMAQv5.2 was employed to resolve both physical and chemical processes involved in the formation of $PM_{2.5}$ during the lockdown period in the BTH region. The IPR results were subsequently used to analyze the individual processes involved in $PM_{2.5}$ formation in the surface layer and full planetary boundary layer (PBL), respectively. For this purpose, the processes considered were the chemistry (gas-phase), emissions, aerosol processes (SOA formation, nucleation, condensation, coagulation, heterogeneous chemistry, mode merging, and aerosol thermodynamics), cloud processes, dry deposition, vertical transport (sum of vertical advection and diffusion), and horizontal transport (sum of horizontal advection and diffusion). Based on their contributions to $PM_{2.5}$ concentrations, atmospheric processes can be grouped into two; source process (concentration increases) and sink process (concentration decreases). Dry deposition and emission belong to the sink and source process, respectively. The IPR of other processes can either be source (positive) or sink (negative). The contributions of individual atmospheric processes to the formation of $PM_{2.5}$ were estimated using the approach of Ye et al. (2022):

$$\mathrm{SOURCE_p} = \frac{\sum_t \mathrm{IPR_{p,t}}}{\sum_p \sum_t \mathrm{IPR_{p,t}}} \times 100\% \quad (\mathrm{IPR_{p,t}} > 0) \qquad (1)$$

$$\mathrm{SINK_p} = \frac{\sum_t \mathrm{IPR_{p,t}}}{\sum_p \sum_t \mathrm{IPR_{p,t}}} \times 100\% \quad (\mathrm{IPR_{p,t}} < 0) \qquad (2)$$

where p is the atmospheric process, and t is the time (in hour). $\mathrm{SOURCE_p}$ and $\mathrm{SINK_p}$ are the proportions of the atmospheric process p in all source and sink processes, respectively. Both source and sink categories are used to reveal how important an atmospheric process is in influencing the changes in $PM_{2.5}$ concentrations.

3. Results and discussion

3.1. WRF model performance

Meteorological parameters play an important role in the formation and transportation of air pollution (Hu et al., 2016; Sulaymon et al., 2021a, 2021b; Wang et al., 2021). In addition, the influences of meteorological parameters on the air quality simulations using chemical transport model have also been established (Hu et al., 2016; Sulaymon et al., 2021a; Wang et al., 2021). To evaluate the WRF model performance, the predicted temperature (T2) and relative humidity (RH) at 2 m above ground level, and wind speeds (WS) and wind directions (WD) at 10 m above surface were compared to the observational data downloaded from the official website of the Chinese Meteorological Agency (http://data.cma.cn/en, last access: January 2023). Table S3 shows the summary statistics including the mean observation (OBS), mean prediction (PRE), mean bias (MB), mean error (ME), and the root mean square error (RMSE). In addition to the BTH region as a whole, four representative cities including Beijing (BJ), Tianjin (TJ), Shijiazhuang (SJZ), and Baoding (BD) were evaluated. Generally, T2 (Table S3) was slightly over-predicted in the BTH and the four representative cities during the lockdown. The MB and ME of T2 in BTH were 0.4 and 1.7, respectively, which fell below the suggested benchmarks (MB≤±0.5; and ME≤2.0) (Emery et al., 2001). These are consistent with a previous study over BTH region (Chang et al., 2019). Except in Tianjin (MB:0.5), the MB values in other three cities (Beijing:2.2; Shijiazhuang:0.6; and Baoding:1.3) exceeded the benchmark. Except in Beijing (ME:2.3), the ME values in all the cities were within the benchmark range. Although there were no suggested benchmarks for the MB and ME indices of RH, however, RH (Table S3) was underpredicted in BTH region and the four representative cities (Ma et al., 2021). Similar results had been reported by previous studies over BTH region (Chang et al., 2018; Li et al., 2021b; Sulaymon et al., 2021a; Zhao et al., 2021) and China as a whole (Hu et al., 2016; Sulaymon et al., 2021b; Wang et al., 2021). Bhati and Mohan (2018) obtained a similar result and attributed it to the influence of the boundary layer parameterization on the weather prediction. The mean observed WS across the cities and BTH ranged from 1.8 to 2.3 m/s, an illustration of relatively calm conditions during the lockdown. Generally, WS (Table S3) was over-predicted (Ma et al., 2021). However, based on the ME, MB, and RMSE indices, the predictions reasonably captured the observations across the four cities and BTH (Li et al., 2021b; Sulaymon et al., 2021a; Zhao et al., 2021). The over-predictions of WS might be due to unresolved topography within the WRF model (Li et al., 2014). The MB values met the suggested benchmark

($\leq\pm0.5$) in BTH and three cities except Shijiazhuang (0.7). During the lockdown, the ME and RMSE values ranged between 0.6-0.9 and 0.7-1.2, respectively, with both indices falling below the recommended benchmarks (≤2.0). WD (Table S3) was generally under-predicted except in Shijiazhuang where the PRE was slightly higher than the OBS. Overall, the MB values were above the suggested criterion range ($\leq\pm10$) except in Baoding (MB: -0.8), Shijiazhuang (MB:2.3), and BTH (MB: -9.6). Also, the ME values in the four cities and BTH region greatly exceeded the benchmark ($\leq\pm30$), especially in Shijiazhuang (ME:101.5), Beijing (ME:78.4), and BTH region (ME:70.5). Similar model performance of WD had been reported (Hu et al., 2016; Sulaymon et al., 2021a, 2021b; Wang et al., 2021). Generally, in this study, the WRF model exhibited better performance when compared to previous studies in BTH region (Chang et al., 2019; Li et al., 2021b; Sulaymon et al., 2021a; Zhang et al., 2021; Zhao et al., 2021) and China as a country (Ma et al., 2021; Sulaymon et al., 2021b; Wang et al., 2021). Since the simulated meteorological parameters were robust, they were used in driving the air quality simulations.

3.2. CMAQ model performance

In evaluating the performance of CMAQ model in predicting $PM_{2.5}$, statistical indices, which include the mean observations (OBS), mean predictions (PRE), mean fractional bias (MFB), mean fractional error (MFE), mean normalized bias (MNB), and mean normalized error (MNE) were calculated. The performance of CMAQ model for $PM_{2.5}$ over the BTH and at four representative cities during the lockdown period based on the two cases are shown in Table S4. Generally, the simulated $PM_{2.5}$ concentrations exhibited good agreement with the observed data with the model performance indices falling within the recommended benchmarks for $PM_{2.5}$ (MFB ≤±0.60 and MFE ≤ 0.75) (Boylan and Russel, 2006) in BTH and the four cities for the two cases. For Case 1, $PM_{2.5}$ was over-estimated in BTH (0.10), Beijing (0.31), and Tianjin (0.41), while it was under-predicted in Shijiazhuang (-0.05) and Baoding (-0.19). Considering Case 2, all of the MFB values were negative except in Tianjin (0.32), an indication that CMAQ under-predicted the total $PM_{2.5}$ concentrations in BTH and the other three cities. Chang et al. (2019) had reported an under-estimation of $PM_{2.5}$ by CMAQ in Beijing and Shijiazhuang, which is consistent with this study for Case 2. Also, the model performances for Case 2 are in line with the findings of Sulaymon et al. (2021a) In addition, under-predictions of $PM_{2.5}$ in all of the prefectural-level cities of BTH region were reported by Jiang et al. (2021). The MFE values for the two cases ranged between 0.40-0.51, which were within the recommended benchmark (MFE≤ 0.75). Overall, the CMAQ model has shown better performance in this study when compared to previous studies across the BTH region (Chang et al., 2019; Jiang et al., 2021; Li et al., 2021b; Sulaymon et al., 2021a; Zhang et al., 2021; Zhao et al., 2021). Thus, the model results were deemed acceptable for further analyses, including the IPR analysis.

3.3. IPR analysis of $PM_{2.5}$ formation at the surface layer

The hourly concentrations of $PM_{2.5}$ as well as the contributions of the individual atmospheric processes to the evolution of $PM_{2.5}$ at the surface layer in the BTH region and four representative cities for the two cases during the lockdown period are illustrated in Fig. 1. In the BTH region as a whole, the emissions (EMIS), horizontal transport (HTRA), and aerosol processes (AERO) were the major positive contributors (sources) to the net surface $PM_{2.5}$.

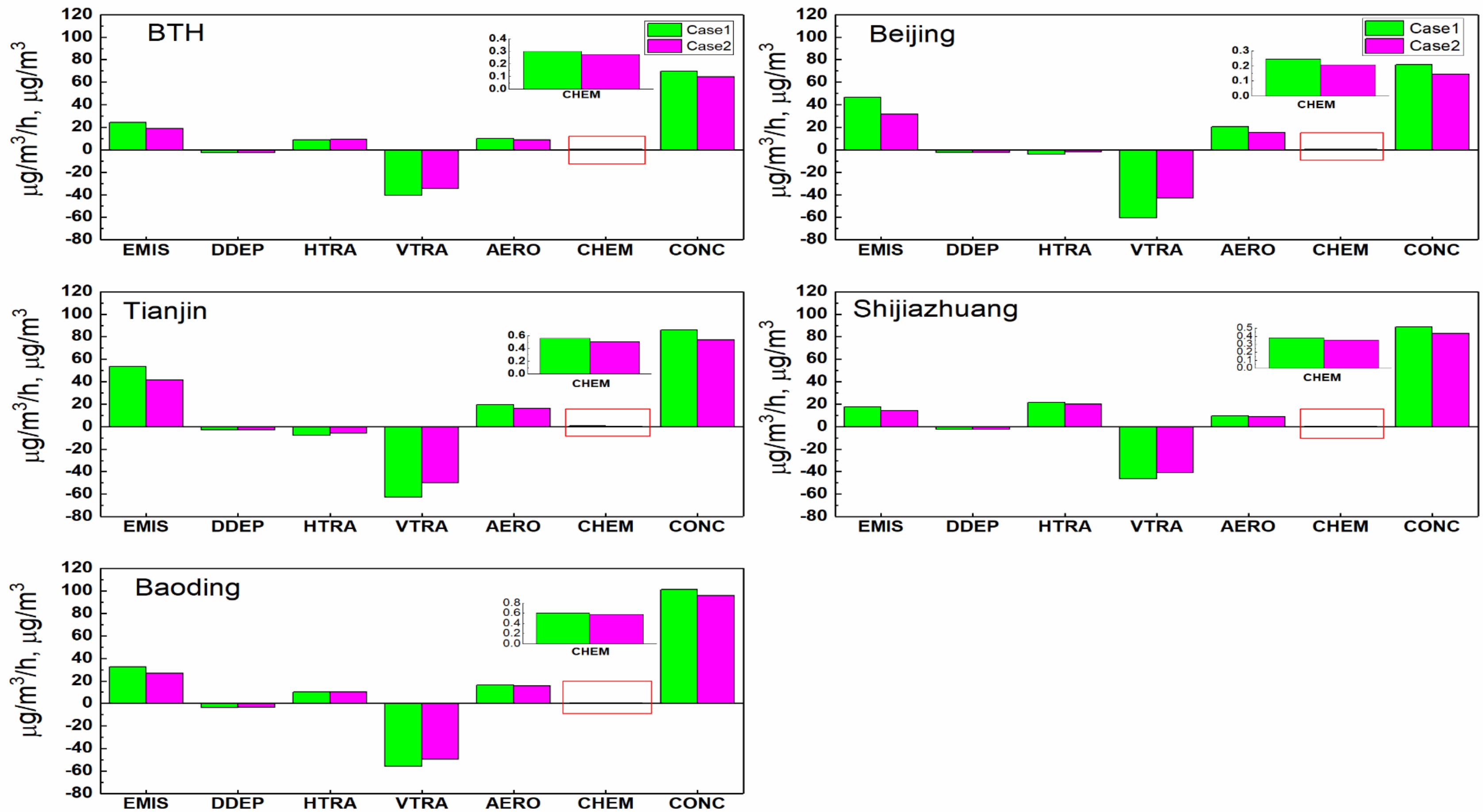

Fig. 1. Contributions of the individual processes to the concentrations of $PM_{2.5}$ at the surface layer in Cases 1 and 2 during the lockdown period. EMIS represents $PM_{2.5}$ input by emissions, DDEP represents $PM_{2.5}$ decrease by dry deposition; HTRA and VTRA represent $PM_{2.5}$ change by horizontal and vertical transport, respectively; AERO represents $PM_{2.5}$ change by the aerosol; and CHEM represents $PM_{2.5}$ change by gas-phase chemistry. The unit of the processes is µg/m^3/h. CONC is the hourly $PM_{2.5}$ concentrations in µg/m^3.

For Case 2, the contributions of EMIS, HTRA, and AERO to $PM_{2.5}$ formation were 42.4, 32.5, and 20.9% (Fig. 2b), respectively, while their contributions in the same order for Case 1 were 46.7, 29.4, and 20.3% (Fig. 2a), respectively. The reduction in the surface layer's $PM_{2.5}$ for the two cases was primarily attributed to the vertical transport (VTRA), while slight removal was also due to dry deposition (DDEP). In Beijing and Tianjin, EMIS and AERO were the predominant processes that contributed to the net surface $PM_{2.5}$ formation (Fig. 1) for both cases. The total contribution ratios of EMIS and AERO in Case 2 were 86.2% and 92.9% for Beijing and Tianjin (Fig. 2b), respectively. The reduction of surface $PM_{2.5}$ in Beijing and Tianjin for the two cases was associated with the VTRA, HTRA, and DDEP processes, with VTRA being the highest sink, with negative contributions of 79.0-81.3% (Beijing) and 80.2-81.0% (Tianjin). The results of the present study are consistent with those reported by Ye et al. (2022) in the coastal city of Kannur, India, where the EMIS, HTRA, and AERO were the dominant processes that positively contributed to $PM_{2.5}$ evolution, while VTRA and DDEP were responsible for surface $PM_{2.5}$ removal during the three periods considered in the study. Also, Fan et al. (2015) reported EMIS and VTRA as the two major processes that influenced $PM_{2.5}$ at the surface layer in the Pearl River Delta (PRD) region of China. Furthermore, Liu et al. (2010) and Xing et al. (2011) had earlier reported EMIS and AERO as the major $PM_{2.5}$ sources in both surface layer and the PBL in Beijing, while Xing et al. (2011) found VTRA as the major $PM_{2.5}$ sink in the surface layer. The $PM_{2.5}$ removal due to HTRA and DDEP in both cases were relatively the same in both Beijing and Tianjin. Considering Shijiazhuang and Baoding, similar trends were obtained regarding the contributions of individual processes to $PM_{2.5}$ formation.

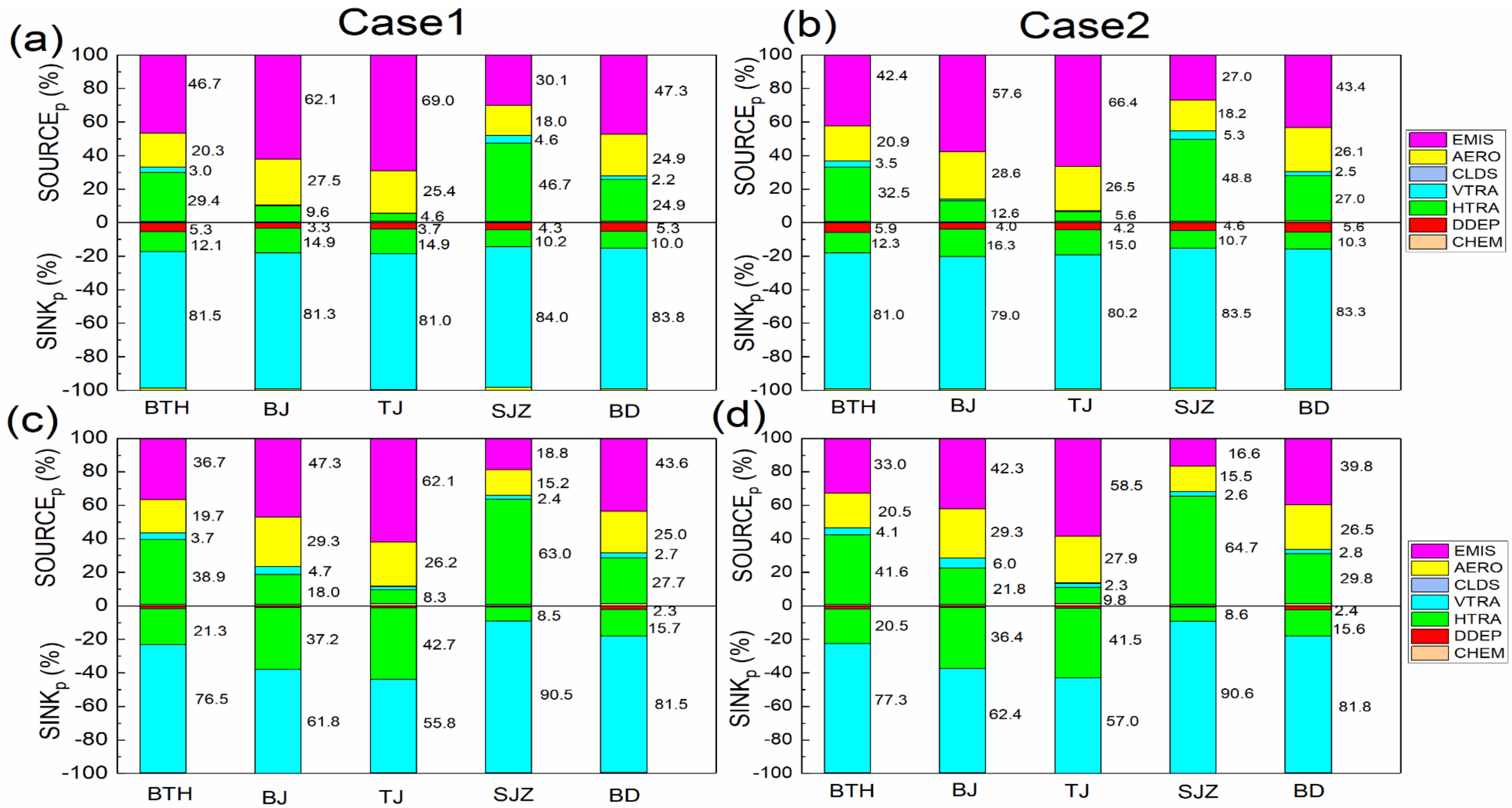

Fig. 2. Positive and negative contribution ratios of the individual processes to $PM_{2.5}$ concentrations (a,b) at the surface layer and (c,d) in the planetary boundary layer in Cases 1 and 2 during the lockdown period. EMIS, AERO, CLDS, VTRA, HTRA, DDEP, and CHEM represent the contributions of the emissions, aerosol, clouds, vertical transport, horizontal transport, dry deposition, and gas-phase chemistry, respectively to $PM_{2.5}$ formation.

The EMIS, AERO, and HTRA processes dominated the positive contributions to the net surface $PM_{2.5}$ in the two cities (Fig. 1), accounting for a total of 94.0 and 96.5% in Shijiazhuang and Baoding, respectively in Case 2 (Fig. 2b), while similar contributions were obtained in Case 1 (Fig. 2a). In addition to EMIS and AERO processes, the horizontal import of $PM_{2.5}$ to the surface layer via HTRA contributed to the elevated $PM_{2.5}$ concentrations in both Shijiazhuang and Baoding relative to Beijing and Tianjin. VTRA dominated the removal of $PM_{2.5}$ from the surface layer to upper layers in both cities, with higher rates in Case 1 relative to Case 2. DDEP process also had negative effects on $PM_{2.5}$ formation in the two cities, with very low contributions, especially in Shijiazhuang. The photochemistry (CHEM) process had positive net impacts on $PM_{2.5}$ evolution for the two cases across the BTH region and the four representative cities, however, the contributions were extremely low and negligible (Fan et al., 2015). This is contrary to what was reported in Kannur (Ye et al., 2022), as CHEM had negative effects on $PM_{2.5}$ in the city. Due to the negligible contributions of cloud (CLDS) processes to $PM_{2.5}$, it was not discussed in this study. It should be noted that the $PM_{2.5}$ concentrations in BTH region and the four cities in Case 2 were relatively low compared to Case 1. This could be attributed to low $PM_{2.5}$ formation from EMIS in Case 2. However, there was no substantive decrease in $PM_{2.5}$ concentrations in Case 2 despite reductions in anthropogenic emissions. This could be explained by the reduced $PM_{2.5}$ export from the surface layer to the upper layers due to low VTRA rates in Case 2 (compared to Case 1), leading to the accumulation of $PM_{2.5}$ in the surface layer, which subsequently led to high $PM_{2.5}$ pollution during the lockdown period.

3.4. IPR analysis of $PM_{2.5}$ formation in the PBL

Fig. S2 shows the mean hourly change rates attributed to individual atmospheric processes to $PM_{2.5}$ production and the concentrations of $PM_{2.5}$ in the PBL during the lockdown. The contributions of the various processes to $PM_{2.5}$ formation within the PBL in BTH and the four cities followed the similar trends as found in the surface layer. However, the contributions of the individual processes to $PM_{2.5}$ were smaller in the PBL compared to the surface layer, as $PM_{2.5}$ concentrations decrease as vertical layers increase (Fan et al., 2015). Generally, the contributions of EMIS and VTRA to the net $PM_{2.5}$ (Case 2) were low in the PBL compared to the surface layer. For instance, relative to what was obtained to the surface layer, the rates due to EMIS and VTRA in the PBL decreased by half in BTH region and all of the representative cities. Similar to the surface layer, the EMIS, HTRA, and AERO were the predominant contributors to the net $PM_{2.5}$ in the whole BTH region and Baoding, while only EMIS and AERO processes contributed substantially to the net $PM_{2.5}$ in Beijing and Tianjin. In Shijiazhuang, however, HTRA was the dominant contributor to $PM_{2.5}$ formation. Compared to other processes, the contributions of CHEM process were extremely low and negligible (Fan et al., 2015; Ye et al., 2022). In addition to VTRA as the major process responsible for the removal of $PM_{2.5}$ across the study areas, $PM_{2.5}$ removal in Beijing and Tianjin was also associated with HTRA. In all of the study areas, slight removal of $PM_{2.5}$ was also attributed to DDEP process. It could be noted that the VTRA and HTRA effects within the PBL were opposite to those to the surface layer. As illustrated in Fig. 2(d), the negative contributions (sinks) due to VTRA in the entire PBL substantially reduced in all of the study areas except Shijiazhuang (increased) when compared to the surface layer. Contrary to the surface layer, the sinks ($PM_{2.5}$ removal) due to HTRA within the PBL increased in all of the study areas except Shijiazhuang (decreased). It is worth noting that despite the decreases in EMIS rates by half (which might have adversely influenced $PM_{2.5}$ formation within the PBL) in comparison to the surface layer, the absolute difference in $PM_{2.5}$ concentrations between the surface layer and PBL was not significant, and ranged between 5.7-9.1 μg/m^3 across the study areas. This could be attributed to reduced $PM_{2.5}$ export due to low VTRA rates, leading to the accumulation of $PM_{2.5}$ within the PBL, and subsequently resulted to high $PM_{2.5}$ concentrations. Overall, in the PBL, EMIS and VTRA served as the two dominant processes that impacted $PM_{2.5}$ in BTH, Beijing, Tianjin, and Baoding, while VTRA and HTRA were the two major processes that influenced $PM_{2.5}$ formation in Shijiazhuang.

3.5. Vertical profiles of the atmospheric processes contributing to $PM_{2.5}$

The mean hourly $PM_{2.5}$ change rates attributed to individual atmospheric processes for the first ten layers (layers 1-10), as well as the vertical profiles of $PM_{2.5}$ evolution for Case 2 during the lockdown period are illustrated in Fig. 3, while that of Case 1 are shown in Fig. S3. As earlier stated in section 3.4, the characteristics of $PM_{2.5}$ concentrations at upper layers (layer 4 and above) were different from near-surface layers, hence, the contributions of emissions sources at upper layers were negligible (Fan et al., 2015). Across the study areas, the contributions from EMIS sources were only found within layers 1-3 (Fig. 3a-e) (Fan et al., 2015; Ye et al., 2022), and this was associated with the height of the emissions sources (Fan et al., 2015; Ye et al., 2022). The highest and lowest contributions of EMIS were found in Tianjin and Shijiazhuang, respectively, and the contribution decreased as the vertical layer increased. Within the first three layers, AERO process was another major source of $PM_{2.5}$ in all of the study areas, and the formation rate of $PM_{2.5}$

through the AERO process decreased as the vertical layer increased. Furthermore, VTRA contributed negatively and served as the predominant sink for removing the near-surface $PM_{2.5}$ at the lower layers in Beijing (layers 1-3), Shijiazhuang (layers 1-4), Tianjin and Baoding (layers 1-2), while it slightly contributed positively (acted as source) at the upper layers. This is consistent with the results of Fan et al. (2015), in which VTRA was reported as a sink in the near-surface layers and a source in the upper layers (layer 4 and above). In Beijing (Fig. 3b) and Tianjin (Fig. 3c), HTRA served as another sink for $PM_{2.5}$ across the vertical layers, and the rate initially increased between layers 1 and 2, but continuously decreased as the vertical layer increased. In Shijiazhuang (Fig. 3d), HTRA contributed positively at the lower layers (layers 1-3) and negatively at the upper layers. Considering Baoding (Fig. 3e), HTRA only acted as the source at the first layer, while it behaved as the sink from the second layer upward. It could be deduced that there were vertical and horizontal exports of $PM_{2.5}$ in Beijing and Tianjin at the surface layer, while Shijiazhuang, Baoding, and the whole BTH region witnessed vertical export and horizontal import of $PM_{2.5}$ in the surface layer. DDEP acted as another sink of $PM_{2.5}$, and only existed at the first layer across the study areas (Fan et al., 2015; Ye et al., 2022). DDEP contributions were only found in the first layer because dry deposition was treated as a bivariate variable by the CMAQ model, and integrated it over the whole atmospheric column (Fan et al., 2015). As shown in Fig. 3(f-j), the highest $PM_{2.5}$ concentration was found in the surface layer, and decreased with increases in vertical layer height (Fan et al., 2015). This result could be attributed to the contributions of EMIS and AERO processes, as well as the decreasing trends of the two processes as the vertical layer increased.

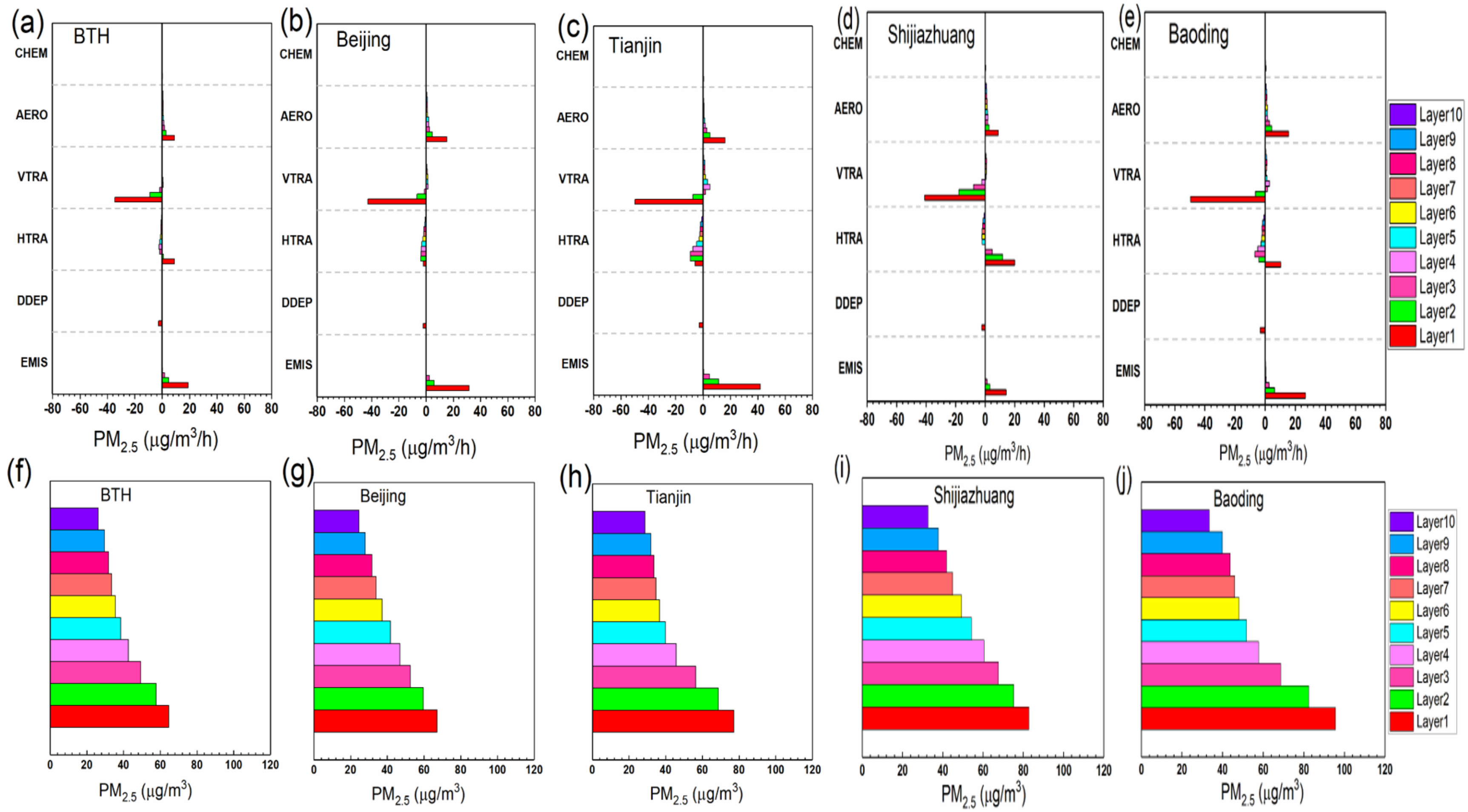

Fig. 3. Hourly $PM_{2.5}$ change rates due to individual atmospheric processes for layers 1-10 (a-e) and evolution of hourly $PM_{2.5}$ vertical profiles (f-j) in Case 2 during the lockdown period. Abbreviations used in this figure are the same as in Fig. 1.

3.6 IPR analysis of $PM_{2.5}$ pollution episodes during lockdown

During the lockdown period, the predicted $PM_{2.5}$ concentrations (in Case 2) (Fig.4; Tables S5-S6) indicated that persistent $PM_{2.5}$ pollution episodes could not be avoided in the BTH region despite reductions in anthropogenic emissions (Sulaymon et al., 2021a). Fig. S6 illustrates the spatial distributions of $PM_{2.5}$ in the BTH region during the lockdown for the two cases. Fig. S6(b) shows that the $PM_{2.5}$ concentrations during the lockdown were higher ($PM_{2.5} \geq 75$ μg/m^3, level II of Chinese air quality standard) in Tianjin and southern Hebei Province, while the northern Hebei was characterized with low concentrations ($PM_{2.5} \leq 50$ μg/m^3). In the prefectural-level cities of BTH region, three severe $PM_{2.5}$ pollution episodes (EPs) (Fig. 4) occurred during the lockdown (Case 2). They are represented as EP1 (January 24-31, 2020), EP2 (February 7-13), and EP3 (February 19-21). It should be noted that EP1 and EP2 coincided with the 2020 Spring (January 25) and Lantern (February 8) festivals, respectively. The statistics for all the EPs in each city are enumerated in Tables S5-S6. For the purpose of process analysis of $PM_{2.5}$ during the EPs, Beijing, Tianjin, Shijiazhuang, and Baoding were selected as the representative cities. As illustrated in Fig. 5, Beijing and Tianjin had the highest $PM_{2.5}$ concentrations during EP2, while Shijiazhuang and Baoding recorded their highest $PM_{2.5}$ concentrations during EP1. Also, during EP2 and EP3, Baoding experienced severe pollution with elevated $PM_{2.5}$ concentrations. This indicates that the region suffered severe pollution episodes during the lockdown. Dai et al. (2021) and Sulaymon et al. (2021a) had previously reported severe haze episodes in the BTH region during the lockdown. Therefore, it becomes pertinent to elucidate the major atmospheric processes responsible for the formation of the EPs.

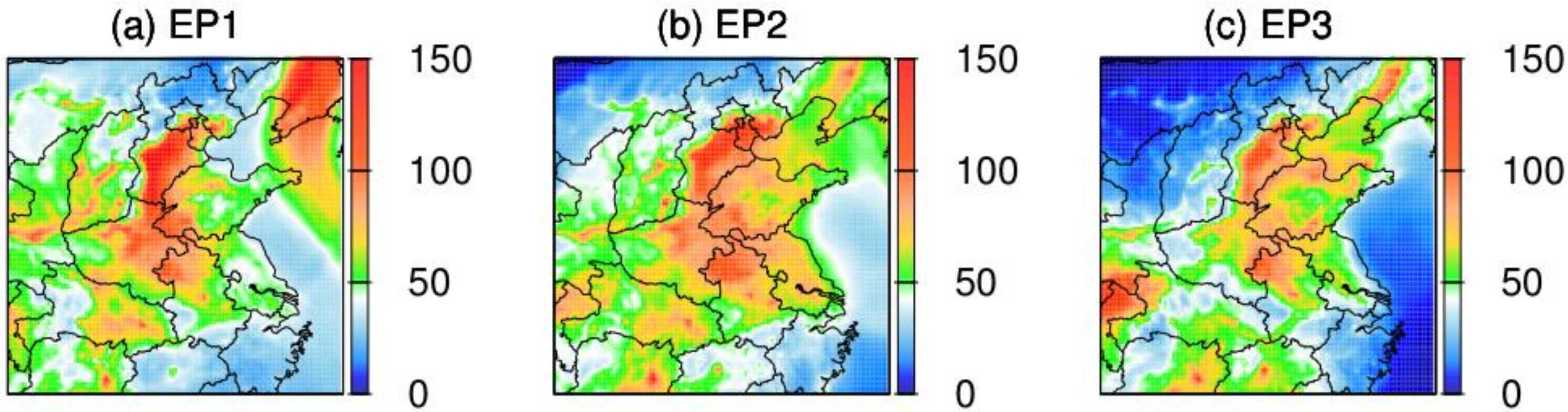

Fig. 4. Spatial distributions of predicted $PM_{2.5}$ (Case 2) during (a) EP1, (b) EP2, and (c) EP3 in the BTH region. Units are $\mu g/m^3$.

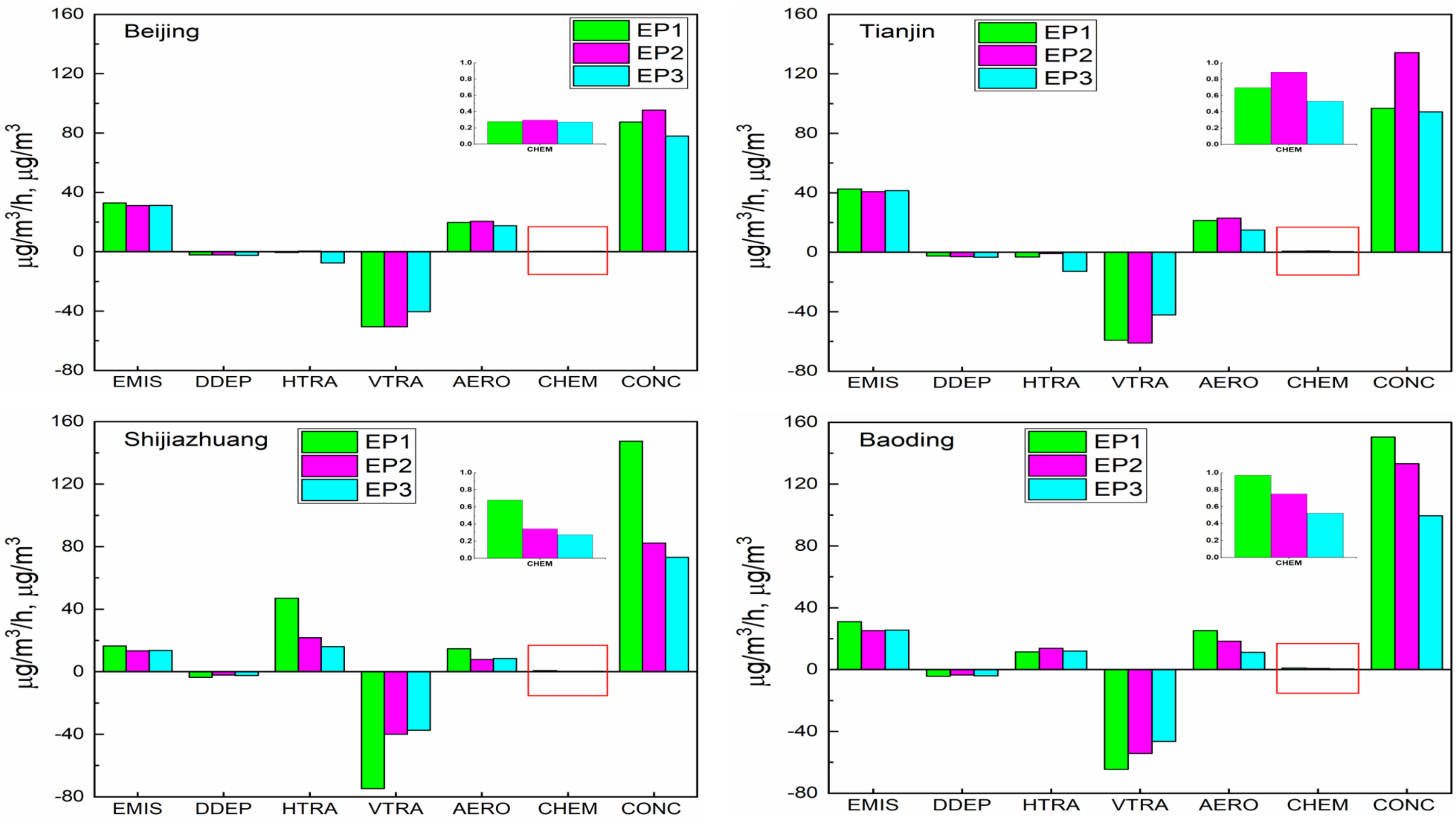

Fig. 5. Contributions of the individual processes to the concentrations of $PM_{2.5}$ (Case 2) at the surface layer during the three pollution episodes in the four representative cities. Abbreviations used in this figure are the same as in Fig. 1.

The contributions of different atmospheric processes to $PM_{2.5}$ formation (in Case 2) during the three EPs in the four representative cities were analyzed. Table S7 shows the average planetary boundary layer height (PBLH) and wind speed for the four cities during the three EPs. The PBLH during the third pollution episode (EP3; PBLH>400 m) was higher than the PBLH during the first two pollution episodes (EP1 and EP2; PBLH<370 m) across the study areas. A thinner boundary layer is more conducive for the accumulation of locally-emitted particles, leading to increased $PM_{2.5}$ concentrations and results in haze events (Fan et al., 2015). As illustrated in Fig. 5, the three pollution episodes in Beijing and Tianjin were principally caused by local emissions (EMIS), while the pollution events in Shijiazhuang and Baoding could be attributed to both local emissions (EMIS) and regional transport (HTRA).

Fig. 5 shows that emissions sources and aerosols were the major positive contributors to $PM_{2.5}$ pollution in Beijing, Tianjin, and Baoding, while horizontal transport was the most significant positive contributor to pollution level in Shijiazhuang, followed by emissions and aerosols. In Baoding, however, HTRA also contributed positively towards $PM_{2.5}$ concentrations throughout the three episodes. There were no significant differences between emissions sources among the three episodes in all of the study areas, and the average total emissions ranged between 13.3-42.6 $\mu g/m^3/h$ across the EPs in the cities. During the three episodes across the four cities, $PM_{2.5}$ was released into the atmosphere through EMIS and AERO processes, and fell back to the surface layer via DDEP process (Fan et al., 2015), with very low rates of dry deposition (ranged between -2.1 $\mu g/m^3/h$ and -4.3 $\mu g/m^3/h$). Also, $PM_{2.5}$ was transported and diffused through VTRA and HTRA processes. In Beijing and Tianjin, there were negligible differences between the contributions from VTRA during the first two episodes, and the total rates were approximately -51 μg/m^3/h and -60 μg/m^3/h in Beijing and Tianjin, respectively. During EP3 in the two cities, the contributions by VTRA (-40 μg/m^3/h in Beijing; and -42 μg/m^3/h in Tianjin) were low relative to the first two episodes. The VTRA contributions in Shijiazhuang (-75 μg/m^3/h) and Baoding (-65 μg/m^3/h) during EP1 were greater than those contributed in Beijing and Tianjin during the same period, and this was due to lower PBLH values (Table S7) in Shijiazhuang and Baoding relative to Beijing and Tianjin. The difference in the VTRA rates between the first two episodes and the third episode in Beijing and Tianjin could be explained by the accumulation of particulates on near-surface layers due to the nature of boundary layer (thinner) (Fan et al., 2015) being exhibited during the first two pollution episodes. Therefore, VTRA had a greater clearing impact for $PM_{2.5}$ during the first two episodes in the two cities. Contrarily, during the third episode in the two cities, a more uniform vertical mixing of $PM_{2.5}$ was achieved, and this was due to the thicker PBLHs during EP3 (Table S7). Hence, the clearing effect of VTRA during EP3 was low compared to EP1 and EP2. In addition, due to higher wind speed during EP3 (Table S7), the negative contributions due to HTRA were higher in Beijing (-8 μg/m^3/h) and Tianjin (-13 μg/m^3/h) during EP3 compared to EP1 and EP2, and this subsequently reduced the contributions from VTRA during EP3. In Shijiazhuang, VTRA also exhibited a very greater clearing effect during EP1 than EP2 and EP3, and similar scenario also occurred in Baoding. In Shijiazhuang, HTRA was the dominant positive contributor to $PM_{2.5}$ throughout the episodes, with the highest contribution rate during EP1. In Baoding, however, there was negligible difference between the contributions from HTRA to $PM_{2.5}$ pollution during the three episodes. Due to availability of several emissions sources in

Beijing and Tianjin, which result to a large quantity of local emissions, $PM_{2.5}$ concentrations were generally higher in the two cities. Hence, the effects of both VTRA and HTRA on pollution levels were negative during the three pollution episodes, and both mainly provided dilution and clearing effects in the two cities (Fan et al., 2015). On the other hand, in both Shijiazhuang and Baoding, horizontal transport contributed positively and significantly increased $PM_{2.5}$ concentrations during the three episodes. It is also worthy to mention that $PM_{2.5}$ concentrations during the three episodes in the four cities were greatly and positively influenced by the planetary boundary layer height, as the episode with the lowest PBLH had the highest $PM_{2.5}$ concentration in a city. The results of the present study are consistent with those reported by Fan et al. (2015) during three pollution episodes over the PRD region. Fan et al. (2015) had reported surface emissions, aerosol processes, and horizontal transport as the major contributors to air pollution episodes over the PRD. In the PBL (Fig. S7), EMIS and AERO were also the dominant contributors to $PM_{2.5}$ concentrations in Beijing and Tianjin, HTRA was the most important source in Shijiazhuang, and EMIS, AERO, and HTRA actively contributed to $PM_{2.5}$ formation in Baoding during the EPs. VTRA was the major removal pathway. However, the contribution and removal rates were low in the PBL relative to the surface layer.

To better understand the roles of the atmospheric processes towards the pollution episodes, $PM_{2.5}$ formation and removal within the PBL (layers 1-10) were analyzed in Tianjin (Fig. 6), while those of other three cities are illustrated in Figs S8-S10. Considering the three EPs in Tianjin, the positive contributions of EMIS and AERO processes to the hourly $PM_{2.5}$ significantly occurred within layers 1-3 (Fig. 6a-c), while they both contributed less at upper layers. Also, there were vertical imports of $PM_{2.5}$ (although very low) at upper layers (layers 3-10 for EP1 and EP2; and layers 3-6 for EP3). Conversely, VTRA (layers 1-2) and HTRA (layers 1-10) served as the predominant sinks and $PM_{2.5}$ removal pathways. DDEP process also acted as another sink for $PM_{2.5}$ during the EPs, and only existed at the first layer (Fan et al., 2015). The contributions by CHEM process were negligible across the vertical layers (Fan et al., 2015; Ye et al., 2022). As shown in Fig. 6(d-f), EP2 was characterized with the highest $PM_{2.5}$ concentrations, followed by EP1 and EP3. Furthermore, the $PM_{2.5}$ formation processes in the surface layer during the EPs were compared. Fig. 7 illustrates the percentage contributions of the atmospheric processes to $PM_{2.5}$ formation/removal during the EPs in the four cities. The total contributions of EMIS and AERO (EMIS+AERO) during the EPs ranged between 80-89% and 88-97% in Beijing (Fig. 7a) and Tianjin (Fig. 7b), respectively. In Shijiazhuang (Fig. 7c), the contributions due to HTRA during the episodes ranged between 44-61%, making it the major $PM_{2.5}$ source. As earlier revealed in Fig. 5, $PM_{2.5}$ formation during the episodes in Baoding (Fig. 7d) was attributed to the contributions of EMIS, AERO, and HTRA, with total contributions of 93-98% during the EPs. In the four cities, $PM_{2.5}$ removal was dominantly influenced by VTRA during the EPs.

Furthermore, the diel variations of the contributions of various atmospheric processes to the formation of $PM_{2.5}$ as well as the hourly variations of $PM_{2.5}$ concentrations at the surface layer during the three episodes are illustrated in Fig. 8. In Beijing, EMIS and AERO processes were the major $PM_{2.5}$ sources, and showed two peaks (07:00 LT and 20:00 LT) during the three episodes.

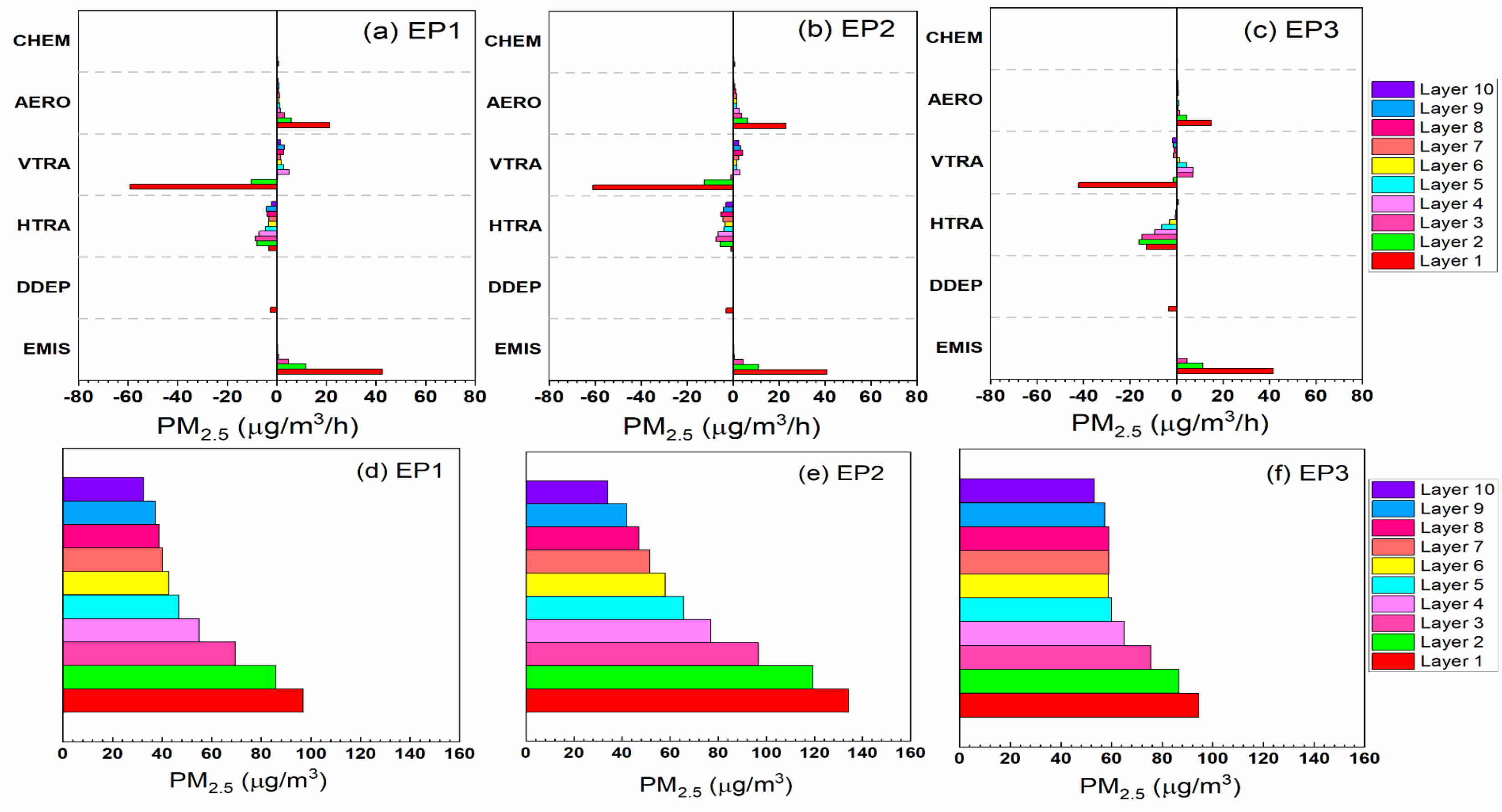

571

572 **Fig. 6.** Hourly $PM_{2.5}$ change rates (Case 2) due to individual atmospheric processes for layers 1-10 (a-c) and evolution of hourly $PM_{2.5}$
573 vertical profiles (d-f) during the three pollution episodes in Tianjin. Abbreviations used in this figure are the same as in Fig. 1.
574

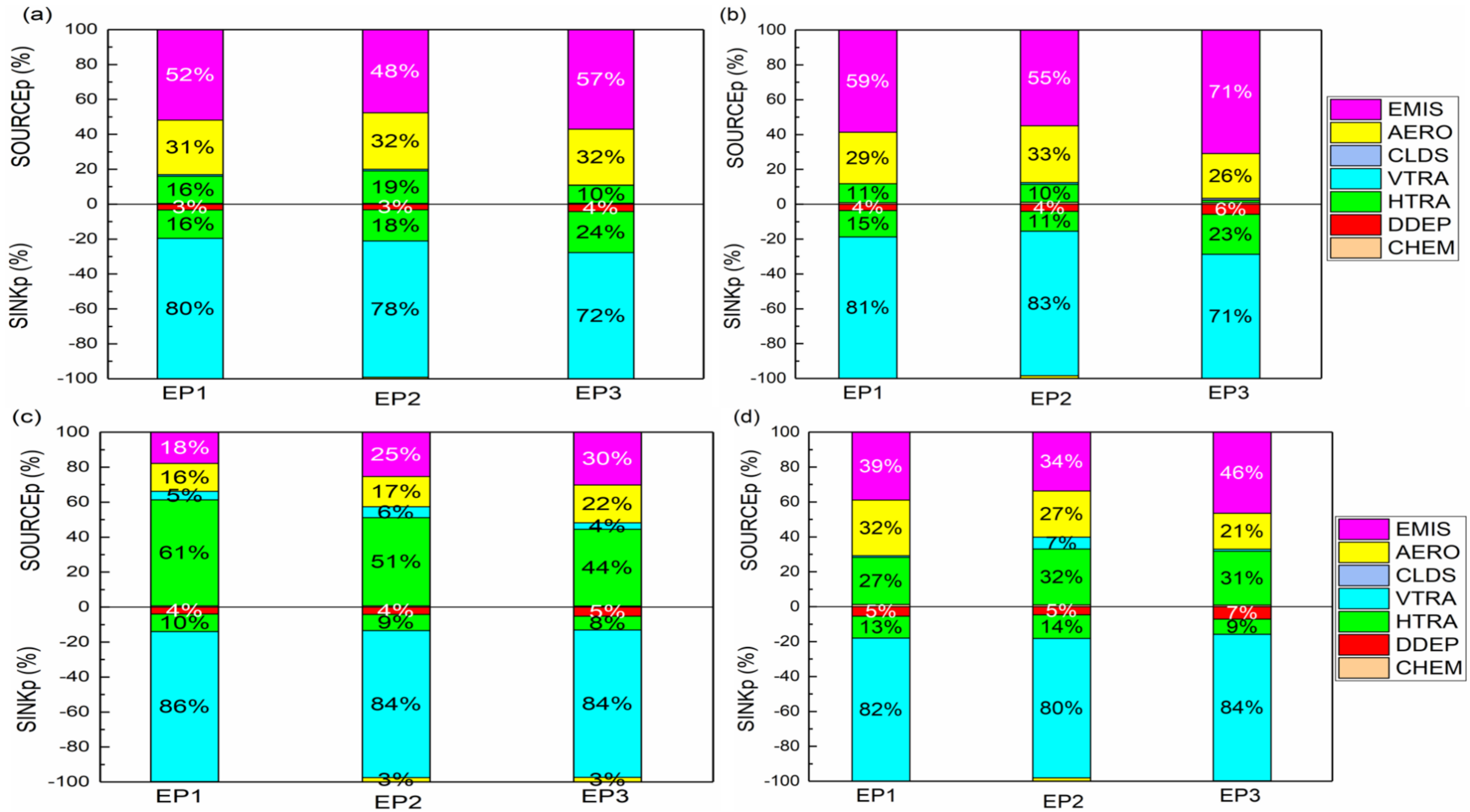

Fig. 7. Positive and negative contribution ratios of the individual processes to $PM_{2.5}$ concentrations (Case 2) at the surface layer in (a) Beijing, (b) Tianjin, (c) Shijiazhuang, and (d) Baoding during the three pollution episodes. Abbreviations used in this figure are the same as in Fig. 2.

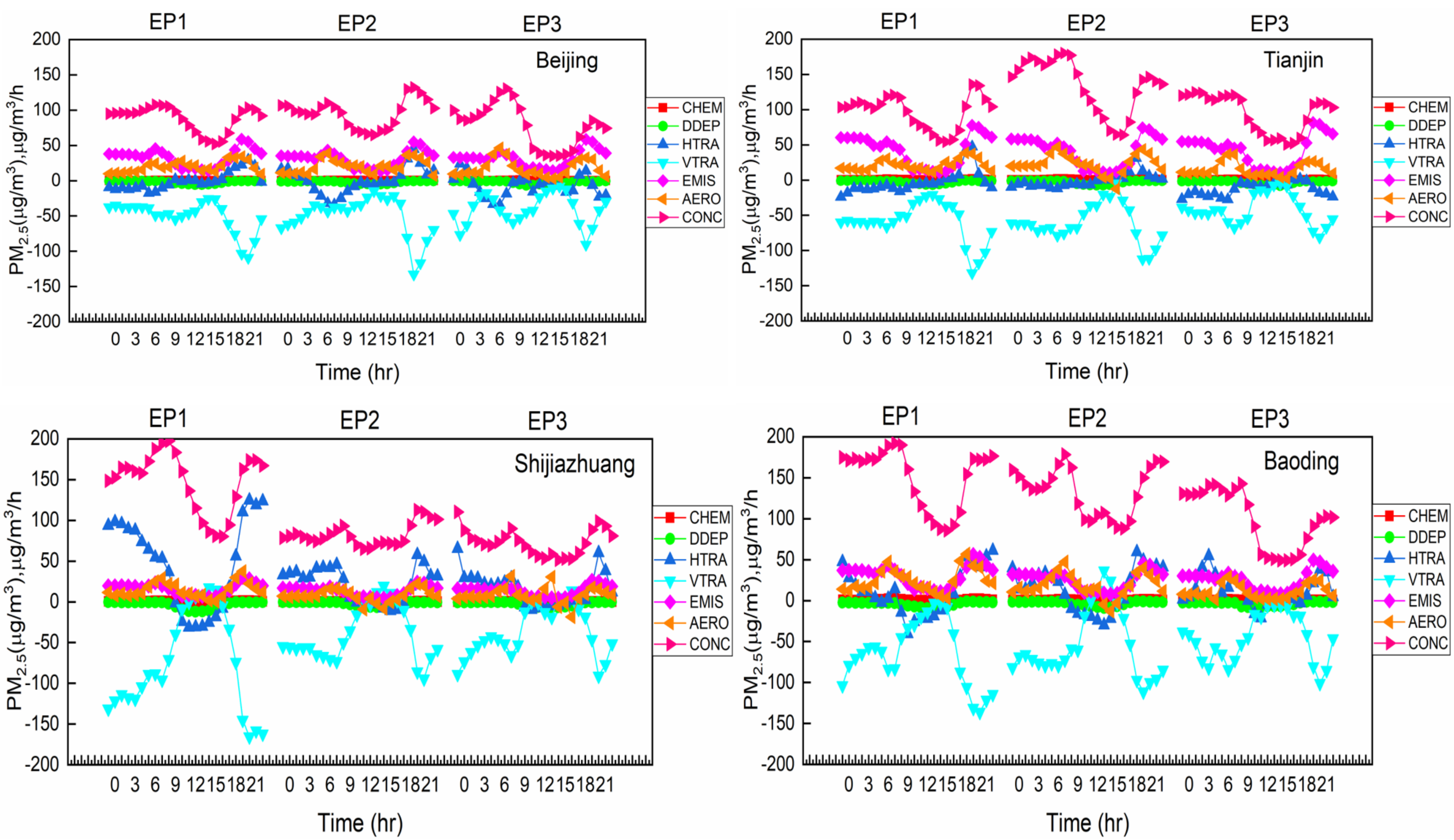

Fig. 8. Diel variations of contributions of individual processes to $PM_{2.5}$ formation (Case 2) at the surface layer during the three pollution episodes in the four representative cities. Abbreviations used in this figure are the same as in Fig. 1.

The highest rates of EMIS during the EPs ranged between 54.8-58.6 μg/m^3/h, all occurred at 20:00 LT. The VTRA dominated the $PM_{2.5}$ removal, with the highest removal rates of -109.3 μg/m^3/h (at 21:00 LT), -132.6 μg/m^3/h (at 20:00 LT), and -90.7 μg/m^3/h (at 20:00 LT) during EP1, EP2, and EP3, respectively. In addition, HTRA was another major $PM_{2.5}$ removal pathway during the EPs. However, HTRA later acted as another $PM_{2.5}$ source during EP1 (17:00-22:00 LT; with maximum rate of 29.6 μg/m^3/h at 21:00 LT), EP2 (00:00-03:00 and 18:00-23:00 LT; with maximum rate of 44.7 μg/m^3/h at 20:00 LT), and EP3 (00:00-02:00 and 19:00-20:00 LT; with highest rate of 24.0 μg/m^3/h at 01:00 LT), leading to the horizontal import of $PM_{2.5}$ during the periods. Considering Tianjin, EMIS process was the dominant $PM_{2.5}$ source and exhibited two distinct peaks (00:00 LT and 20:00 LT) during the three episodes. The highest contributions of EMIS during EP1, EP2, and EP3 were 77.7 μg/m^3/h, 74.1 μg/m^3/h, and 81.7 μg/m^3/h, respectively, all occurred at 20:00 LT. AERO process was another $PM_{2.5}$ source with two peaks during EP1 (07:00 LT and 19:00 LT), EP2 and EP3 (07:00 LT and 20:00 LT). The negative contributions of VTRA made it the dominant $PM_{2.5}$ sink throughout the 24hrs period, with the maximum removal rates of -132.1 μg/m^3/h (at 20:00 LT), -112.5 μg/m^3/h (at 20:00 LT), and -81.3 μg/m^3/h (at 21:00 LT) during EP1, EP2, and EP3, respectively. Besides VTRA, HTRA served as the second major $PM_{2.5}$ sink during the three EPs. However, HTRA later became another $PM_{2.5}$ source during EP1 (16:00-21:00 LT; with maximum rate of 47.5 μg/m^3/h), EP2 (14:00-23:00; with maximum rate of 31.1 μg/m^3/h), and EP3 (17:00-18:00 LT; with very low rates). In Shijiazhuang, HTRA was the major $PM_{2.5}$ contributor, and showed two peaks during EP1 (98.3 μg/m^3/h at 01:00 LT and 124.8 μg/m^3/h at 21:00 LT), EP2 (45.8 μg/m^3/h at 08:00 LT and 57.8 μg/m^3/h at 20:00 LT), and EP3 (65.2 μg/m^3/h at 00:00 LT and 60.3 μg/m^3/h at 21:00 LT). The VTRA was the dominant $PM_{2.5}$ removal pathway, with the highest rates of -165.6 μg/m^3/h, -94.5 μg/m^3/h, and -91.0 μg/m^3/h during EP1, EP2, and EP3, respectively, all at 21:00 LT. However, VTRA later became positive and served as another $PM_{2.5}$ source during EP1 (13:00-16:00 LT; with maximum rate of 17.4 μg/m^3/h at 15:00 LT), EP2 (14:00-17:00 with maximum rate of 19.4 μg/m^3/h at 15:00 LT), and EP3 (15:00-17:00 with highest rate of 13.6 μg/m^3/h at 17:00 LT), resulting to the vertical import of $PM_{2.5}$ during the periods. In Baoding, EMIS, AERO, and HTRA were the major $PM_{2.5}$ formation pathways during nighttime, while EMIS and AERO were the dominant sources during daytime. Being the major $PM_{2.5}$ removal pathway, VTRA had the highest rates of -136.3 μg/m^3/h (21:00 LT), -111.4 μg/m^3/h (20:00 LT), and -101.1 μg/m^3/h (21:00 LT) during EP1, EP2, and EP3, respectively. During EP2, VTRA shortly behaved as another $PM_{2.5}$ source (13:00-15:00 LT, with highest rate of 36.5 μg/m^3/h. With very low rates during the episodes, DDEP and CHEM processes served as $PM_{2.5}$ sink and source, respectively across the four cities. The $PM_{2.5}$ concentrations peaked in Beijing (EP1: 107.8 μg/m^3 at 07:00 LT; EP2: 132.1 μg/m^3 at 20:00 LT; EP3: 130.3 μg/m^3 at 08:00 LT), Tianjin (EP1: 135.7 μg/m^3 at 20:00 LT; EP2: 180.1 μg/m^3 at 08:00 LT; EP3: 124.6 μg/m^3 at 02:00 LT), Shijiazhuang (EP1: 197.6 μg/m^3 at 09:00 LT; EP2: 112.6 μg/m^3 at 20:00 LT; EP3: 110.3 μg/m^3 at 00:00 LT), and Baoding (EP1: 192.0 μg/m^3 at 08:00 LT; EP2: 178.2 μg/m^3 at 08:00 LT; EP3: 142.8 μg/m^3 at 09:00 LT).

4. Conclusions

This study employed the PA tool in the CMAQ model to identify and quantify the contributions of individual atmospheric processes and meteorology to the three $PM_{2.5}$ pollution episodes that occurred during the COVID-19 lockdown in the BTH region even with the required reductions in human activities. Due to emission reductions, the total $PM_{2.5}$ concentrations across the BTH decreased by 6.2-11.0%. However, the region still experienced three $PM_{2.5}$ pollution episodes during the lockdown. The IPR results showed that the EMIS and AERO processes were the dominant positive contributors to the net surface $PM_{2.5}$ in Beijing and Tianjin, while the EMIS, HTRA, and AERO pathways dominated the net surface $PM_{2.5}$ formation in Shijiazhuang and Baoding. In Case 2, the decrease in surface $PM_{2.5}$ concentrations across the BTH was primarily attributed to the reduced EMIS and AERO processes, which shows the reduction in the primary source of $PM_{2.5}$ as well as decrease in the formation of secondary aerosol through gas-to-particle conversion. Both vertical and horizontal transport had significant impacts on the changes in surface $PM_{2.5}$. Elevated $PM_{2.5}$ concentrations (in Case 2) in the BTH region during the lockdown could be attributed to a low vertical transport rate of $PM_{2.5}$ from the surface layer to the upper layers. Furthermore, during the three pollution episodes, EMIS and AERO processes were the dominant sources of $PM_{2.5}$ formation in Beijing, Tianjin, and Baoding, while HTRA was the major source in Shijiazhuang. In all of the four cities, vertical transport served as the major $PM_{2.5}$ sink throughout the episodes, with differences in vertical rates between the episodes in each city. The pollution levels in the four cities were greatly and positively influenced by the PBLH, as the episode with the lowest PBLH had the highest $PM_{2.5}$ concentration in a city. This study reveals the various atmospheric processes and meteorological factors governing the $PM_{2.5}$ formation during the severe pollution episodes in the BTH region, as well as the changes in the individual atmospheric processes and $PM_{2.5}$ concentrations due to the lockdown measures, and shows that the existing emissions control strategies could not prevent pollution episodes in the region, especially during the winter period. Since it is not possible to control the aerosol and transport processes, only further changes in emissions will reduce the severity of the episodes. Thus, better forecasting of the conditions that would foment such episodes combined with more effective emissions control strategies are urgently required to be able to mitigate such future severe pollution episodes in the BTH region.

Acknowledgements

This work was supported by the National Natural Science Foundation of China (42007187).

Conflict of Interest

The authors declare that they have no conflict of interest.

Open Research

The simulated and the observation data ($PM_{2.5}$ and meteorological variables) used in this study for model evaluation and postprocessing (Figures and Tables) can be found in Sulaymon et al. (2023).

References

Ambient air pollution (2021). Retrieved 28 October 2021, from https://www.who.int/airpollution/ambient/health-impacts/en

Bashir, M. F., MA, B. J., Bilal, Komal, B., Bashir, M. A., Farooq, T. H., Iqbal, N., & Bashir, M. (2020). Correlation between environmental pollution indicators and COVID-19 pandemic: A brief study in Californian context. Environmental Research, 187. https://doi.org/10.1016/j.envres.2020.109652

Bhati, S., & Mohan, M. (2018). WRF-urban canopy model evaluation for the assessment of heat island and thermal comfort over an urban airshed in India under varying land use/land cover conditions. Geoscience Letters, 5(1). https://doi.org/10.1186/s40562-018-0126-7

Boylan, J. W., & Russel, A. G. (2006). PM and light extinction model performance metrics, goals, and criteria for three-dimensional air quality models. Atmospheric Environment, 40, 4946-4959. https://doi.org/10.1016/j.atmosenv.2005.09.087

Chang, X., Wang, S., Zhao, B., Cai, S., & Hao, J. (2018). Assessment of inter-city transport of particulate matter in the Beijing-Tianjin-Hebei region. Atmospheric Chemistry and Physics, 18(7), 4843-4858. https://doi.org/10.5194/acp-18-4843-2018

Chang, X., Wang, S., Zhao, B., Xing, J., Liu, X., Wei, L., Song, Y., Wu, W., Cai, S., Zheng, H., Ding, D., & Zheng, M. (2019). Contributions of inter-city and regional transport to $PM_{2.5}$ concentrations in the Beijing-Tianjin-Hebei region and its implications on regional joint air pollution control. Science of the Total Environment, 660, 1191-1200. https://doi.org/10.1016/j.scitotenv.2018.12.474

Chauhan A., & Singh, R.P. (2020). Decline in $PM_{2.5}$ concentrations over major cities around the world associated with COVID-19. Environ. Res. 187, 109634. 10.1016/j.envres.2020.109634

Chauhan, A.K., & Singh, R.P. (2021). Effect of lockdown on HCHO and trace gases over India during March 2020. AAQR, Volume 21, Issue 4, Article Number 200445. 10.4209/aaqr.2020.07.0445.

Chen, D., Xia, L., Guo, X., Lang, J., Zhou, Y., Wei, L., & Fu, X. (2021). Impact of inter-annual meteorological variation from 2001 to 2015 on the contribution of regional transport to PM2.5 in Beijing, China. Atmospheric Environment, 260. https://doi.org/10.1016/j.atmosenv.2021.118545

Chen, L., Shi, M., Gao, S., Li, S., Mao, J., Zhang, H., Sun, Y., Bai, Z., & Wang, Z. (2017). Assessment of population exposure to $PM_{2.5}$ for mortality in China and its public health benefit based on BenMAP. Environmental Pollution, 221, 311-317. https://doi.org/10.1016/j.envpol.2016.11.080

Croft, D. P., Zhang, W., Lin, S., Thurston, S. W., Hopke, P. K., Masiol, M., Squizzato, S., van Wijngaarden, E., Utell, M. J., & Rich, D. Q. (2019). The association between respiratory infection and air pollution in the setting of air quality policy and economic change. Annals of the American Thoracic Society, 16(3), 321-330. https://doi.org/10.1513/AnnalsATS.201810-691OC

Cui, Y., Ji, D., Maenhaut, W., Gao, W., Zhang, R., & Wang, Y. (2020). Levels and sources of hourly PM2.5-related elements during the control period of the COVID-19 pandemic at a rural site between Beijing and Tianjin. Science of the Total Environment, 744. https://doi.org/10.1016/j.scitotenv.2020.140840

Dai, Q., Ding, J., Hou, L., Li, L., Cai, Z., Liu, B., Song, C., Bi, X., Wu, J., Zhang, Y., Feng, Y., & Hopke, P. K. (2021). Haze episodes before and during the COVID-19 shutdown in Tianjin, China: Contribution of fireworks and residential burning. Environmental Pollution, 286. https://doi.org/10.1016/j.envpol.2021.117252

Dai, Q., Ding, J., Song, C., Liu, B., Bi, X., Wu, J., Zhang, Y., Feng, Y., & Hopke, P. K. (2021). Changes in source contributions to particle number concentrations after the COVID-19 outbreak: Insights from a dispersion normalized PMF. Science of the Total Environment, 759. https://doi.org/10.1016/j.scitotenv.2020.143548

Dai, Q., Liu, B., Bi, X., Wu, J., Liang, D., Zhang, Y., Feng, Y., & Hopke, P. K. (2020). Dispersion normalized PMF provides insights into the significant changes in source contributions to $PM_{2.5}$ after the CoviD-19 outbreak. Environmental Science and Technology, 54(16), 9917-9927. https://doi.org/10.1021/acs.est.0c02776

Emery, C., Tai, E., & Yarwood, G. (2001). Enhanced Meteorological Modeling and Performance Evaluation for Two Texas Ozone Episodes, Prepared for the Texas Natural Resource Conservation Commission. Environ International Corporation, Novato, CA.

Fan, Q., Lan, J., Liu, Y., Wang, X., Chan, P., Hong, Y., Feng, Y., Liu, Y., Zeng, Y., & Liang, G. (2015). Process analysis of regional aerosol pollution during spring in the Pearl River Delta region, China. Atmos. Environ. 122, 829-838.

Fan, H., Zhao, C., & Yang, Y. (2020). A comprehensive analysis of the spatio-temporal variation of urban air pollution in China during 2014-2018. Atmospheric Environment, 220. https://doi.org/10.1016/j.atmosenv.2019.117066

Fu, X.,Wang, T., Gao, J., Wang, P., Liu, Y., Wang, S., Zhao, B., & Xue, L. (2020). Persistent heavy winter nitrate pollution by increased photochemical oxidants in Northern China. Environ. Sci. Technol., 54, 3881-3889.

Gao, C., Li, S., Liu, M., Zhang, F., Achal, V., Tu, Y., Zhang, S., & Cai, C. (2021). Impact of the COVID-19 pandemic on air pollution in Chinese megacities from the perspective of traffic volume and meteorological factors. Science of the Total Environment, 773. https://doi.org/10.1016/j.scitotenv.2021.145545

Hopke, P. K., Croft, D., Zhang, W., Lin, S., Masiol, M., Squizzato, S., Thurston, S. W., van Wijngaarden, E., Utell, M. J., & Rich, D. Q. (2019). Changes in the acute response of respiratory diseases to PM 2.5 in New York State from 2005 to 2016. Science of the Total Environment, 677, 328-339. https://doi.org/10.1016/j.scitotenv.2019.04.357

Hu, J., Chen, J., Ying, Q., & Zhang, H. (2016). One-year simulation of ozone and particulate matter in China using WRF/CMAQ modeling system. Atmospheric Chemistry and Physics, 16(16), 10333-10350. https://doi.org/10.5194/acp- 16-10333-2016

Hu, J., Wu, L., Zheng, B., Zhang, Q., He, K., Chang, Q., Li, X., Yang, F., Ying, Q., & Zhang, H. (2015). Source contributions and regional transport of primary particulate matter in China. Environmental Pollution, 207, 31-42. https://doi.org/10.1016/j.envpol.2015.08.037

Hua, J., Zhang, Y., de Foy, B., Shang, J., Schauer, J. J., Mei, X., Sulaymon, I. D., & Han, T. (2021). Quantitative estimation of meteorological impacts and the COVID-19 lockdown reductions on NO2 and PM2.5 over the Beijing area using Generalized Additive Models (GAM). Journal of Environmental Management, 291. https://doi.org/10.1016/j.jenvman.2021.112676

Huang, J.P., Fung, J.C.H., Lau, A.K.H., & Qin, Y. (2005). Numerical Simulation and Process Analysis of Typhoon-Related Ozone Episodes in Hong Kong, p. 110.

Jiang, Y., Xing, J., Wang, S., Chang, X., Liu, S., Shi, A., Liu, B., & Sahu, S. K. (2021). Understand the local and regional contributions on air pollution from the view of human health impacts. Frontiers of Environmental Science and Engineering, 15(5). https://doi.org/10.1007/s11783-020-1382-2

Kwok, R. H. F., Napelenok, S. L., & Baker, K. R. (2013). Implementation and evaluation of $PM_{2.5}$ source contribution analysis in a photochemical model. Atmospheric Environment, 80, 398-407. https://doi.org/10.1016/j.atmosenv.2013.08.017

Li, L., Chen, C.H., Huang, C., Huang, H.Y., Zhang, G.F., Wang, Y.J., Wang, H.L., Lou, S.R., Qiao, L.P., Zhou, M., Chen, M.H., Chen, Y.R., Streets, D.G., Fu, J.S., & Jang, C.J. (2012). Process analysis of regional ozone formation over the Yangtze River Delta, China using the Community Multi-scale Air Quality modeling system. Atmos. Chem. Phys. 12, 10971-10987.

Li, L., Li, Q., Huang, L., Wang, Q., Zhu, A., Xu, J., Liu, Z., Li, H., Shi, L., Li, R., Azari, M., Wang, Y., Zhang, X., Liu, Z., Zhu, Y., Zhang, K., Xue, S., Ooi, M. C. G., Zhang, D., & Chan, A. (2020). Air quality changes during the COVID-19 lockdown over the Yangtze River Delta Region: An insight into the impact of human activity pattern changes on air pollution variation. Science of the Total Environment, 732. https://doi.org/10.1016/j.scitotenv.2020.139282

Li, M., Song, Y., Huang, X., Li, J., Mao, Y., Zhu, T., Cai, X., & Liu, B. (2014). Improving mesoscale modeling using satellite-derived land surface parameters in the Pearl River Delta region, China. Journal of Geophysical Research, 119(11), 6325-6346. https://doi.org/10.1002/2014JD021871

Li, M., Zhang, Z., Yao, Q., Wang, T., Xie, M., Li, S., Zhuang, B., & Han, Y. (2021). Nonlinear responses of particulate nitrate to NOx emission controls in the megalopolises of China. Atmospheric Chemistry and Physics, 21(19), 15135-15152. https://doi.org/10.5194/acp-21-15135-2021

Li, X., Huang, L., Li, J., Shi, Z., Wang, Y., Zhang, H., Ying, Q., Yu, X., Liao, H., & Hu, J. (2019). Source contributions to poor atmospheric visibility in China. Resources, Conservation & Recycling, 143: 167-177.

Liu, J., Mauzerall, D. L., Chen, Q., Zhang, Q., Song, Y., Peng, W., Klimont, Z., Qiu, X. H., Zhang, S. Q., Hu, M., Lin, W. L., Smith, K. R., & Zhu, T. (2016) Air pollutant emissions from Chinese households: A major and underappreciated ambient pollution source. P. Natl. Acad. Sci. USA, 113, 7756-7761.

Liu, P., & Zhang, Y. (2011). Use of a process analysis tool for diagnostic study on fine particulate matter predictions in the U.S. Part II: analyses and sensitivity simulations. Atmos. Poll. Res. 2, 61-71.

Liu, T., Wang, X., Hu, J., Wang, Q., An, J., Gong, K., Sun, J., Li, L., Qin, M., Li, J., Tian, J., Huang, Y., Liao, H., Zhou, M., Hu, Q., Yan, R., Wang, H., & Huang, C. (2020). Driving Forces of Changes in Air Quality during the COVID-19 Lockdown Period in the Yangtze River Delta Region, China. Environmental Science and Technology Letters, 7(11), 779-786. https://doi.org/10.1021/acs.estlett.0c00511

Liu, X.H., Zhang, Y., Xing, J., Zhang, Q., Wang, K., Streets, D.G., Jang, C., Wang, W.X., & Hao, J.M. (2010). Understanding of regional air pollution over China using CMAQ. Part II: process analysis and sensitivity of ozone and particulate matter to precursor emissions. Atmos. Environ. 44, 3719-3727.

Ma, J., Shen, J., Wang, P., Zhu, S., Wang, Y., Wang, P., Wang, G., Chen, J., & Zhang, H. (2021). Modeled changes in source contributions of particulate matter during the COVID-19 pandemic in the Yangtze River Delta, China. Atmospheric Chemistry and Physics, 21(9), 7343-7355. https://doi.org/10.5194/acp-21-7343-2021

Mishra, R., Mishra, N.C., Singh, R., & Mishra, R. (2021). Improvement of atmospheric pollution in the capital cities of US during COVID-19, https://doi.org/10.1002/essoar.10505250.2

Muhammad, S., Long, X., & Salman, M. (2020). COVID-19 pandemic and environmental pollution: A blessing in disguise? Science of the Total Environment, 728. https://doi.org/10.1016/j.scitotenv.2020.138820

Orak, N. H., & Ozdemir, O. (2021). The impacts of COVID-19 lockdown on PM_{10} and SO_2 concentrations and association with human mobility across Turkey. Environmental Research, 197. https://doi.org/10.1016/j.envres.2021.111018.

Qiao, X., Tang, Y., Hu, J., Zhang, S., Li, J., Kota, S. H., Wu, L., Gao, H., Zhang, H., & Ying, Q. (2015). Modeling dry and wet deposition of sulfate, nitrate, and ammonium ions in Jiuzhaigou National Nature Reserve, China using a source-oriented CMAQ model: Part I. Base case model results. Science of the Total Environment, 532, 831-839. https://doi.org/10.1016/j.scitotenv.2015.05.108

Querol, X., Massagué, J., Alastuey, A., Moreno, T., Gangoiti, G., Mantilla, E., Duéguez, J. J., Escudero, M., Monfort, E., Pérez García-Pando, C., Petetin, H., Jorba, O., Vázquez, V., de la Rosa, J., Campos, A., Muñóz, M., Monge, S., Hervás, M., Javato, R., & Cornide, M. J. (2021). Lessons from the COVID-19 air pollution decrease in Spain: Now what? Science of the Total Environment, 779. https://doi.org/10.1016/j.scitotenv.2021.146380

Shang, X., Zhang, K., Meng, F., Wang, S., Lee, M., Suh, I., Kim, D., Jeon, K., Park, H., Wang, X., & Zhao, Y. (2018). Characteristics and source apportionment of fine haze aerosol in Beijing during the winter of 2013. Atmospheric Chemistry and Physics, 18(4), 2573-2584. https://doi.org/10.5194/acp-18-2573-2018

Sharma, S., Zhang, M., Anshika, Gao, J., Zhang, H., & Kota, S. H. (2020). Effect of restricted emissions during COVID-19 on air quality in India. Science of the Total Environment, 728. https://doi.org/10.1016/j.scitotenv.2020.138878

Shen, J., Zhao, Q., Cheng, Z., Huo, J., Zhu, W., Zhang, Y., Duan, Y., Wang, X., Antony Chen, L. W., & Fu, Q. (2020). Evolution of source contributions during heavy fine particulate matter (PM2.5) pollution episodes in eastern China through online measurements. Atmospheric Environment, 232. https://doi.org/10.1016/j.atmosenv.2020.117569

Shen, L., Wang, H., Zhu, B., Zhao, T., Liu, A., Lu, W., Kang, H., & Wang, Y. (2021). Impact of urbanization on air quality in the Yangtze River Delta during the COVID-19 lockdown in China. Journal of Cleaner Production, 296. https://doi.org/10.1016/j.jclepro.2021.126561

Shen, L., Zhao, T., Wang, H., Liu, J., Bai, Y., Kong, S., Zheng, H., Zhu, Y., & Shu, Z. (2021). Importance of meteorology in air pollution events during the city lockdown for COVID-19 in Hubei Province, Central China. Science of the Total Environment, 754. https://doi.org/10.1016/j.scitotenv.2020.142227

Shi, Z., Huang, L., Li, J., Ying, Q., Zhang, H., & Hu, J. (2020). Sensitivity analysis of the surface ozone and fine particulate matter to meteorological parameters in China. Atmospheric Chemistry and Physics, 20(21), 13455-13466. https://doi.org/10.5194/acp-20-13455-2020

Shi, Z., Li, J., Huang, L., Wang, P., Wu, L., Ying, Q., Zhang, H., Lu, L., Liu, X., Liao, H., & Hu, J. (2017). Source apportionment of fine particulate matter in China in 2013 using a source-oriented chemical transport model. Science of the Total Environment, 1476-1487. https://doi.org/10.1016/j.scitotenv.2017.06.019

Singh, R.P., & Chauhan, A.K. (2020). Impact of lockdown on air quality in India during COVID-19 pandemic. Air Quality, Atmosphere and Health, Volume: 13, Issue: 8, 921-928.

Srivastava, A. (2021). COVID-19 and air pollution and meteorology-an intricate relationship: A review. In Chemosphere (Vol. 263). Elsevier Ltd. https://doi.org/10.1016/j.chemosphere.2020.128297

Sulaymon, I. D., Mei, X., Yang, S., Chen, S., Zhang, Y., Hopke, P. K., Schauer, J. J., & Zhang, Y. (2020). $PM_{2.5}$ in Abuja, Nigeria: Chemical characterization, source apportionment, temporal variations, transport pathways and the health risks assessment. Atmospheric Research, 237. https://doi.org/10.1016/j.atmosres.2019.104833

Sulaymon, I. D., Zhang, Y., Hopke, P. K., Hu, J., Zhang, Y., Li, L., Mei, X., Gong, K., Shi, Z., Zhao, B., & Zhao, F. (2021a). Persistent high PM2.5 pollution driven by unfavorable meteorological conditions during the COVID-19 lockdown period in the Beijing-Tianjin-Hebei region, China. Environmental Research, 198. https://doi.org/10.1016/j.envres.2021.111186

Sulaymon, I. D., Zhang, Y., Hu, J., Hopke, P. K., Zhang, Y., Zhao, B., Xing, J., Li, L., & Mei, X. (2021b). Evaluation of regional transport of PM2.5 during severe atmospheric pollution episodes in the western Yangtze River Delta, China. Journal of Environmental Management, 293. https://doi.org/10.1016/j.jenvman.2021.112827

Sulaymon, I. D., Zhang, Y., Hopke, P. K., Zhang, Y., Hua, J., & Mei, X. (2021c). COVID-19 pandemic in Wuhan: Ambient air quality and the relationships between criteria air pollutants and meteorological variables before, during, and after lockdown. Atmospheric Research, 250. https://doi.org/10.1016/j.atmosres.2020.105362

Sulaymon, I. D., Zhang, Y., Hopke, P. K., Hu, J., Rupakheti, D., Xie, X., Zhang, Y., Ajibade, F. O., Hua, J., & She, Y. (2021d). Influence of transboundary air pollution and meteorology on air quality in three major cities of Anhui Province, China. Journal of Cleaner Production, 129641. https://doi.org/10.1016/j.jclepro.2021.12964

Sulaymon, I.D., Zhang, Y., Hopke, P.K., Guo, S., Ye, F., Sun, J., Zhu, Y., & Hu, J. (2023). Quantifying the contributions of atmospheric processes and meteorology to severe $PM_{2.5}$ pollution episodes during the COVID-19 lockdown in the Beijing-Tianjin-Hebei, China. [Dataset]. Zenodo. https://doi.org/10.5281/zenodo.7711747

Tang, L., Shang, D., Fang, X., Wu, Z., Qiu, Y., Chen, S., Li, X., Zeng, L., Guo, S., & Hu, M. (2021). More significant impacts from new particle formation on haze formation during COVID-19 lockdown. *Geophysical Research Letters*, *48*, e2020GL091591. https://doi.org/10.1029/2020GL091591

Wang, B., Qiu, T., & Chen, B. (2014). Photochemical process modeling and analysis of ozone generation. Chin. J. Chem. Eng. 22, 721-729.

Wang, N., Lyu, X. P., Deng, X. J., Guo, H., Deng, T., Li, Y., Yin, C. Q., Li, F., & Wang, S. Q. (2016). Assessment of regional air quality resulting from emission control in the Pearl River Delta region, southern China. Science of the Total Environment, 573, 1554-1565. https://doi.org/10.1016/j.scitotenv.2016.09.013

Wang, P., Chen, K., Zhu, S., Wang, P., & Zhang, H. (2020). Severe air pollution events not avoided by reduced anthropogenic activities during COVID-19 outbreak.

Resources, Conservation and Recycling, 158. https://doi.org/10.1016/j.resconrec.2020.104814

Wang, P., Ying, Q., Zhang, H., Hu, J., Lin, Y., & Mao, H. (2018). Source apportionment of secondary organic aerosol in China using a regional source-oriented chemical transport model and two emission inventories. Environmental Pollution, 237, 756-766. https://doi.org/10.1016/j.envpol.2017.10.122

Wang, X., Li, L., Gong, K., Mao, J., Hu, J., Li, J., Liu, Z., Liao, H., Qiu, W., Yu, Y., Dong, H., Guo, S., Hu, M., Zeng, L., & Zhang, Y. (2021). Modelling air quality during the EXPLORE-YRD campaign - Part I. Model performance evaluation and impacts of meteorological inputs and grid resolutions. Atmospheric Environment, 246. https://doi.org/10.1016/j.atmosenv.2020.118131

Wang, X., Zhang, Y., Hu, Y., Zhou, W., Lu, K., Zhong, L., Zeng, L., Shao, M., Hu, M., & Russell, A.G. (2010). Process analysis and sensitivity study of regional ozone formation over the Pearl River Delta, China, during the PRIDE-PRD2004 campaign using the Community Multiscale Air Quality modeling system. Atmos. Chem. Phys. 10, 4423-4437.

Wu, C., Wang, H., Cai, W., He, H., Ni, A., & Peng, Z. (2021). Impact of the COVID-19 lockdown on roadside traffic related air pollution in Shanghai, China. Building and Environment, 194. https://doi.org/10.1016/j.buildenv.2021.107718

Xing, J., Zhang, Y., Wang, S.X., Liu, X.H., Cheng, S.H., & Zhang, Q. (2011). Modeling study on the air quality impacts from emission reductions and atypical meteorological conditions during the 2008 Beijing Olympics. Atmos. Environ. 45, 1786-1798.

Xing, J., Li, S., Jiang, Y., Wang, S., Ding, D., Dong, Z., Zhu, Y., & Hao, J. (2020). Quantifying the emission changes and associated air quality impacts during the COVID-19 pandemic on the North China Plain: A response modeling study. Atmospheric Chemistry and Physics, 20(22), 14347-14359. https://doi.org/10.5194/acp-20-14347-2020

Xue, T., Liu, J., Zhang, Q., Geng, G., Zheng, Y., Tong, D., Liu, Z., Guan, D., Bo, Y., Zhu, T., He, K., & Hao, J. (2019). Rapid improvement of PM2.5 pollution and associated health benefits in China during 2013-2017. Science China Earth Sciences, 62(12), 1847-1856. https://doi.org/10.1007/s11430-018-9348-2

Xu, W., Song, W., Zhang, Y., Liu, X., Zhang, L., Zhao, Y., Liu, D., Tang, A., Yang, D., Wang, D., Wen, Z., Pan, Y., Fowler, D., Collett, J. L., Willem Erisman, J., Goulding, K., Li, Y., & Zhang, F. (2017). Air quality improvement in a megacity: Implications from 2015 Beijing Parade Blue pollution control actions. Atmospheric Chemistry and Physics, 17(1), 31-46. https://doi.org/10.5194/acp-17-31-2017

Yan, D., Lei, Y., Shi, Y., Zhu, Q., Li, L., & Zhang, Z. (2018). Evolution of the spatiotemporal pattern of PM2.5 concentrations in China - A case study from the Beijing-Tianjin-Hebei region. Atmospheric Environment, 183, 225-233. https://doi.org/10.1016/j.atmosenv.2018.03.041

Ye, F., Rupakheti, D., Huang, L., T, Nishanth., MK, S.K., Li, L., KT, V., & Hu, J. (2022). Integrated process analysis retrieval of changes in ground-level ozone and fine particulate matter during the COVID-19 outbreak in the coastal city of Kannur, India. Environmental Pollution, 307. https://doi.org/10.1016/j.envpol.2022.119468

Yin, P., Brauer, M., Cohen, A.J., Wang, H., Li, J., Burnett, R.T., Stanaway, J.D., Causey, K., Larson, S., Godwin, W., Frostad, J., Marks, A., Wang, L., Zhou, M., & Murray, C.J.L. (2020). The effect of air pollution on deaths, disease burden, and life expectancy across China and its provinces, 1990-2017: an analysis for the Global Burden of Disease Study 2017. The Lancet Planetary Health 4, e386–e398.

Zhang, Y., Ma, Z., Gao, Y., & Zhang, M. (2021). Impacts of the meteorological condition versus emissions reduction on the PM2.5 concentration over Beijing-Tianjin-Hebei during the COVID-19 lockdown. Atmospheric and Oceanic Science Letters, 14(4). https://doi.org/10.1016/j.aosl.2020.100014

Zhao, N., Wang, G., Li, G., Lang, J., & Zhang, H. (2020). Air pollution episodes during the COVID-19 outbreak in the Beijing-Tianjin-Hebei region of China: An insight into the transport pathways and source distribution. Environmental Pollution, 267. https://doi.org/10.1016/j.envpol.2020.115617

Zhao, X., Wang, G., Wang, S., Zhao, N., Zhang, M., & Yue, W. (2021). Impacts of COVID-19 on air quality in mid-eastern China: An insight into meteorology and emissions. Atmospheric Environment, 266. https://doi.org/10.1016/j.atmosenv.2021.118750

Zheng, B., Zhang, Q., Geng, G., Chen, C., Shi, Q., Cui, M., Lei, Y., & He, K. (2021). Changes in China's anthropogenic emissions and air quality during the COVID-19 pandemic in 2020. Earth System Science Data, 13(6), 2895-2907. https://doi.org/10.5194/essd-13-2895-2021

Zheng, B., Zhang, Q., Geng, G., Shi, Q., Lei, Y., & He, K. (2020). Changes in China's anthropogenic emissions during the COVID-19 pandemic. Earth System Science Data Discussions, 1-20. https://doi.org/10.5194/essd-2020-355

Zhou, C., Zhou, H., Holsen, T. M., Hopke, P. K., Edgerton, E. S., & Schwab, J. J. (2019). Ambient Ammonia Concentrations Across New York State. Journal of Geophysical Research: Atmospheres, 124(14), 8287-8302. https://doi.org/10.1029/2019JD030380

Zhu, N., Zhang, D., Wang, W., Li, X., Yang, B., Song, J., Zhao, X., Huang, B., Shi, W., Lu, R., Niu, P., Zhan, F., Ma, X., Wang, D., Xu, W., Wu, G., Gao, G. F., & Tan, W. (2020). A Novel Coronavirus from Patients with Pneumonia in China, 2019. New England Journal of Medicine, 382(8), 727-733. https://doi.org/10.1056/nejmoa2001017

Supplementary Material for

Quantifying the contributions of atmospheric processes and meteorology to severe $PM_{2.5}$ pollution episodes during the COVID-19 lockdown in the Beijing-Tianjin-Hebei, China

Ishaq Dimeji Sulaymon[a], Yuanxun Zhang[b,c], Philip K. Hopke[d,e], Song Guo[f], Fei Ye[a], Jinjin Sun[a], Yanhong Zhu[a], Jianlin Hu[a*]

[a] *Jiangsu Key Laboratory of Atmospheric Environment Monitoring and Pollution Control, Collaborative Innovation Center of Atmospheric Environment and Equipment Technology, School of Environmental Science and Engineering, Nanjing University of Information Science and Technology, Nanjing, 210044, China*

[b] *College of Resources and Environment, University of Chinese Academy of Sciences, Beijing 100049, China*

[c] *CAS Center for Excellence in Regional Atmospheric Environment, Chinese Academy of Sciences, Xiamen, 361021, China*

[d] *Center for Air Resources Engineering and Science, Clarkson University, Potsdam, NY 13699, USA*

[e] *Department of Public Health Sciences, University of Rochester School of Medicine and Dentistry, Rochester, NY 14642, USA*

[f] *State Key Joint Laboratory of Environmental Simulation and Pollution Control, College of Environmental Sciences and Engineering, Peking University, Beijing, 100871, China*

[*] Corresponding author. *E-mail address:* sulaymondimeji@nuist.edu.cn; jianlinhu@nuist.edu.cn

Text S1. Materials and methods

To evaluate the effects of the reduction in anthropogenic emissions sectors on air quality, two scenarios were simulated for comparison (Table S2). For the base case scenario (Case 1), the original anthropogenic emission inventory of the Multi-resolution Emission Inventory for China based on year 2016 (MEIC16) was used. In scenario 2 (Case 2), the industrial, transportation, and power emissions sectors were scaled with a factor of 0.80 (20% reduction), 0.20 (80% reduction), and 0.90 (10% reduction), respectively. The transportation sector was greatly reduced (80%) as both public and private transport systems except those rendering essential services (such as security operatives and hospital vehicles) were shut down nationwide during the lockdown period. The industrial sector was only reduced by 20% as industries producing essential items (such as food, toiletries, face mask, drugs, and so on) were allowed to operate (though not at full scale) during the lockdown period. The emissions from power plants were reduced by 10% in Case 2 due to the closure of offices, schools, restaurants, business centers, non-essential industries, shopping malls, and other public outlets that were also consumers of electricity aside the residential usage. In addition, since the lockdown period coincided with the winter period, the demand for and consumption of power for home heating as well as lighting became highly necessary, hence, no substantive reduction (>10%) in power sector could be justified during the lockdown. The emissions from residential sector were held constant in Case 2 (similar to Case1) since people were mandated to stay at home as a physical way of curtailing the spread of the pandemic. In the absence of official emission inventory during the lockdown, the emission scaling factors used in this study followed the suggestions by the Chinese Research Academy of Environmental Sciences (CRAES 2020) regarding the status of emission inventory in China during the lockdown and were also consistent with those of Sulaymon et al. (2021a) and Wang et al. (2020).

Text S2. Diel variations of atmospheric processes contributing to $PM_{2.5}$ at the surface layer

The diel variations for the contributions of individual atmospheric processes to the formation of $PM_{2.5}$ and the hourly variations of $PM_{2.5}$ concentrations at the surface layer for the two cases are presented in Fig. S4. Considering Case 2, the positive contributions of EMIS process exhibited two slight increasing trends during 05:00 local time (LT) to 07:00 LT and 15:00-20:00 LT in BTH, Beijing, Shijiazhuang, and Baoding, while it only showed a small increasing trend in Tianjin during 15:00-20:00 LT. EMIS process displayed a bimodal feature in BTH, Beijing, Shijiazhuang, and Baoding at 07:00 LT and 20:00 LT. Also, the positive contributions due to AERO process showed two increasing trends in BTH (04:00-08:00 LT and 15:00-20:00 LT), Beijing (04:00-07:00 LT and 15:00-19:00 LT), Tianjin (04:00-07:00 LT and 16:00-20:00 LT), Shijiazhuang (04:00-08:00 LT and 15:00-20:00 LT), and Baoding (03:00-07:00 LT and 15:00-20:00 LT). AERO process exhibited two peaks in Tianjin and Baoding (07:00 LT and 20:00 LT), BTH and Shijiazhuang (08:00 LT and 20:00 LT), and Beijing (07:00 LT and 19:00 LT). The first peak of $PM_{2.5}$ concentration occurred at 07:00 LT (in Beijing and Tianjin) and 08:00 LT (in BTH region, Shijiazhuang, and Baoding). During the first periods of increasing trends of EMIS and AERO in Beijing and Tianjin, both HTRA and VTRA were the major sinks, resulting into vertical and horizontal exports of $PM_{2.5}$ in the two cities. Contrarily, in BTH, Shijiazhuang, and Baoding, HTRA, just like EMIS and AERO, also contributed positively to the net

$PM_{2.5}$, especially during the nighttime and early hours of the day, while VTRA served as the predominant sink, resulting into horizontal import and vertical export of $PM_{2.5}$. During the nighttime and early hours of the day, the contributions of HTRA were the dominant $PM_{2.5}$ import in Shijiazhuang, with the two peaks occurring at 00:00 LT and 21:00 LT. However, HTRA changed from positive to negative in BTH (11:00-15:00 LT), Shijiazhuang (10:00-17:00 LT), and Baoding (09:00-16:00 LT) and acted as another sink. It is worthy to note that during 13:00-1600 LT and 14:00-1500 LT in Shijiazhuang and Baoding, respectively, the contributions of VTRA became positive, resulting into vertical import and horizontal export of $PM_{2.5}$. The positive effects of EMIS (07:00-15:00 LT in Beijing; 07:00-11:00 LT in Shijiazhuang, Baoding, and BTH) and AERO (07:00-14:00 LT in Beijing; 08:00-12:00 LT in Shijiazhuang; 07:00-15:00 LT in Baoding; and 08:00-15:00 LT in BTH) became weakened and their contributions decreased during the periods. Therefore, the net effects of these positive processes (EMIS and AERO) were insufficient to offset the continuous negative effects of VTRA on $PM_{2.5}$ concentrations, leading to downward trends in $PM_{2.5}$ across the study areas during the periods. It should also be noted that the HTRA effects changed from negative to positive in BTH (16:00-23:00 LT), Beijing (18:00-22:00 LT), Tianjin (15:00-20:00 LT), Shijiazhuang (18:00-23:00 LT), and Baoding (17:00-23:00 LT) and served as another contributor to the net $PM_{2.5}$. As a result of the positive contributions of the EMIS, AERO, and HTRA processes during the nighttime, the already flattened $PM_{2.5}$ levels began to rise again, and the second $PM_{2.5}$ peak occurred at 21:00 LT (in BTH, Beijing, Tianjin, and Shijiazhuang) and 22:00 LT in Baoding. Generally, the EMIS process was the vital source of hourly $PM_{2.5}$ concentrations at the surface, with the highest contributions in BTH region (25.3 μg/m^3/h in daytime; 34.4 μg/m^3/h in nighttime), Beijing (43.6 μg/m^3/h in daytime; 55.7 μg/m^3/h in nighttime), Tianjin (53.2 μg/m^3/h in daytime; 76.2 μg/m^3/h in nighttime), and Baoding (36.9 μg/m^3/h in daytime; 48.4 μg/m^3/h in nighttime), while HTRA was the dominant source in Shijiazhuang (37.4 μg/m^3/h in daytime; 48.4 μg/m^3/h in nighttime). Contrarily, $PM_{2.5}$ was substantially removed from the surface layer and transported to the upper layers through the VTRA process, especially during nighttime, with the maximum removal rates of 67.4 μg/m^3/h (21:00 LT), 89.7 μg/m^3/h (20:00 LT), 94.4 μg/m^3/h (20:00 LT), 85.6 μg/m^3/h (21:00 LT), and 94.7 μg/m^3/h (21:00 LT) in BTH region, Beijing, Tianjin, Shijiazhuang, and Baoding, respectively. DDEP and CHEM processes had slight contributions and served as the sink and source of $PM_{2.5}$, respectively. It is worthy to note that the trends of the atmospheric processes and $PM_{2.5}$ in Case 1 were similar to in Case 2 in each of the study areas, however, the contributions of the individual processes to the net $PM_{2.5}$ and the resultant magnitudes of $PM_{2.5}$ changes were higher in Case 1 than Case 2. This was due to the effects of emissions reductions implemented in Case 2.

Text S3. Diel variations of atmospheric processes contributing to $PM_{2.5}$ in the PBL

As illustrated in Fig. S5, the trends of hourly contributions of individual atmospheric processes to the formation of $PM_{2.5}$ as well as the diel distributions of $PM_{2.5}$ concentrations in the PBL were similar to that of surface layer except that the magnitudes were low in PBL relative to the surface layer. Similar to the surface layer, the EMIS process was the major source of $PM_{2.5}$ concentrations in the PBL, with the maximum contributions in BTH region (14.9 μg/m^3/h in daytime; 14.7 μg/m^3/h in nighttime), Beijing (19.6 μg/m^3/h in daytime; 19.1 μg/m^3/h in nighttime), Tianjin (27.1 μg/m^3/h in daytime; 29.6 μg/m^3/h in nighttime), and Baoding (32.4 μg/m^3/h in daytime; 26.9 μg/m^3/h in nighttime), while

HTRA was the dominant $PM_{2.5}$ import in Shijiazhuang (30.2 μg/m^3/h in daytime; 41.0 μg/m^3/h in nighttime). Vertical transport (VTRA) was the major $PM_{2.5}$ removal pathway during most hours of the day except for some hours during the daytime, with the highest removal rates of 32.6 μg/m^3/h, 33.2 μg/m^3/h, 30.8 μg/m^3/h, 55.1 μg/m^3/h, and 60.1 μg/m^3/h in BTH region, Beijing, Tianjin, Shijiazhuang, and Baoding, respectively. Contrary to the surface layer, whose highest VTRA removal rates occurred at the nighttime in all of the study areas, the highest VTRA removal rates in Tianjin and BTH region occurred at 08:00 LT, while that of Baoding occurred at 07:00 LT. Although, the positive contributions of EMIS, AERO, and HTRA pathways to $PM_{2.5}$ formation were low in the PBL relative to the surface layer, however, high $PM_{2.5}$ concentrations were still obtained across the study areas. This could be primarily explained by the low VTRA exports from the PBL compared to the surface layer, resulting to the accumulation of $PM_{2.5}$ within the PBL.

Table S1. The major physics options and the schemes used in the WRF model.

Physics option	Scheme
Microphysics	Thompson scheme
Shortwave radiation	RRTMG scheme
Longwave radiation	RRTMG scheme
Surface layer	Revised MM5 Monin-Obukhov scheme
Land surface	Unified Noah land-surface scheme
Planetary boundary layer	YSU scheme
Cumulus parameterization	Grell-Freitas ensemble scheme

Table S2. Emission scaling factors and the configuration of simulation scenarios

Source sectors	Case 1	Case 2
Residential	No changes	No changes
Industry	No changes	20% reduction
Transportation	No changes	80% reduction
Power	No changes	10% reduction
Agriculture	No changes	No changes

Table S3. Model performance of meteorological factors during the COVID-19 lockdown (OBS: observed mean; PRE: predicted mean; MB: mean bias; ME: mean error; RMSE: root mean square error). The values that do not meet the criteria are highlighted in bold.

		BTH	Beijing	Tianjin	Shijiazhuang	Baoding	Benchmark[a]
T2 (K)	OBS	274.2	273.7	275.1	277.0	274.9	
	PRE	274.6	275.9	275.6	277.6	276.2	
	MB	0.4	**2.2**	0.5	**0.6**	**1.3**	≤±0.5
	ME	1.7	**2.3**	1.1	1.3	1.9	≤2.0
	RMSE	2.1	2.7	1.4	1.6	2.2	
RH (%)	OBS	63.9	63.7	67.5	65.9	68.4	
	PRE	47.5	41.1	49.1	42.9	44.0	
	MB	-16.4	-22.5	-18.4	-23.0	-24.4	
	ME	18.2	22.5	18.4	23.0	24.4	
	RMSE	20.6	24.7	20.3	24.1	26.4	
WS (m/s)	OBS	2.2	2.3	2.3	2.2	1.8	
	PRE	2.7	2.4	2.7	2.9	2.3	
	MB	0.5	0.2	0.4	**0.7**	0.5	≤±0.5
	ME	0.9	0.6	0.6	0.8	0.7	≤2.0
	RMSE	1.2	0.7	0.8	1.1	0.9	≤2.0
WD (°)	OBS	181.6	172.6	195.4	190.7	130.3	
	PRE	172.0	151.7	166.7	192.9	129.5	
	MB	-9.6	**-20.9**	**-28.7**	2.3	-0.8	≤±10
	ME	**70.5**	**78.4**	**45.2**	**101.5**	**50.0**	≤±30
	RMSE	96.9	108.8	69.7	119.8	80.3	

a. The benchmarks used were suggested by Emery et al. (2001).

Table S4. Model performance of $PM_{2.5}$ during the COVID-19 lockdown for the two cases (OBS: observed average; PRE: predicted average; MFB: mean fractional bias; MFE: mean fractional error; MNB: mean normalized bias; MNE: mean normalized error). The performance criteria for $PM_{2.5}$ were suggested by Boylan and Russell (2006).

		BTH	Beijing	Tianjin	Shijiazhuang	Baoding	Benchmark
Case 1							
$PM_{2.5}$ (μg/m^3)	OBS	73.40	75.13	75.81	98.87	106.85	
	PRE	74.75	81.35	93.14	86.04	102.87	
	MFB	0.10	0.31	0.41	-0.05	-0.19	≤±0.60
	MFE	0.50	0.51	0.51	0.40	0.50	≤0.75
	MNB	0.41	0.77	0.91	0.08	0.55	
	MNE	0.70	0.94	0.99	0.43	0.79	
Case 2							
$PM_{2.5}$ (μg/m^3)	OBS	73.40	75.13	75.81	98.87	106.85	
	PRE	68.99	72.53	83.98	79.20	96.42	
	MFB	-0.03	-0.20	0.32	-0.13	-0.13	≤±0.60
	MFE	0.49	0.50	0.48	0.41	0.49	≤0.75
	MNB	0.30	0.56	0.72	-0.01	0.43	
	MNE	0.64	0.80	0.85	0.41	0.72	

Table S5. Averaged predicted $PM_{2.5}$ concentrations of the three pollution episodes (EPs) for Case 2 during COVID-19 lockdown in the BTH region.

Pollution Episodes City	EP1 $PM_{2.5}$ ($\mu g/m^3$)	EP2 $PM_{2.5}$ ($\mu g/m^3$)	EP3 $PM_{2.5}$ ($\mu g/m^3$)
Beijing	82.8	100.5	77.9
Tianjin	91.7	129.7	92.2
Shijiazhuang	125.1	83.2	66.6
Baoding	133.4	120.4	94.4
Cangzhou	75.0	92.8	79.1
Tangshan	103.6	138.8	98.2
Langfang	85.4	124.6	94.5
Handan	103.6	84.2	68.8
Hengshui	88.6	88.9	82.8
Xingtai	91.7	80.0	60.1

Table S6. Maximum hourly $PM_{2.5}$ concentrations of the three pollution episodes (EPs) for Case 2 during COVID-19 lockdown in the BTH region.

Pollution Episodes City	EP1 $PM_{2.5}$ ($\mu g/m^3$)	EP2 $PM_{2.5}$ ($\mu g/m^3$)	EP3 $PM_{2.5}$ ($\mu g/m^3$)
Beijing	175.8	200.8	179.0
Tianjin	207.9	233.6	193.6
Shijiazhuang	235.5	222.7	132.0
Baoding	333.1	258.0	187.1
Cangzhou	165.8	178.4	168.0
Tangshan	308.0	308.8	279.1
Langfang	191.6	285.4	211.9
Handan	219.2	165.4	132.4
Hengshui	227.4	163.8	178.4
Xingtai	183.8	186.4	114.1

Table S7. Averaged predicted PBLH and wind speed during the three pollution episodes (EPs) in the four cities.

	PBLH (m)			Wind Speed (m)		
City	EP1	EP2	EP3	EP1	EP2	EP3
Beijing	356.9	255.1	636.5	1.69	1.61	2.33
Tianjin	366.9	262.2	471.7	1.84	1.76	2.42
Shijiazhuang	294.2	341.1	650.6	1.87	2.96	3.63
Baoding	286.9	238.5	517.1	1.79	1.67	2.87

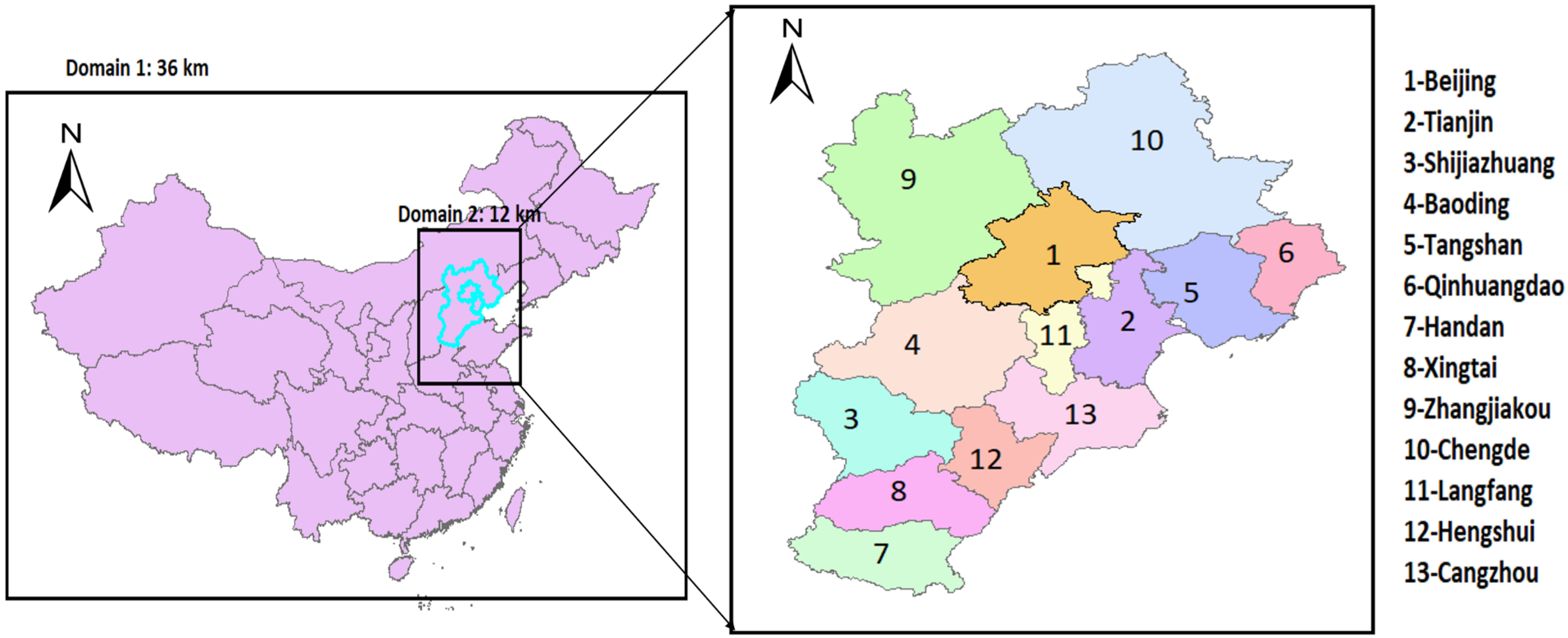

Figure S1. The simulation domains used in this study (left) and the Beijing-Tianjin-Hebei (BTH) region (right). The representative cities were numbered 1-4.

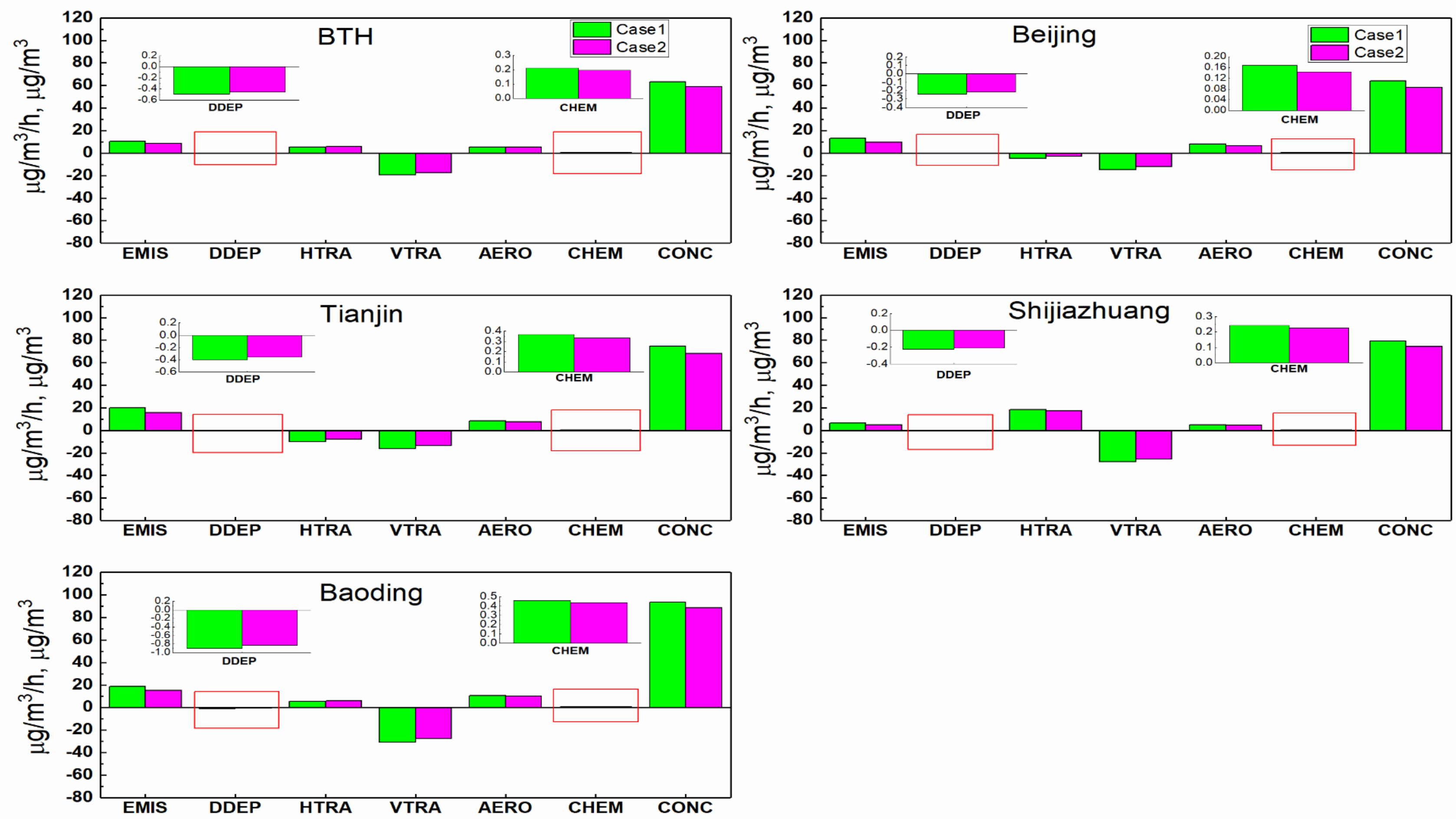

Figure S2. Contributions of the individual processes to the concentrations of $PM_{2.5}$ in the planetary boundary layer (PBL) in Cases 1 and 2 during the lockdown period. Abbreviations used in this figure are the same as in Fig. 1.

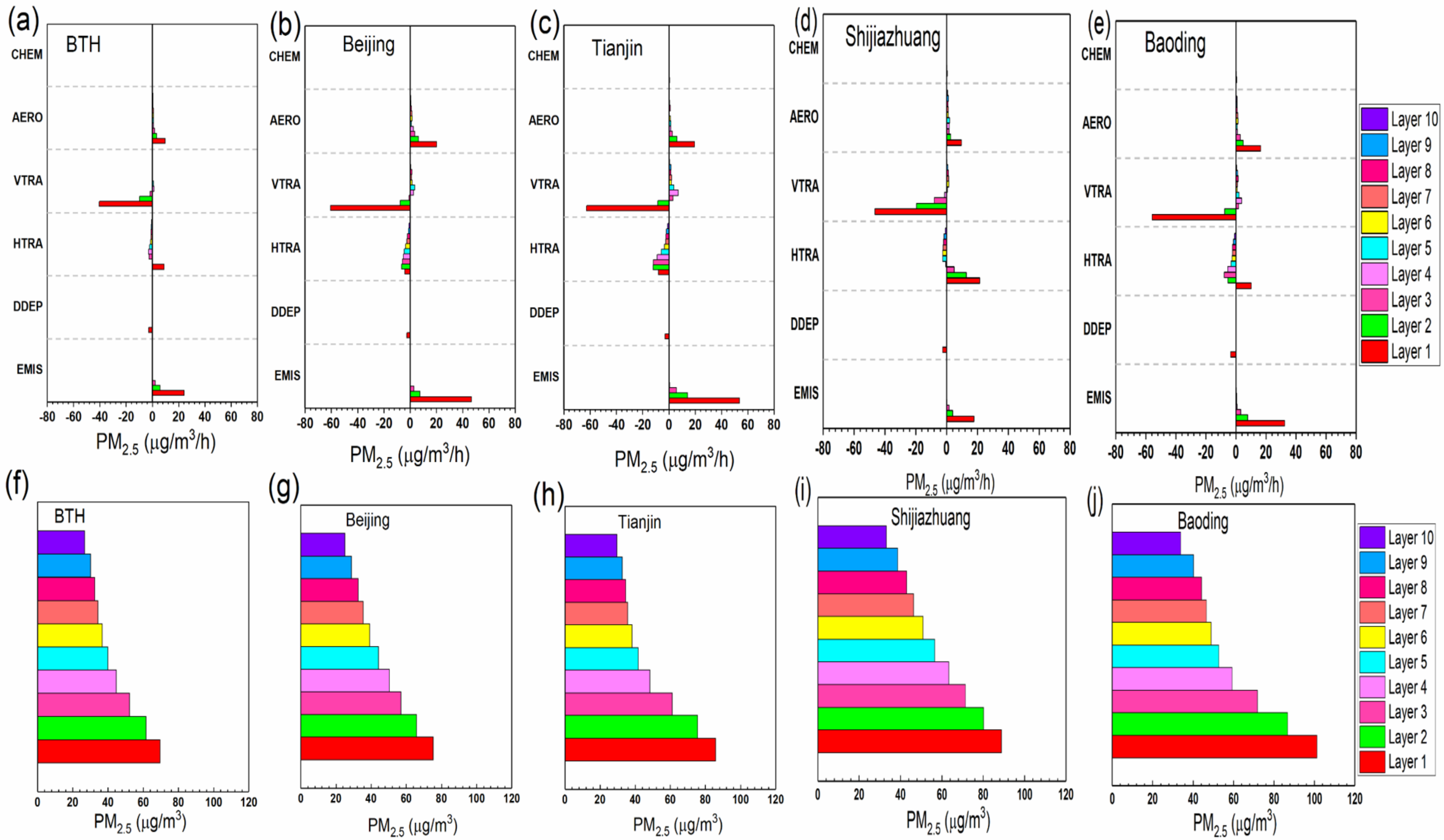

Figure S3. Hourly $PM_{2.5}$ change rates due to individual atmospheric processes for layers 1-10 (a-e) and evolution of hourly $PM_{2.5}$ vertical profiles (f-j) in Case 1 during the lockdown period. Abbreviations used in this figure are the same as in Fig. 1.

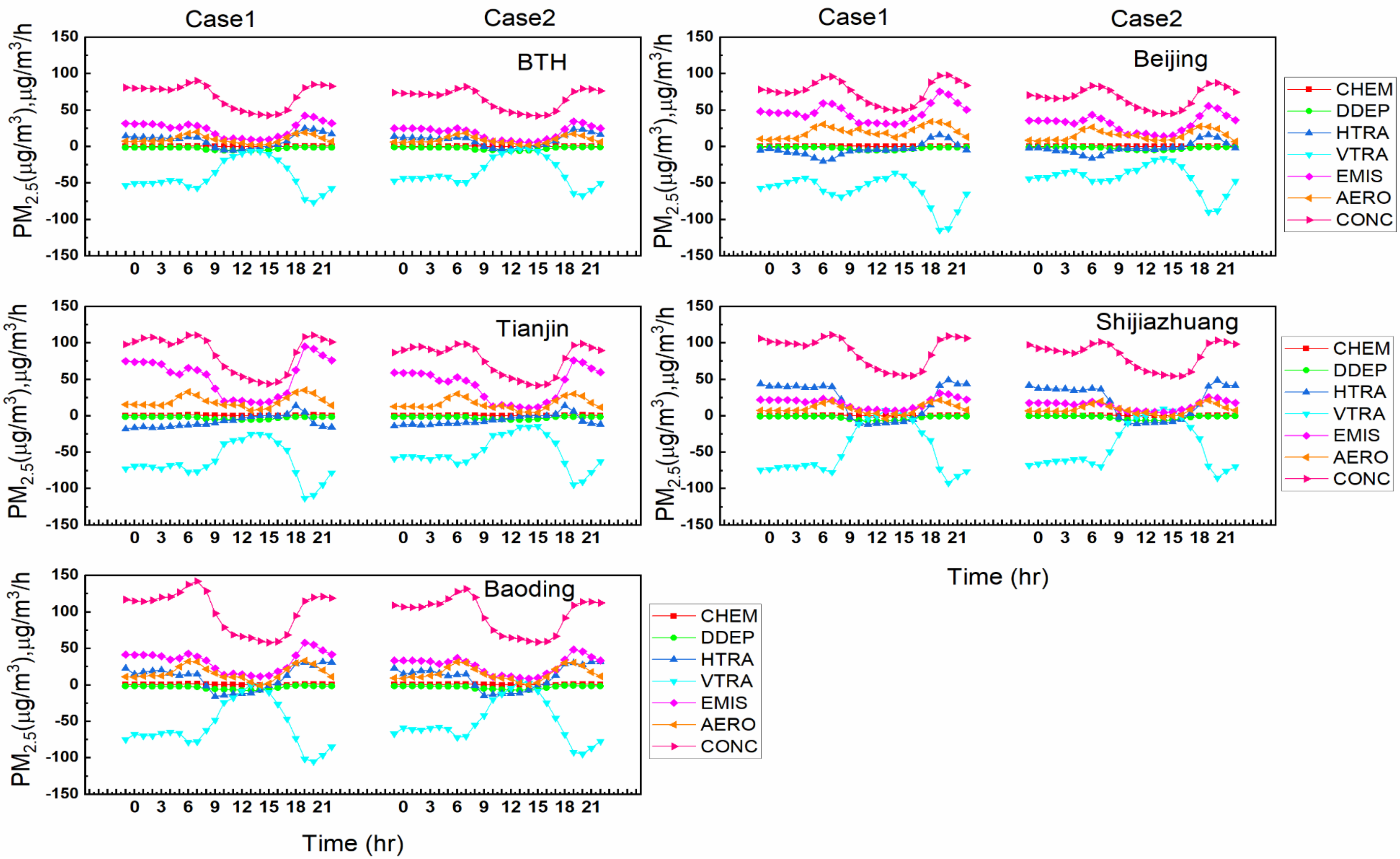

Figure S4. Diel variations of contributions of individual processes to $PM_{2.5}$ formation at the surface layer in Cases 1 and 2 during the lockdown period. Abbreviations used in this figure are the same as in Fig. 1.

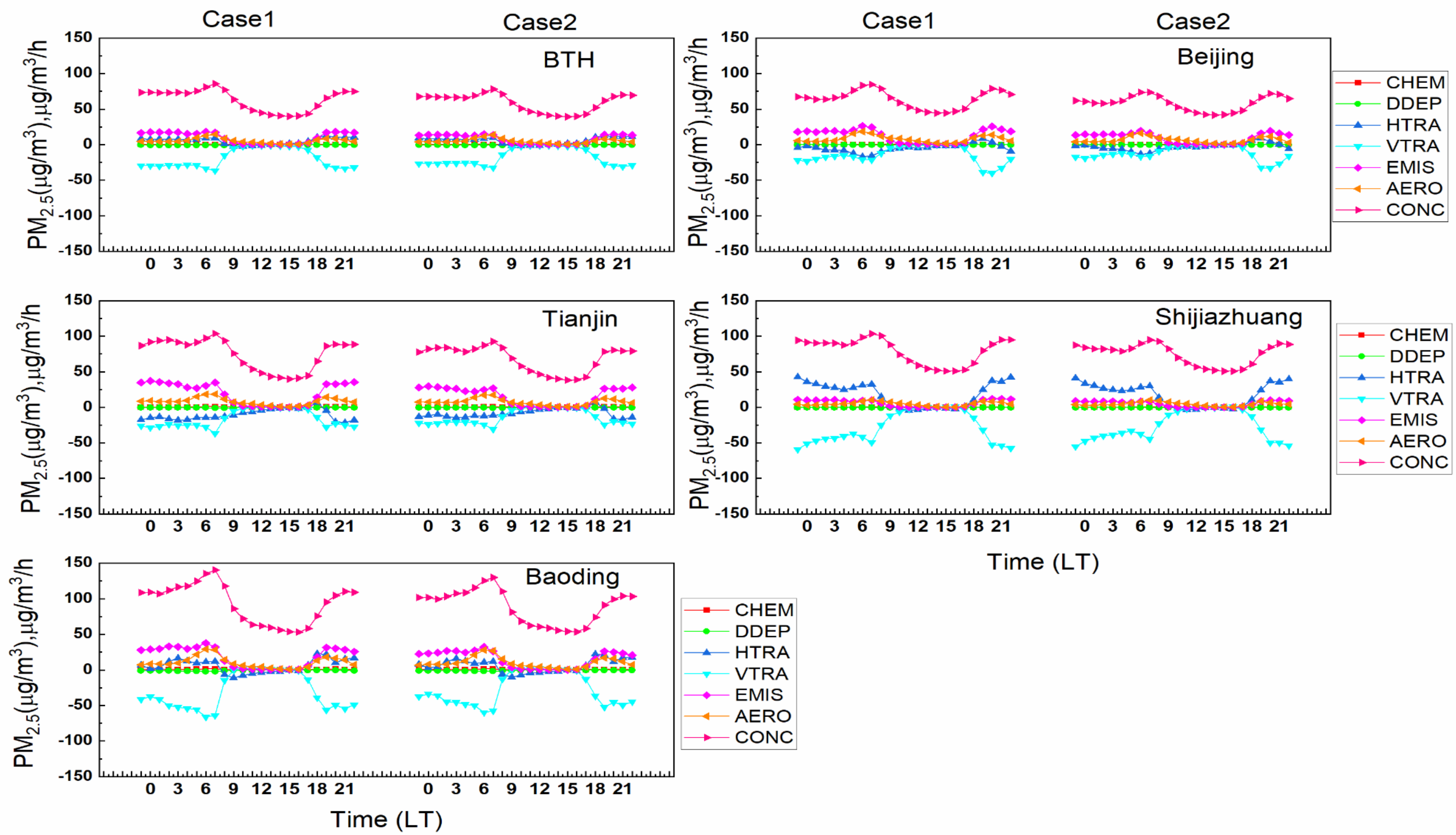

Figure S5. Diel variations of contributions of individual processes to $PM_{2.5}$ formation in the planetary boundary layer (PBL) in Cases 1 and 2 during the lockdown period. Abbreviations used in this figure are the same as in Fig. 1.

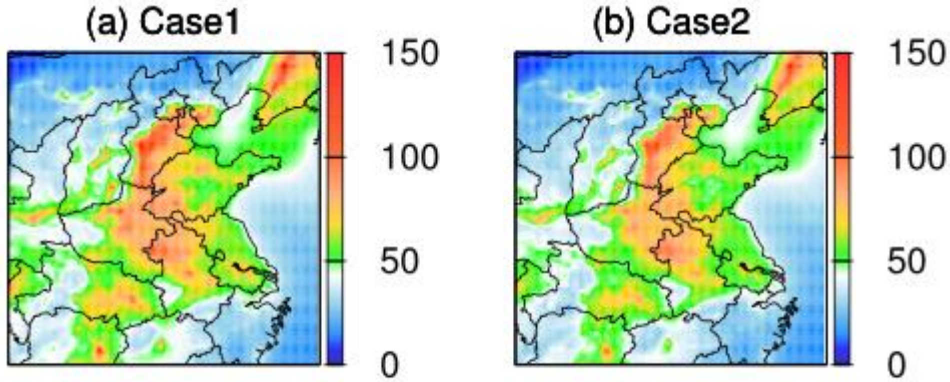

Figure S6. Spatial distributions of predicted $PM_{2.5}$ during lockdown (a) Case1 and (b) Case2 in the BTH region. Units are μg/m^3.

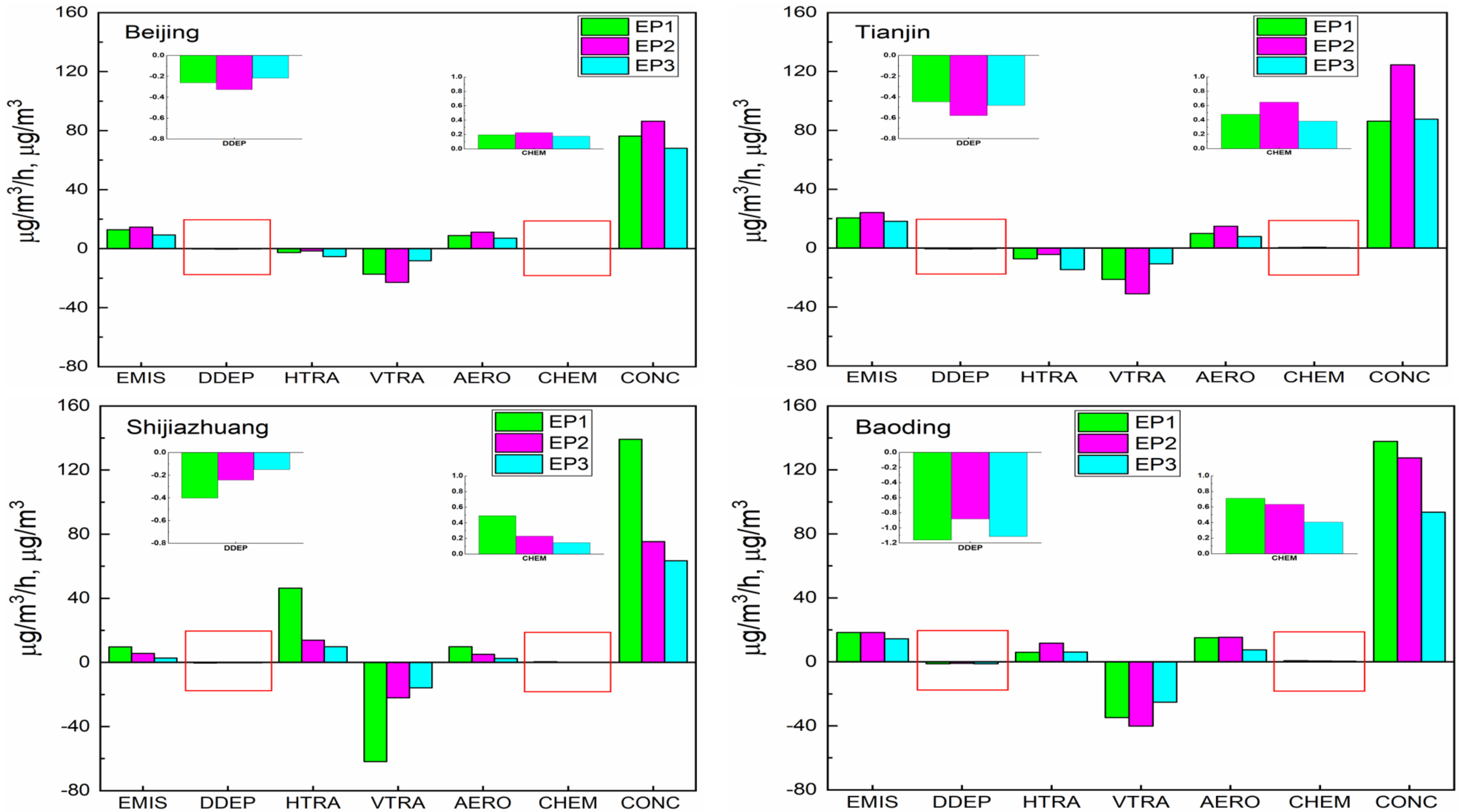

Figure S7. Contributions of the individual processes to the concentrations of $PM_{2.5}$ (Case 2) in the PBL during the three pollution episodes in the four representative cities. Abbreviations used in this figure are the same as in Fig. 1.

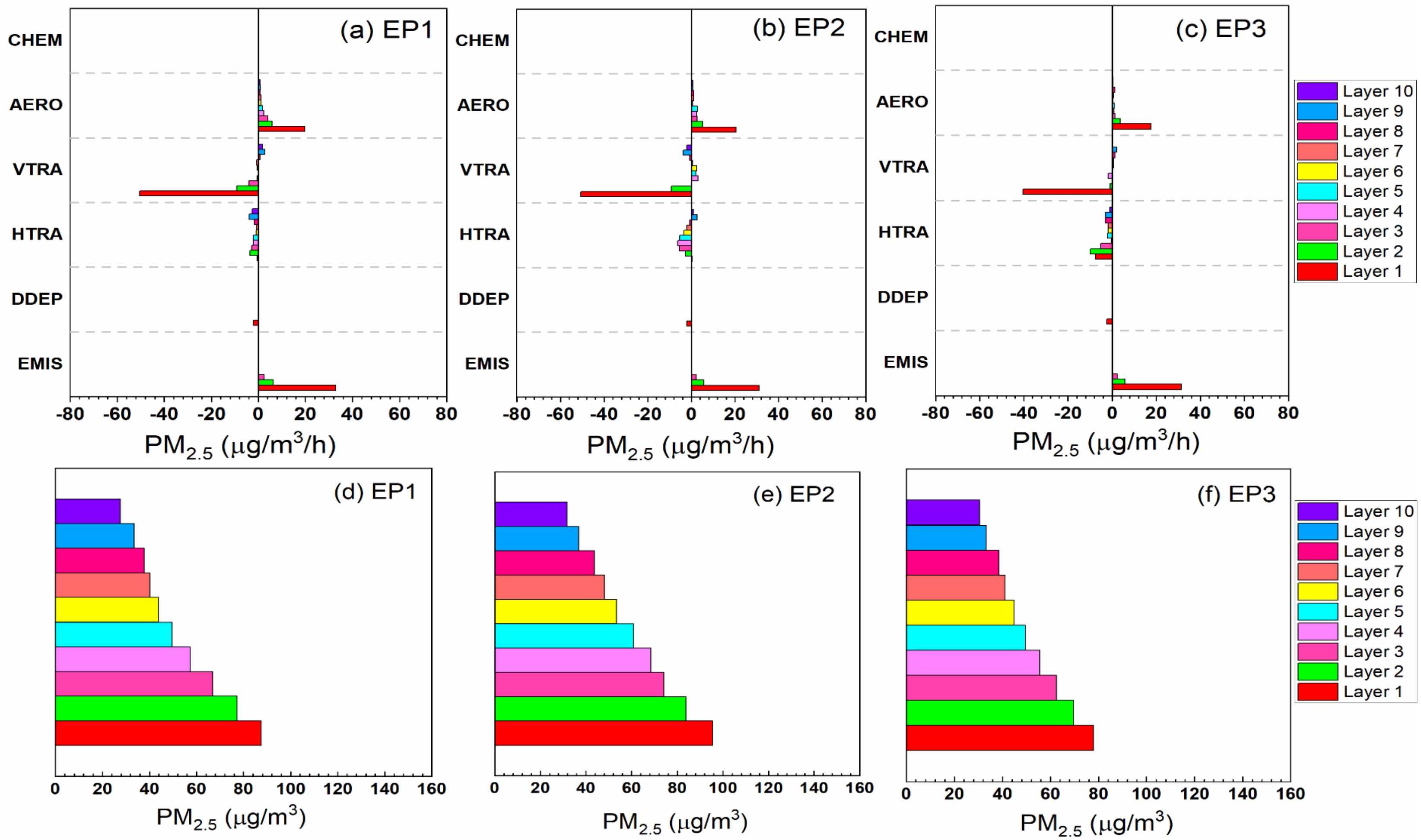

Figure S8. Hourly $PM_{2.5}$ change rates (Case 2) due to individual atmospheric processes for layers 1-10 (a-c) and evolution of hourly $PM_{2.5}$ vertical profiles (d-f) during the three pollution episodes in Beijing. Abbreviations used in this figure are the same as in Fig. 1.

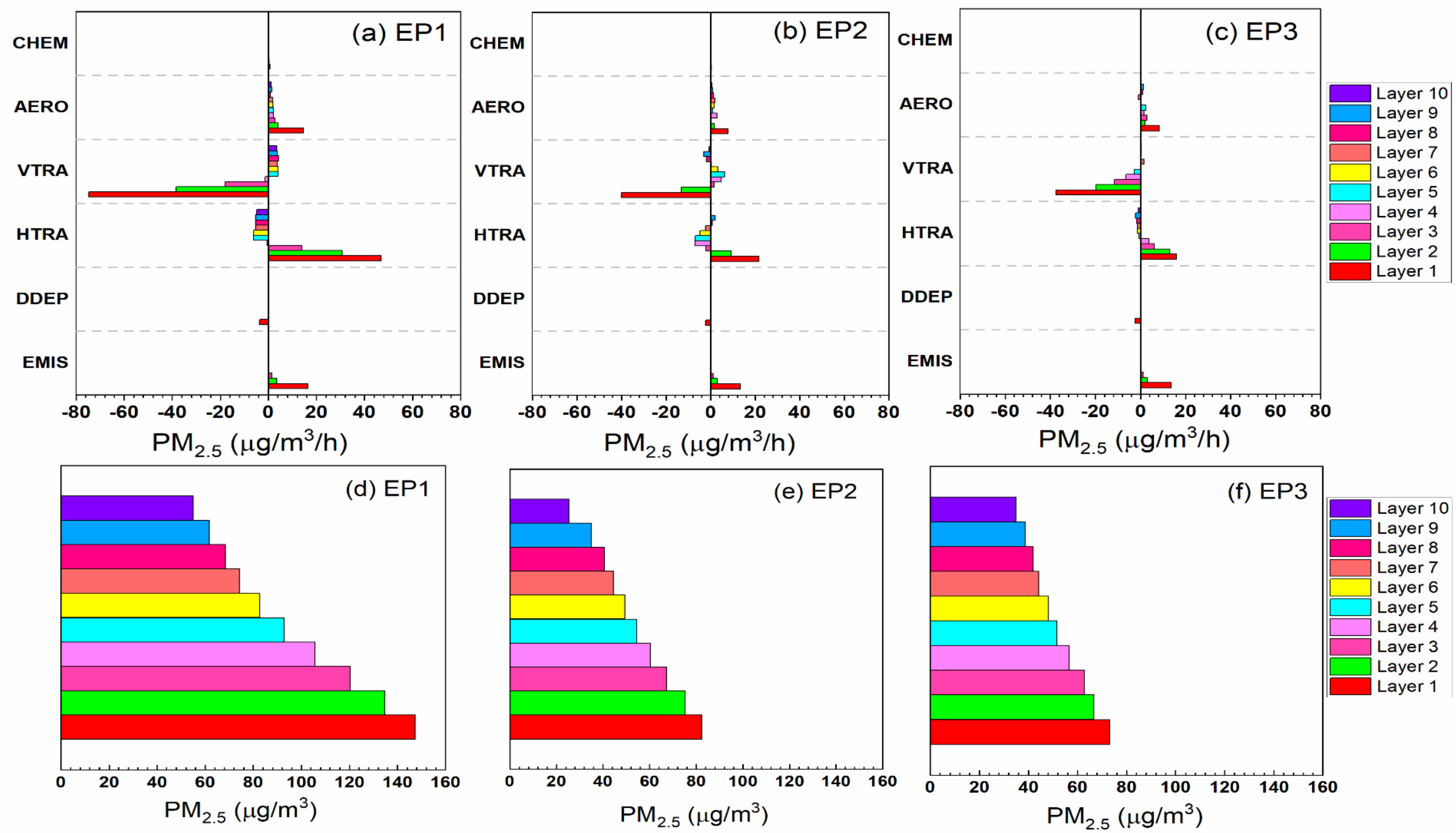

Figure S9. Hourly $PM_{2.5}$ change rates (Case 2) due to individual atmospheric processes for layers 1-10 (a-c) and evolution of hourly $PM_{2.5}$ vertical profiles (d-f) during the three pollution episodes in Shijiazhuang. Abbreviations used in this figure are the same as in Fig. 1.

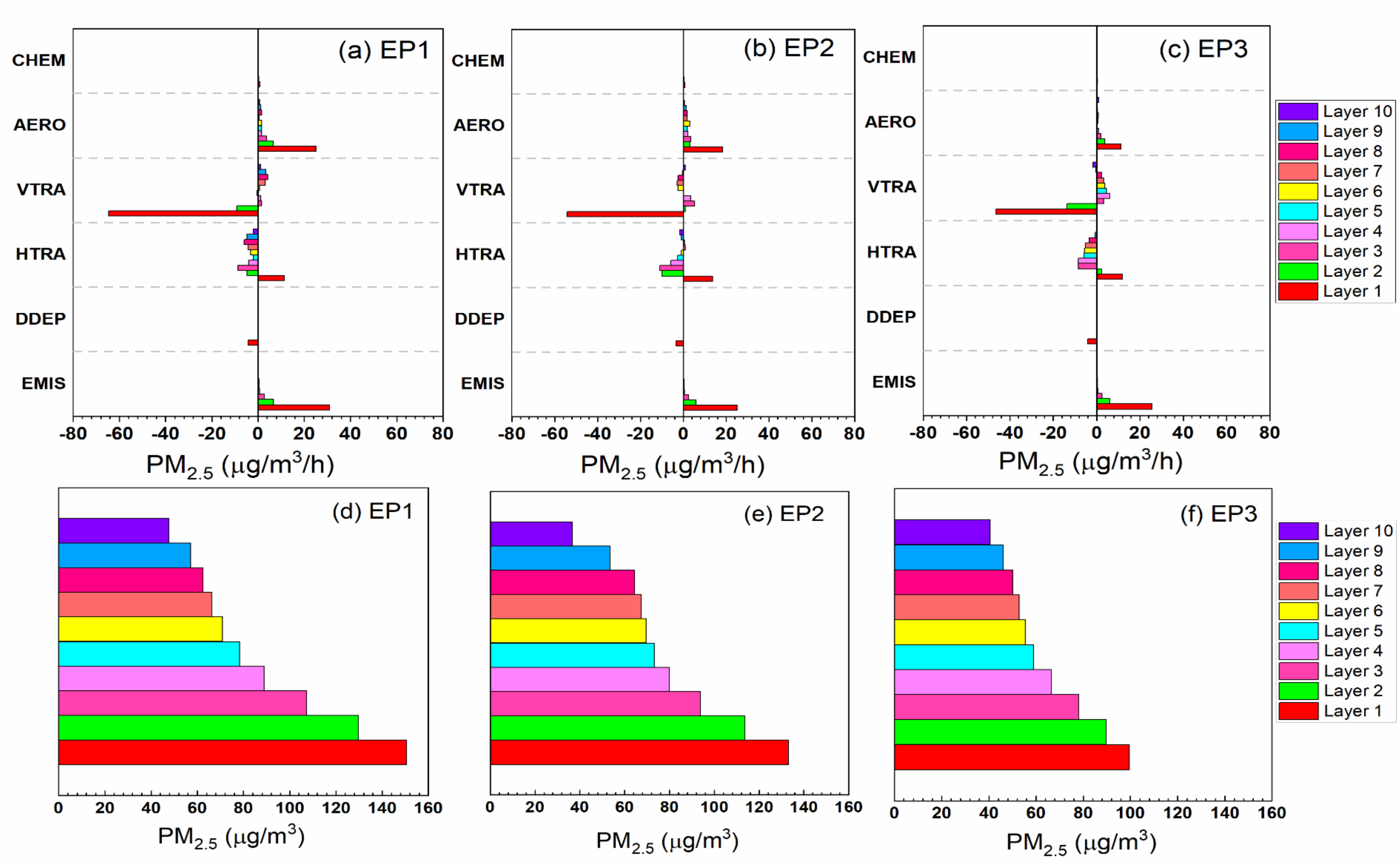

Figure S10. Hourly $PM_{2.5}$ change rates (Case 2) due to individual atmospheric processes for layers 1-10 (a-c) and evolution of hourly $PM_{2.5}$ vertical profiles (d-f) during the three pollution episodes in Baoding. Abbreviations used in this figure are the same as in Fig. 1.

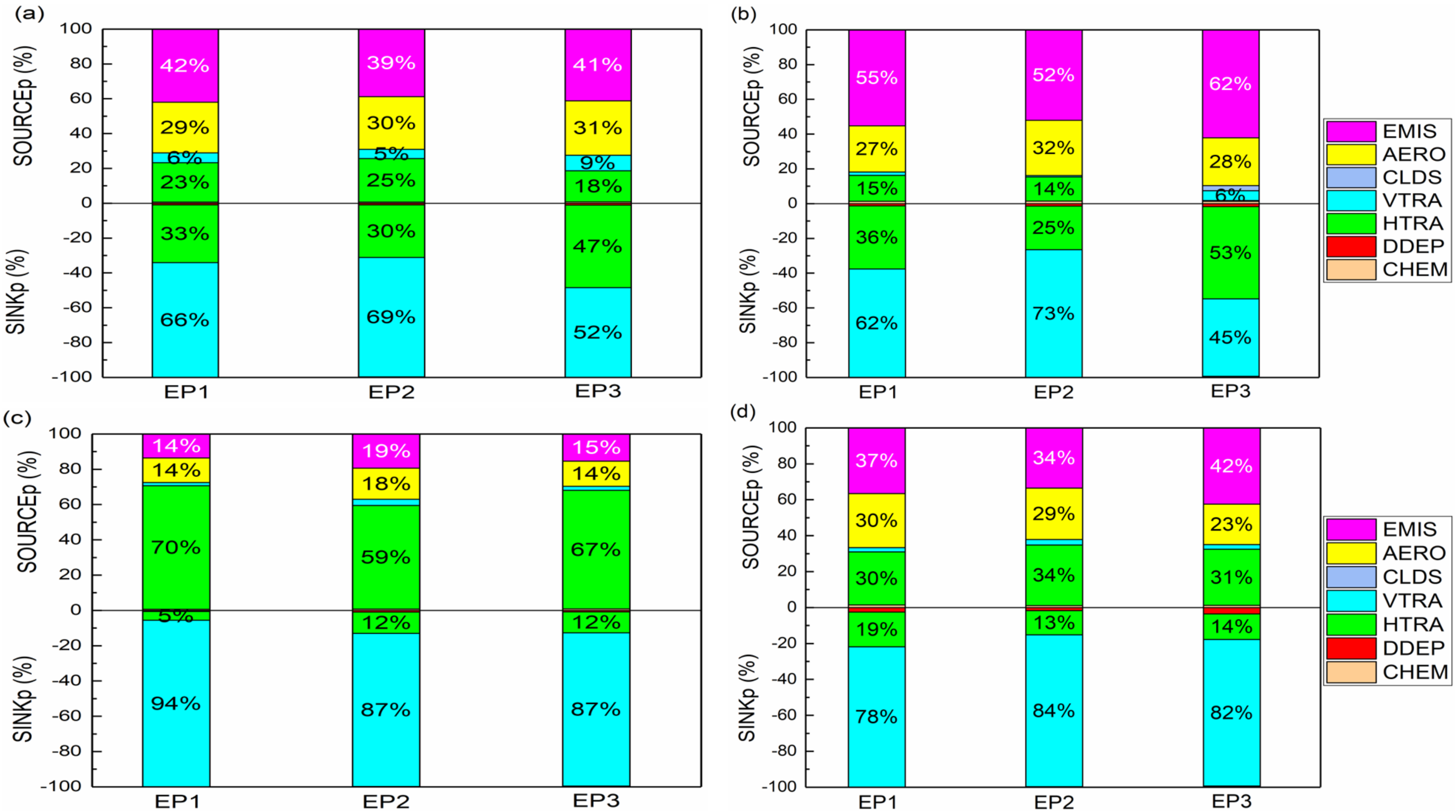

Figure S11. Positive and negative contribution ratios of the individual processes to $PM_{2.5}$ concentrations (Case 2) in the PBL in (a) Beijing, (b) Tianjin, (c) Shijiazhuang, and (d) Baoding during the three pollution episodes. Abbreviations used in this figure are the same as in Fig. 2.

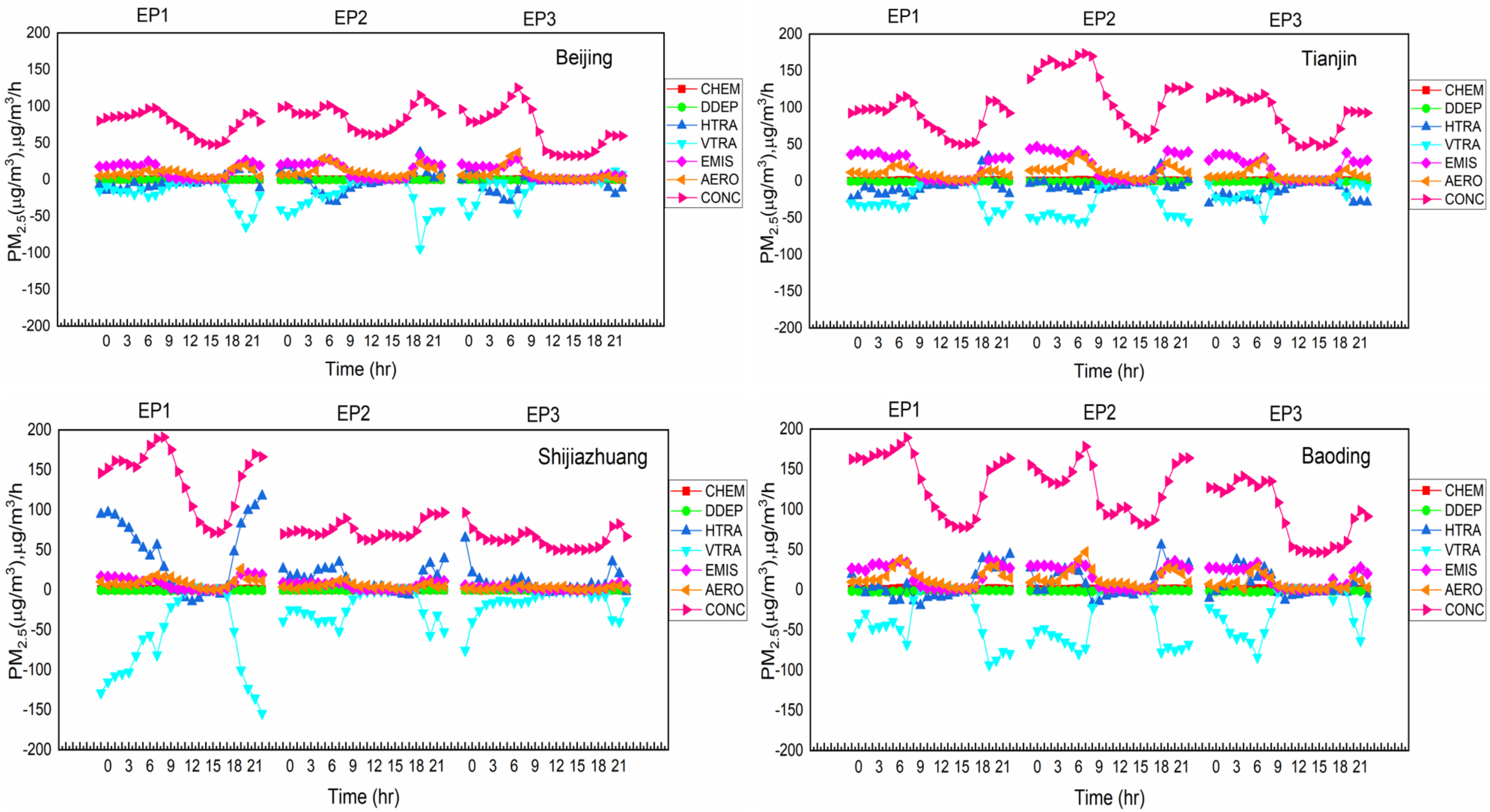

Figure S12. Diel variations of contributions of individual processes to $PM_{2.5}$ formation (Case 2) in the PBL during the three pollution episodes in the four representative cities. Abbreviations used in this figure are the same as in Fig. 1.

References

Emery, C., Tai, E., Yarwood, G. (2001). Enhanced Meteorological Modeling and Performance Evaluation for Two Texas Ozone Episodes, Prepared for the Texas Natural Resource Conservation Commission. Environ International Corporation, Novato, CA.

Sulaymon, I. D., Zhang, Y., Hopke, P. K., Hu, J., Zhang, Y., Li, L., Mei, X., Gong, K., Shi, Z., Zhao, B., Zhao, F. (2021a). Persistent high PM2.5 pollution driven by unfavorable meteorological conditions during the COVID-19 lockdown period in the Beijing-Tianjin-Hebei region, China. Environmental Research, 198. https://doi.org/10.1016/j.envres.2021.111186

Tang, L., Shang, D., Fang, X., Wu, Z., Qiu, Y., Chen, S., Li, X., Zeng, L., Guo, S., Hu, M. (2021). More significant impacts from new particle formation on haze formation during COVID-19 lockdown. *Geophysical Research Letters*, *48*, e2020GL091591. https://doi.org/10.1029/2020GL091591

Wang, P., Chen, K., Zhu, S., Wang, P., Zhang, H. (2020). Severe air pollution events not avoided by reduced anthropogenic activities during COVID-19 outbreak. Resources, Conservation and Recycling, 158. https://doi.org/10.1016/j.resconrec.2020.104814